

Analysis of herpes simplex virus 1 and host miRNAs during productive and latent infection

Zubković, Andreja

Doctoral thesis / Disertacija

2023

Degree Grantor / Ustanova koja je dodijelila akademski / stručni stupanj: **University of Rijeka / Sveučilište u Rijeci**

Permanent link / Trajna poveznica: <https://urn.nsk.hr/urn:nbn:hr:193:836855>

Rights / Prava: [In copyright](#) / [Zaštićeno autorskim pravom.](#)

Download date / Datum preuzimanja: **2024-05-19**

Repository / Repozitorij:



[Repository of the University of Rijeka, Faculty of Biotechnology and Drug Development - BIOTECHRI Repository](#)



UNIVERSITY OF RIJEKA
DEPARTMENT OF BIOTECHNOLOGY

Andreja Zubković

**Analysis of herpes simplex virus 1 and
host miRNAs during productive and
latent infection**

DOCTORAL THESIS

Rijeka, 2023

UNIVERSITY OF RIJEKA
DEPARTMENT OF BIOTECHNOLOGY

Andreja Zubković

**Analysis of herpes simplex virus 1 and
host miRNAs during productive and
latent infection**

DOCTORAL THESIS

Mentor: Igor Jurak, Ph.D.; Associate professor
Co-mentor: Michael Hackenberg, Ph.D.; Professor

Rijeka, 2023

SVEUČILIŠTE U RIJECI
ODJEL ZA BIOTEHNOLOGIJU

Andreja Zubković

**Analiza miRNA domaćina i herpes
simpleks virusa 1 tijekom produktivne i
latentne infekcije**

DOKTORSKA DISERTACIJA

Mentor: izv. prof. dr. sc. Igor Jurak
Komentor: prof. dr. sc. Michael Hackenberg

Rijeka, 2023

Thesis mentor: Igor Jurak, Ph.D.; Associate professor

Thesis co-mentor: Michael Hackenberg, Ph.D.; Professor

Doctoral thesis was defended on March 29th, 2023 at the Department of Biotechnology, University of Rijeka, in front of the committee:

1. assistant professor Željka Maglica, PhD (president of the committee)
2. assistant professor Berislav Lisnić, PhD (member)
3. associate professor Felix Wensveen, PhD (member)

Doctoral thesis contains 166 pages, 43 figures, 22 tables and 159 references

I would like to express my gratitude to my mentor, associate professor Igor Jurak, for his invaluable guidance and for always pushing our limits, continuous advice and critical feedback, and the support he offered, not only throughout research projects but in other areas as well.

I would also like to thank my co-mentor, professor Michael Hackenberg in welcoming me in his group during my stay in Granada. His expertise, insight, and encouragement helped me to tackle on the large amounts of data and to complete this study.

Many thanks to former lab members and colleagues Marina Pribanić Matešić, PhD, Maja Cokarić Brdovčak, PhD, Maja Jekić and Ines Žarak, for contributing to the experiments, for always being there to help troubleshoot problems, and for valuable feedback they have provided.

Many thanks to current lab members for their continuous moral support and advice through my final year - thank you Mia Cesarec, PhD, also for providing feedback on my drafts, Adwait Parchure, Justina Echeta, Vlatka Ivanišević, and all other master's students, and all other colleagues who were there for me at the Department of Biotechnology.

Posebno veliko hvala Vedranu i mami, te mojoj obitelji i prijateljima na moralnoj podršci, pomoći i razumijevanju za sve moje obaveze, hvala što ste tu uz mene.

FUNDING

The work was performed at the Department of Biotechnology, University of Rijeka, Rijeka, Croatia. The study was supported by the Croatian Science Foundation research grants IP-2014-09-8790 “Roles of non-coding RNAs in regulation of herpes simplex virus 1 infection” and IP-2020-02-2287 „Roles od ADAR proteins in herpes simples virus 1 infection“, FP7-PEOPLE-2013-MC-CIG, University of Rijeka Research Support Grant # 18-178-1331, the European Regional Development Fund (“Strengthening the capacity of the Scientific Center of Excellence CerVirVac for research in viral immunology and vaccinology”; KK.01.1.1.01.0006), and the Croatian Academy of Sciences and Arts project („Utjecaj povećane ekspresije staničnih mikroRNA miR-183/96/182 na replikaciju herpes simpleks virusa 1“).

SUMMARY

Viruses significantly perturb cell metabolism during infection and guide their functions toward efficient virus replication. Previous studies have shown that herpes simplex virus 1, while also encoding its own microRNAs (miRNAs), leads to significant changes in host miRNA expression. However, the exact role of such deregulation has not been elucidated. In this study, we comprehensively analyzed host and HSV-1 encoded miRNAs during productive and latent infection by applying a next-generation sequencing approach and bioinformatic analyses followed by functional studies.

Firstly, to study host miRNA changes during productive HSV-1 infection, we determined differentially expressed miRNAs in various HSV-1 infected cells in culture. We found a cluster of co-expressed host miRNAs, miR-183/96/182, that was reproducibly upregulated in primary cells. Interestingly, we found that miRNAs of this cluster share common targets, including the Forkhead box O (FoxO) family of transcription factors. We observed a slight increase followed by a decrease of FoxO1 and FoxO3 transcripts and proteins during HSV-1 infection, which coincided with the expression of the miR-183/96/182. However, we found that overexpression of the miR-183/96/182 cluster is not required for the depletion of FoxO proteins. Nonetheless, to further examine the roles of these proteins in infection, we generated cells deficient for FoxO1 and FoxO3 using the CRISPR-Cas9 technology. Our results show that individual FoxO1 or FoxO3 protein is not required for efficient virus infection.

In the second part of the study, we analyzed HSV-1 miRNAs in great detail by comparing a large number of sequencing experiments (i.e., datasets). One part of the datasets was generated in-house by sequencing, and the other was obtained from public databases. Thus far, 29 mature miRNAs have been found encoded by HSV-1, the functions of which are largely unknown. However, we have noticed significant discrepancies between reports including a lack of consistency in miRNA sequences.

To determine the exact sequences (i.e. most dominant isomiRs) of HSV-1 encoded miRNAs and to examine their expression variation between different latency models and latency in humans, we analyzed miRNAs expressed by different viral strains and clinical isolates during productive and latent infection. Extensive bioinformatics analysis showed inconsistencies between these HSV-1 miRNAs and published reference sequences. In our study, we defined the most dominant HSV-1 miRNA sequences for 29 mature miRNAs in different stages of the infection to facilitate future functional analyses of these miRNA molecules. All known HSV-1 miRNAs were categorized, suggesting that some previously published miRNAs may not be genuine regulatory molecules but rather sequencing artifacts or degradation products. Furthermore, we found significant post-transcriptional editing of hsv1-miR-H2-3p in latently infected human ganglia which confers a broadening of potential targets for the regulation of latency. This study contributes to basic knowledge and understanding of HSV-1 encoded miRNAs and their roles in regulating HSV-1 infection.

Key words: herpes simplex virus 1; microRNA; virus-host interaction, miR-H2, posttranscriptional editing

SAŽETAK

Tijekom infekcije virusi značajno mijenjaju biologiju stanice, te pritom podređuju i usmjeravaju njezine funkcije u smjeru efikasne virusne replikacije. Prethodne studije su pokazale da herpes simpleks virus 1, osim što kodira svoje mikroRNA (miRNA), dovodi i do značajnih promjena u ekspresiji miRNA domaćina, za što se smatra da bi moglo dovoditi do stvaranja pogodnih uvjeta za replikaciju virusa, no točne uloge tih promjena nisu detaljno analizirane. Kako bi opširnije prikazali analizu miRNA domaćina te HSV-1, istraživanje je podijeljeno na dva dijela, prvi dio, koji čini analiza diferencijalnih promjena miRNA domaćina tijekom infekcije te drugi dio gdje su detaljnije analizirane miRNA HSV-1.

Prvo, kako bi proučili promjene miRNA domaćina tijekom infekcije HSV-1, napravili smo profil diferencijalno eksprimiranih miRNA, te pokazali da je klaster miRNA domaćina koje se zajedno eksprimiraju, miR-183/96/182, reproducibilno povećano eksprimiran u primarnim stanicama u kulturi. Traženjem zajedničkih meta navedenih miRNA, od potencijalnih kandidata izdvojili smo Forkhead box O (FoxO) porodicu transkripcijskih faktora te uočili njihovo blago povećanje nakon kojeg slijedi opadanje razine transkripata te proteina tokom infekcije HSV-1. Kako bi ispitali ulogu FoxO u infekciji, metodom CRISPR-Cas9 generirali smo stanice deficitentne za FoxO1 i FoxO3, no, uspoređujući replikaciju, uočili smo da FoxO1 ili FoxO3 ne igraju značajnu ulogu u replikaciji HSV-1.

Drugo, kako bi detaljnije analizirali miRNA HSV-1, generirali smo i prikupili setove podataka dobivene sekvenciranjem malih RNA molekula uzoraka inficiranih sa HSV-1. Istraživanja su do sada pokazala da HSV-1 kodira 29 zrelih miRNA, čija funkcija nije u potpunosti razjašnjena. U tim dosadašnjim otkrićima sudjelovale su različite istraživačke grupe koje su u svojim istraživanjima primjenjivale različite kriterije za otkrića novih miRNA što je na kraju rezultiralo brojnim odstupanjima, uključujući i točne sekvence miRNA HSV-1. Kako bismo odredili točne sekvence miRNA HSV-1, te ispitali ekspresiju miRNA u latenciji u uzorcima čovjeka, usporedili smo sekvence miRNA između različitih virusnih sojeva i kliničkih izolata. Opsežna bioinformatička analiza pokazala je odstupanja sekvenci miRNA HSV-1 od objavljenih referentnih sekvenci, čime smo definirali

najdominantnije sekvence 29 zrelih miRNA molekula HSV-1 u različitim fazama HSV-1 infekcije kako bi doprinijeli razumijevanju i olakšali buduće funkcionalne analize ovih miRNA molekula. Također smo kategorizirali sve poznate miRNA HSV-1 te sugeriramo da neke od prije objavljenih miRNA možda nisu izvorne regulatorne molekule, već artefakti sekvenciranja. Nadalje, opisujemo značajno posttranskripcijsko uređivanje hsv1-miR-H2-3p u latentno inficiranim ganglijima čovjeka, za razliku od *in vitro* uzoraka u produktivnoj fazi infekcije. Ovi rezultati ukazuju na to da virus koristi stanične procese kako bi proširio repertoar mogućih meta miRNA ili na taj način utječe na njihovu stabilnost.

Ključne riječi: herpes simpleks virus 1, mikroRNA, interakcija virusa i domaćina, posttranskripcijsko uređivanje

TABLE OF CONTENTS

1. INTRODUCTION	1
1.1. Herpes simplex viruses	1
1.1.1. Taxonomy of herpesviruses	1
1.1.2. Structure of HSV-1 and HSV-2	2
1.1.3. HSV-1 entry and replication cycle	4
1.1.4. Latency and reactivation	7
1.1.5. Host immune response and HSV-1 strategy for successful replication - modification of the cellular environment and deregulation of miRNAs	9
1.2. microRNAs (miRNAs)	11
1.2.1. Biogenesis of miRNAs and processing	11
1.2.2. Ago preference	13
1.2.3. Function and targeting	14
1.2.4. Modifications affecting miRNA stability and targeting	15
1.2.5. Viral miRNAs.....	16
1.3. HSV-1 encoded miRNAs.....	17
1.3.1. HSV-1 miRNAs targeting viral transcripts	18
1.3.2. HSV-1 miRNAs targeting host transcripts	20
1.4. HSV-1 deregulates host miRNAs	22
1.4.1. Host miRNAs with functions in regulation of apoptosis	24
1.4.2. Host miRNAs with functions in antiviral immunity	25
1.4.3. Host miRNAs with functions in inhibition of viral replication	28
1.4.4. Other host miRNAs with unknown targets	29
1.4.5. Relationship between HSV-1 latency and miR-138	30
1.5. Potential targets of host miR-183/96/182	31

1.5.1. FoxO transcriptional factors	31
1.5.2. The role of TF FoxO in the antiviral response of the cell.....	32
2. RESEARCH AIMS	34
3. MATERIALS AND METHODS	36
3.1. Materials.....	36
3.1.1. Cell lines	36
3.1.2. Cell culture media	36
3.1.3. Viruses.....	37
3.1.4. <i>Reagents – buffers, solutions and kits</i>	38
3.1.5. Bacterial strains and medium.....	41
3.1.6. Plasmids	41
3.1.7. CRISPR/Cas9 constructs.....	42
3.1.8. Antibodies used for Western Blot and Immunofluorescence.....	43
3.1.9. siRNA.....	43
3.1.10. PCR Primers	43
3.1.11. Data sets collected from databases obtained by massively parallel sequencing of HSV-1 or HSV-2 infected samples	45
3.2. Methods	52
3.2.1. Culturing of the cells	52
3.2.2. Infection	52
3.2.3. Determination of viral titer using plaque assay	52
3.2.4. Plasmid isolation and bacterial transformation.....	53
3.2.5. Transfection of mimics and siRNA molecules.....	53
3.2.6. RNA extraction and quantitative RT-PCR (RT-qPCR)	54
3.2.7. Protein extraction and Western Blot.....	54
3.2.8. Immunofluorescence.....	55

3.2.9. Crispr-Cas9 constructs and validation of knockout (^{-/-}) cells	55
3.2.10. Ago immunoprecipitation	56
3.2.11. Small RNA sequencing and data analysis	56
3.2.12. Transcriptome sequencing and analysis	57
3.2.13. Statistical analysis.....	57
4. RESULTS	58
4.1. Comprehensive analysis of host miRNAs in HSV-1 infection.....	58
4.1.1. A number of host miRNAs are deregulated during HSV-1 infection. 58	
4.1.2. miR-183/96/182 cluster is upregulated in HSV-1 infected primary HFF and WI38 cells	61
4.2. Upregulated host miRNAs miR-183, -96 and -182 regulate 33 common targets	63
4.3. Members of the FoxO protein family as potential targets of miR-182/-96/- 183	64
4.3.1. HSV-1 productive infection induces FoxO1 and FoxO3 expression. 64	
4.3.2. FoxO family of proteins is upregulated during MCMV infection	67
4.3.3. FoxO family of proteins gets induced after IFN-β or poly(I:C) stimulation.....	69
4.3.4. Induction of FoxO1 and FoxO3 expression is dependent on MOI ...	70
4.3.5. FoxO1 re-localizes during herpesvirus infection	71
4.3.6. FoxO1 or FoxO3 are not required for efficient HSV-1 replication in SH-SY5Y cells	73
4.4. Comprehensive analysis of HSV-1 encoded miRNAs	77
4.4.1. HSV-1 microRNA profiling using deep sequencing data sets	77
4.4.2. Posttranscriptional modification detected in human trigeminal ganglia samples	92
4.4.3. Functional analysis of edited miR-H2-3p	95

4.4.4. HSV-1 miRNA processing and loading into the RISC	98
5. DISCUSSION	100
6. CONCLUSIONS	107
7. REFERENCES	109
SUPPLEMENTAL DATA	124
CURRICULUM VITAE	151

1. INTRODUCTION

1.1. Herpes simplex viruses

Herpes simplex virus 1 (HSV-1) is a well-known pathogen that causes cold sores, usually in the orolabial region. In rare cases, it can cause serious diseases such as viral encephalitis or keratitis in individuals with compromised immunity.

HSV-1 belongs to the *Simplexvirus* genus, together with herpes simplex virus 2 (HSV-2), a common human pathogen causing genital herpes. It is estimated that over 67% of the world's population under the age of 49 is infected with HSV-1, while HSV-2 prevalence was estimated to be 13.2% [1]. HSV infection is most often asymptomatic or leads to mild illnesses. However, in people with a weakened immune system, it can lead to the development of serious diseases, such as encephalitis, or even death [2].

1.1.1. Taxonomy of herpesviruses

HSV-1 belongs to the *Herpesvirales* order, which consists of more than a hundred highly divergent dsDNA viruses that share a number of biological properties, including the morphology of the virion. It is divided into three different families based on their hosts, including herpesviruses of mammals, birds, and reptiles (the *Herpesviridae* family); herpesviruses of fish and amphibians (the *Alloherpesviridae* family), and herpesviruses infecting bivalves (the *Malacoherpesviridae* family) [2]. Members of the *Herpesviridae* family infect humans and can cause various diseases. The family name, *Herpesviridae* is derived from the Greek word "herpein" which means "to creep", probably alluding to the creeping spread of the HSV-1 skin lesions. The main feature of all herpesviruses is the ability to establish latency after lytic infection. Based on host range, genetic organization and replication strategies, viruses from the *Herpesviridae* family are further classified into three distinct subfamilies – *Alpha*-, *Beta*-, and *Gammaherpesvirinae*. Of more than one hundred viruses, only nine herpesviruses are known to infect humans. Herpes simplex viruses – HSV-1, HSV-2, and varicella-zoster virus (VZV) belong to the *Alphaherpesvirinae*, and are characterized by short reproductive cycle, destruction of infected cells in productive infection, rapid spread in culture, and the ability to establish latency in neurons. Human

cytomegalovirus (HCMV), Human herpesviruses 6 - HHV-6A and HHV-6B, and Human herpesvirus 7 (HHV-7), belong to the *Betaherpesvirinae* subfamily. *Betaherpesvirinae* have narrow host range, longer replication cycle and slow spread in cultured cells, and the ability to establish latency generally in cells of the monocyte lineage. Epstein-Barr virus (EBV) and human virus associated with Kaposi's sarcoma (KSHV) are classified into *Gammapherpesvirinae* subfamily and are characterized by the restriction to the family or order of the natural host, specific for either T or B lymphocytes, and can establish latent infection in lymphoid tissue [2].

1.1.2. Structure of HSV-1 and HSV-2

A typical herpesvirion consists of a core containing a linear double-stranded DNA (dsDNA), which ranges from 124–295 kb in length; an icosahedral capsid approximately 125 nm in diameter with a hole running down its long axis, which comprises nucleocapsid. Nucleocapsid is surrounded by a layer known as the tegument that is in turn bounded by a host-derived lipid envelope studded with viral glycoproteins that mediate viral attachment and entry [2]. A schematic illustration of a representative member of the *Herpesviridae* family virion, herpes simplex 1, is shown in Figure 1.

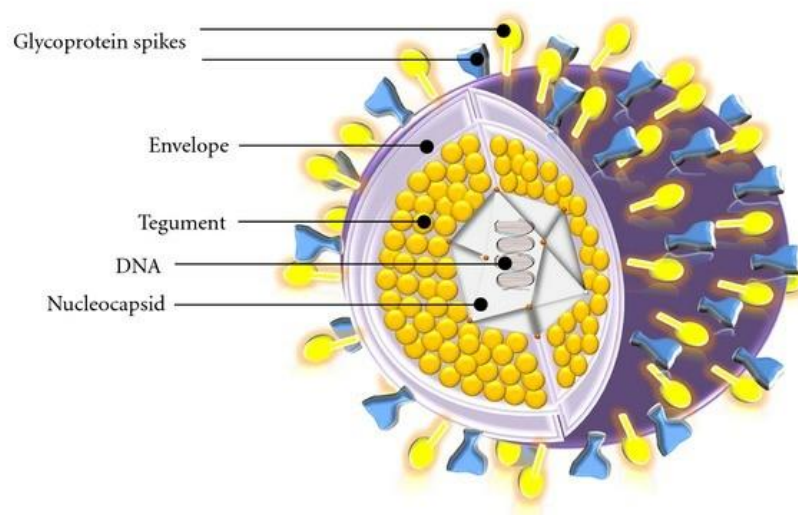
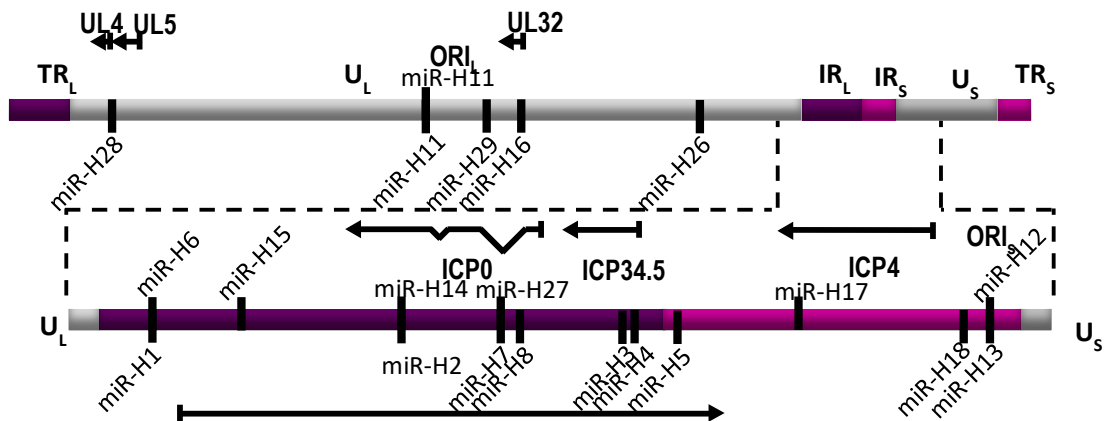


Figure 1. Herpes simplex virus 1 (HSV-1) virion. HSV-1 belongs to the *Herpesviridae* family because of its biological properties and the structure of virion, which consists of a dsDNA genome, icosahedral capsid shell, tegument with numerous viral proteins and envelope studded with 12 different viral glycoproteins. Adapted from [3].

Genomes of HSV-1 and HSV-2 consist of about 150 kb long double-stranded DNA (dsDNA) and are highly GC rich (about 70%). Genomes of HSV-1 (strain 17, accession number NC_001806) and HSV-2 (strain HG52, accession number NC_001798) share about 50% sequence identity but are considered different virus species. Interestingly, different HSV-1 and HSV-2 isolates show less than 0.7% variability. The main differences between HSV-1 and HSV-2 at the molecular level are in the sizes of the encoded proteins and the endonuclease cleavage sites. HSV-1 encodes approximately 80 genes, comprised of proteins involved in viral replication, in evasion of host immune response, viral capsid proteins, and transcripts involved in establishment and maintenance of latency [2]. The HSV genome consists of two covalently linked regions: the unique long region (U_L) and the unique short region (U_S). The U_L region encodes at least 56 different proteins involved in DNA replication and capsid formation, while the U_S region encodes 12 proteins, primarily for proteins important in host immune evasion. U_L is surrounded by a long terminal repeat region (TR_L) and a long inverted internal repeat region (IR_L), while the U_S is surrounded by a short terminal repeat region, (TR_S) and the short inverted internal repeat region (IR_S) (Figure 2). The repetitive regions, present in two copies, contain mostly immediate-early genes (IE), including ICP0 and ICP4 (ICP-infected cell polypeptide), and encode latency-associated transcripts (LATs), and a number of virus microRNAs (miRNAs) (Figure 2). Viral genome replication can be initiated at redundant replication origins, Ori_L and Ori_S . Ori_L is located within the U_L region, whereas the two copies of Ori_S are found in the short repeat regions (IR_S/TR_S) [2].

In this study, we investigated primarily regulatory molecules encoded by HSV-1, and thus, further descriptions will focus primarily on HSV-1.

A



B

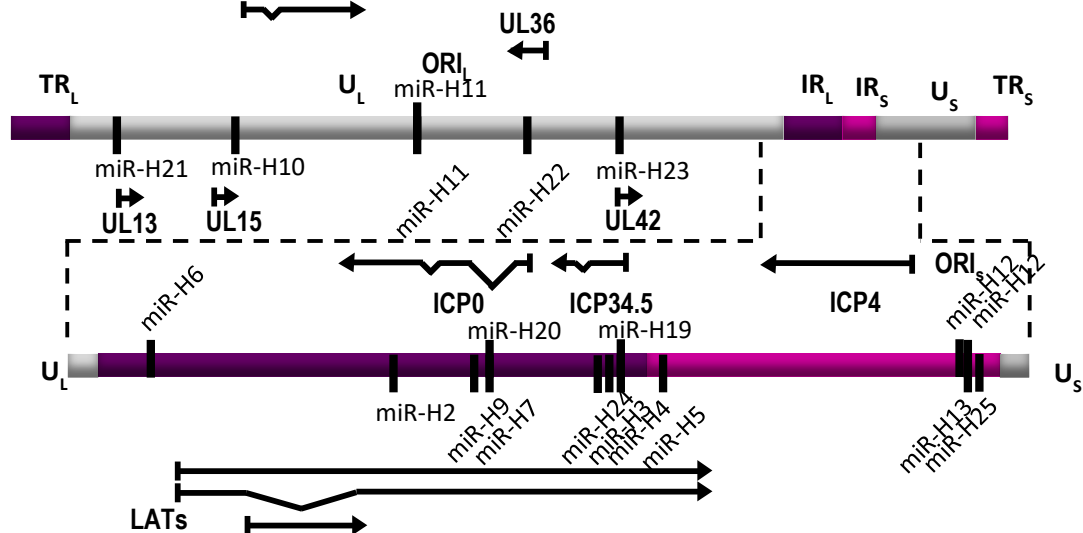


Figure 2. Schematic representation of HSV-1 and HSV-2 genome organization. A) HSV-1 and B) HSV-2 genomes consisting of unique long (UL) and unique short (US) regions surrounded by long (TRL) and short terminal region (TRS), marked purple and pink, respectively, and their inverted regions (IRL, IRS) where loci encoding miRNAs are located, marked with miR-H1-miR-H29. The locations of important viral transcripts encoded within the miRNA encoded loci are indicated with solid lines with arrows (ICP0, ICP34.5, ICP4, UL4, etc.)

1.1.3. HSV-1 entry and replication cycle

The HSV-1 entry mechanism depends on the cell type. The viral entry to the host cell is initiated by the interaction between viral glycoprotein B (gB) and/or glycoprotein C (gC) and host surface receptors, which induces the changes in the cell membrane. A key step in the fusion of a viral particle with a cell membrane is the interaction of the gD with specific receptors. gD interacts with three types of receptors:

herpes virus entry mediator (HVEM), which is expressed mainly on immune cells and is responsible for alerting the immune system to the presence of viral antigens; nectin 1 and 2, expressed on epithelial and neuronal cells; and 3-O-heparan sulfate, which results from modification of the heparan sulfate by the heparan sulfate 3-O-sulfotransferase which is present in the brain. Interaction of the gD with receptors is followed by the formation of a complex of glycoproteins important for entry, including gH/gL, and fusion of the viral envelope with the cell membrane and entry of the viral capsid and tegument into the cytoplasm of the host cell. The capsid reaches the nuclear pores, where it releases the HSV-1 genome in a linear form [4]. The incoming genome circularizes and binds proteins. [5].

Transcription of HSV-1 genes is stimulated by viral tegument protein 16 (VP16, encoded by *UL48*) protein, which induces the cascade of gene expression: first immediate early (IE or α), then early (E or β), followed by late (L or γ) genes further subdivided into leaky-late (γ_1) and true late (γ_2) viral genes transcribed by RNA Polymerase II (Figure 3).

Upon viral entry, VP16, also called alpha gene transactivating factor (α -TIF) creates a complex with host proteins Oct-1 (octamer binding protein 1) and HCF-1 (host cell factor 1). This interaction results in the de-repression of IE promoters and it facilitates the recruitment of other host transcriptional factors to IE promoters, which results in the induction of IE gene transcription [2]. In this phase of the infection, another well-described tegument protein, virion host shutoff protein (vhs, encoded by *UL41*) plays an important role in degradation of cellular mRNAs and priming cell for virus production [2]. The newly transcribed IE gene ICP4 (encoded by *RS1*) protein works as a major viral transcription factor and induces the transcription of E and L genes. ICP4 can also recruit other host genes that are beneficial for the HSV-1 infection. Other IE proteins that include ICP0 (encoded by *RL2*), ICP22 (encoded by *US1*), ICP27 (encoded by *UL54*) and ICP47 (encoded by *US12*) are also involved in the regulation of the efficient transcription of viral early and late genes or in the inhibition of the host innate immune antiviral response [2]. ICP0 acts as an E3 ubiquitin ligase whose activity is required at low MOIs to activate gene expression, to degrade most of the cellular proteins and damage the nuclear structures [2]. ICP27 is a multifunctional regulatory protein important for mRNA splicing, 3' processing and export, and also induction of the expression of early and late genes [2]. All IE genes

have multiple functions but are generally considered transcriptional regulators and intrinsic antiviral immunity modulators.

E gene products are primarily involved in viral DNA synthesis. They include genes such as ICP8 (single-strand DNA binding protein), viral DNA polymerase (UL30) and others, which are essential for DNA synthesis [2].

DNA synthesis, which is fully required for the expression of γ_2 genes, is initiated at the origins of replication (ORI_L and ORI_S). ORI_S are activated by the origin-binding protein, OBP (encoded by the *UL9*) after which DNA synthesis continues to be carried out by replisome, which consists of viral DNA polymerase and its processivity factor (encoded by the *UL30* and *UL42*, respectively), a three-subunit helicase-primase complex encoded by the *UL5*, *UL8*, and *UL52* genes; and an ssDNA-binding protein ICP8 (encoded by the *UL29*), which is important for the formation of the replication compartment (RC) in which viral genome replication takes place. By promoting L gene expression, ICP8 also triggers the shift from the early to late phase. L genes largely encode structural proteins required for virion assembly, which occurs in tandem with E gene expression [2]. Capsid is assembled from the structural proteins and genomes are then packaged into capsids.

The newly formed nucleocapsids emerge from the nucleus, and by passing through the nuclear membrane they obtain an envelope. The viral particles travel through the cytoplasm to the cell membrane where they are released. The newly formed viral particles travel to uninfected cells and repeat their replication cycle (Figure 3).

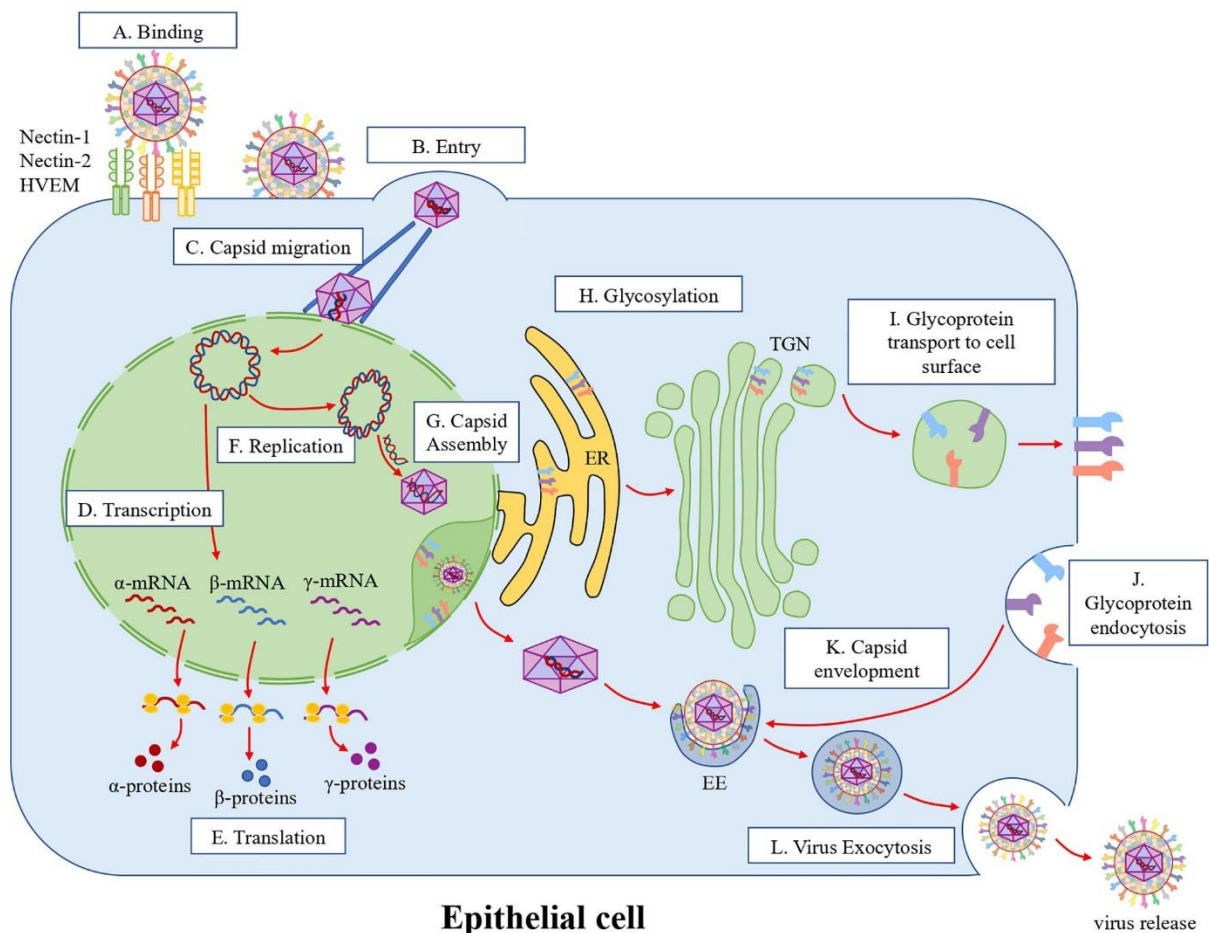


Figure 3. The schematic representation of the productive stages of HSV-1 infection. The mucosal epithelium is usually the primary site of infection, where the virus enters the cells and starts its productive infection and generation of new virus particles. It entails first binding to the host through specific receptors such as Nectin-1, Nectin-2 and HVEM (A), leading to membrane fusion and entry of the capsid and tegument in the cell (B). The capsid then migrates to the nucleus (C), and genetic material is pushed through the nuclear pore into the nucleus. The viral genome circularizes and the cascade of gene expression ensues - immediate early (IE) and early (E) genes, which are necessary for viral DNA replication (F), which will induce transcription and translation of the viral late (L) genes (D, E), followed by capsid and virion assembly (G) which includes glycosylation (H) and transport of glycoproteins to the cell surface (I) and their endocytosis (J). Capsid is then enveloped (K), and the infectious virus gets released (L). TGN - trans-Golgi network, EE – early endosomes, Adapted from [6].

1.1.4. Latency and reactivation

After primary infection in the epithelial cells, HSV-1 capsids travel by retrograde transport to the cell body of the sensory trigeminal ganglia (TGs) where it establishes latent infection, a clinically most relevant phase of HSV-1 infection [7]. Due to the number of technical challenges in investigating latency *in vivo* and developing the

latency models of the infection, the exact molecular mechanisms governing the establishment, maintenance, and reactivation from the latency are still poorly understood [2].

During the latent phase, the viral DNA is in circular episomal form, and there is a selective and limited transcription of viral genes with no virus replication. During latent infection, the only highly expressed species are non-coding gene products such as latency-associated transcripts (LATs) and miRNAs.

LATs extend through the R_L and R_S regions and can be found in 2 copies in the HSV-1 genome. Multiple LAT transcripts are transcribed, including an unstable 8.3-kb primary transcript which after processing produces stable introns 1.5 and 2-kb in length. Additionally, primary transcript gives rise to the number of miRNAs located within LAT itself [8]. The exact functions of the LAT transcript are not yet fully elucidated; however, it is known to participate in many important processes, including the inhibition of apoptosis and in lowering the level of transcripts encoding proteins needed to re-activate the productive phase of the infection [8].

Occasionally, certain stimuli can initiate reactivation, which can be asymptomatic, or lesions, usually lower intensity than primary infection, may appear. During reactivation, it has been shown that levels of IE proteins increase and their promoters are associated with the markers for active chromatin, while the LAT levels decrease. Moreover, newly formed viral particles travel by anterograde transport through the axon to the peripheral tissue, and restart the productive phase of the cycle the site of primary infection [7] (Figure 4).

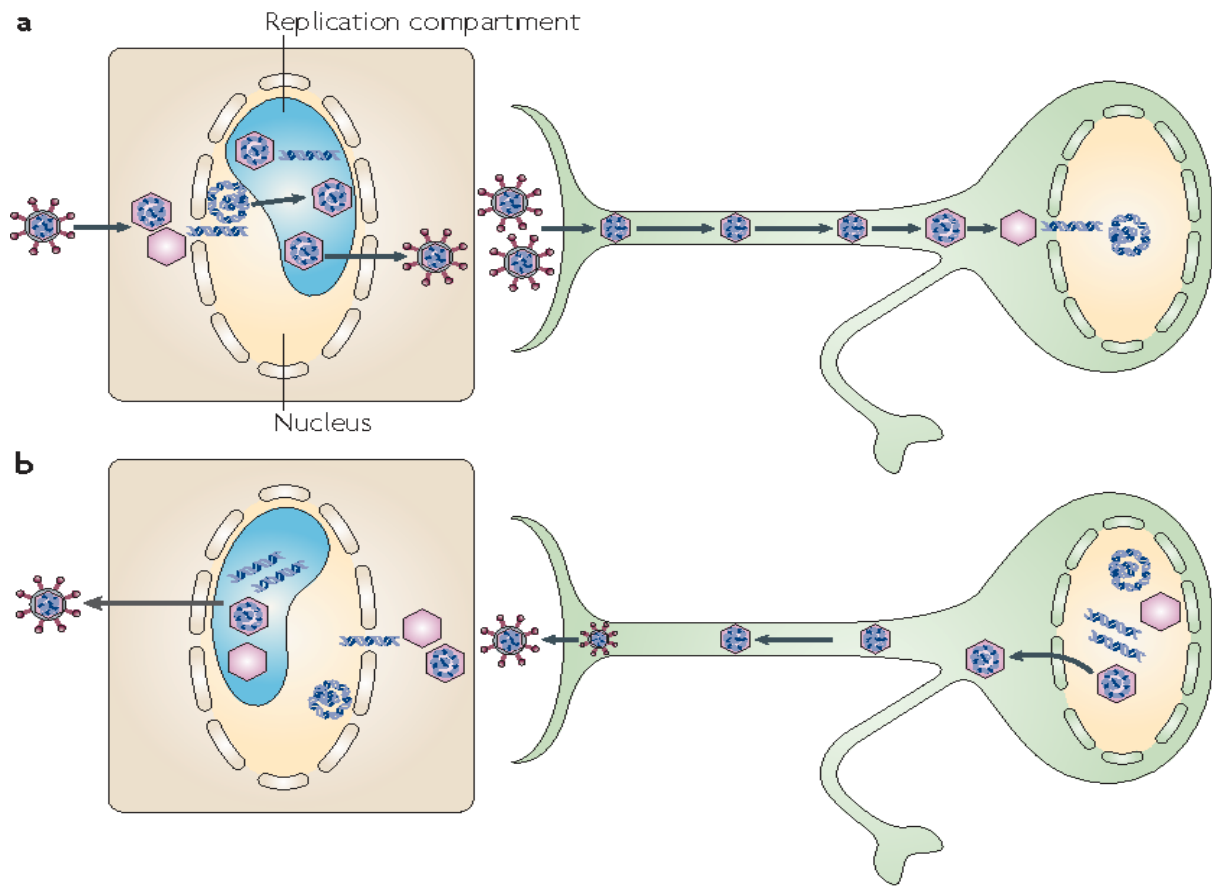


Figure 4. Schematic representation of HSV-1 entering the latent phase of infection and reactivation. (A) After primary infection, HSV-1 enters the sensory neurons and travels to the neuronal cell body by retrograde transport, where it establishes latency, hallmarked by the episomal form of DNA. (B) Due to the various external stimuli, the reactivation of the virus can occur. The virus travels by anterograde transport through the neuron to the site of primary infection. Adapted from [7]).

1.1.5. Host immune response and HSV-1 strategy for successful replication - modification of the cellular environment and deregulation of miRNAs

Viruses can take over many cellular processes and molecules to enable their efficient virus replication by using the essential machinery of a host. It has been shown that HSV-1 infection broadly alters cell structure and processes such as margination of chromatin, enlargement of the cell nucleus, formation of the replication compartments, disruption of the nuclear lamina and nucleoli and Golgi apparatus and microtubules [9].

Host have developed numerous defense mechanisms to protect themselves from viruses. At the same time, viruses have developed their own counterdefenses, such as manipulation and/or avoidance of the host's immune response, which enable

them to establish more favorable conditions for viral replication and efficient spread from host to host [9].

Innate immunity is predominantly responsible for the first line of defense against pathogens and rapid response to infections. The main components of innate immunity are physical and chemical barriers, such as epithelium and antimicrobial chemicals produced at the epithelial surface, phagocytic cells (neutrophils, macrophages, dendritic cells), and natural killer (NK) cells and other innate lymphoid cells and blood proteins, including the complement system and other mediators of inflammation.

HSV-1 infection activates innate immune response by stimulating different Pattern Recognition Receptors (PRRs), which can structurally be classified into several major families, including Toll-like receptors (TLRs), RIG-I like receptor (RLRs), cyclic GMP-AMP synthase (cGAS), and other. TLR2, TLR4, and HVEM act as primary receptors for virus glycoprotein recognition and entry, then DNA sensors such as TLR9, cGAS, IFI16, DAI/ZBP1, and dsRNA sensors such as TLR3, MDA5, RIG-I, PKR (reviewed in [10]). Their activation ultimately leads to the type I interferon (IFN- α and IFN- β) induction or cell death. The IFN- α/β produced leads to the activation of interferon-stimulated genes (ISGs) and eventually stimulates anti-inflammatory cytokine secretion, leading to a decrease in HSV-1 replication. Although many immune responses get activated due to infection, HSV-1 has also developed a number of mechanisms to counteract host antiviral immune responses on many levels [11].

Multiple cellular effector pathways play an important role in establishing the antiviral state. For example, promyelocytic leukemia (PML) protein forms ND10 nuclear structures, which have been implicated in a number of cellular antiviral processes. An increase in the replication of HSV-1 ICP0 mutant in primary fibroblasts by knocking down PML by shRNA has been shown, indicating a mechanism that is inhibited by the wt HSV-1 [12, 13]. ICP0, a viral E3 ubiquitin ligase, induces degradation of PML and subsequent disassembly of ND10 nuclear bodies counteracting its activity that way. Protein kinase R (PKR) is an IFN-inducible dsRNA-binding protein that phosphorylates and inhibits the activity of the eukaryotic translation initiation factor eIF2 α , thus preventing host, as well as viral gene expression. Accordingly, mice deficient in PKR have increased susceptibility to HSV-1 and HSV-2 [14]. Two HSV-1 encoded genes, ICP34.5 and Us11, counteract PKR activity by dephosphorylating eIF2 α and competing for dsRNA binding, respectively [15, 16]. Finally, the HSV-encoded viral host shutoff (vhs) protein inhibits host gene

expression and decreases type I IFN production, confirming the importance of this signaling pathway [17].

HSV-1 causes induction of apoptosis, a well-defined programmed cell death performed by caspases. However, virus has also developed multiple mechanisms that block caspase activation and apoptosis by producing several anti-apoptotic molecules [18].

In addition to the mechanisms mentioned above, HSV-1 utilizes many other mechanisms to create a favorable environment for replication, including the production of microRNA (miRNA) molecules or manipulation of cellular gene expression via miRNAs [19]. For that reason, the biogenesis and function of miRNAs will be discussed in further detail.

1.2. microRNAs (miRNAs)

The above-mentioned manipulations of the host environment include miRNAs, a class of small non-coding RNA molecules typically 20 – 25 nucleotides long. miRNAs have been found in mammals, plants and several virus families, including herpesviruses, retroviruses, adenoviruses, and polyomaviruses, etc., many of which are highly conserved across different species, i.e., conservation has been shown in most metazoans, plants and different virus families [20]. Many miRNAs participate in important and diverse developmental, cellular, and physiological processes, and, by supporting transcriptional programs and reducing aberrant transcripts, they play a role in conferring robustness to biological processes. Various miRNAs are grouped into families based on the identity of their seed regions (nucleotides 2-8), and for many, severe phenotypes have been observed only after the disruption of multiple family members. On the other hand, phenotypes have been visible in case of the disruption of the preferentially expressed member of the miRNA family.

1.2.1. Biogenesis of miRNAs and processing

The process of miRNA formation begins in the nucleus by formation of primary transcripts (pri-miRNA) by RNA polymerase II (Figure 5). The RNase III enzyme Drosha recognizes the stem-loop, also referred to as the hairpin structure of the pri-miRNA, and, together with its subunit DGCR8 (DiGeorge syndrome critical region 8) in the Microprocessor complex, cleaves it and releases the precursor miRNA (pre-

miRNA), approximately 60 base pairs in length. Pre-miRNA is then transferred from the nucleus to the cytoplasm by the Exportin 5/ GTP-binding nuclear protein Ran (RAN-GTP) transport complex. In the cytoplasm, another RNase III enzyme Dicer, with co-factors such as trans-activation response RNA-binding protein (TRBP) or protein activator of protein kinase R (PACT), recognizes the structure of pre-miRNA, and cleaves it into duplex that consists of two mature ~22 base pairs long RNA molecules. These two arms usually have two unpaired nucleotides at the 3' end at both complementary RNA strands. One arm will generally be loaded with Argonaute proteins (guide arm) into a multi-protein RNA-induced silencing complex (RISC), while the other will be degraded (passenger arm). These miRNA arms are annotated as miR-5p and miR-3p, indicating the arm from which the sequence was obtained. In addition, other biogenesis pathways independent of RNA polymerase II, Dicer, or Drosha, have been shown, and for only a small number of miRNAs, processing is non-canonical [21].

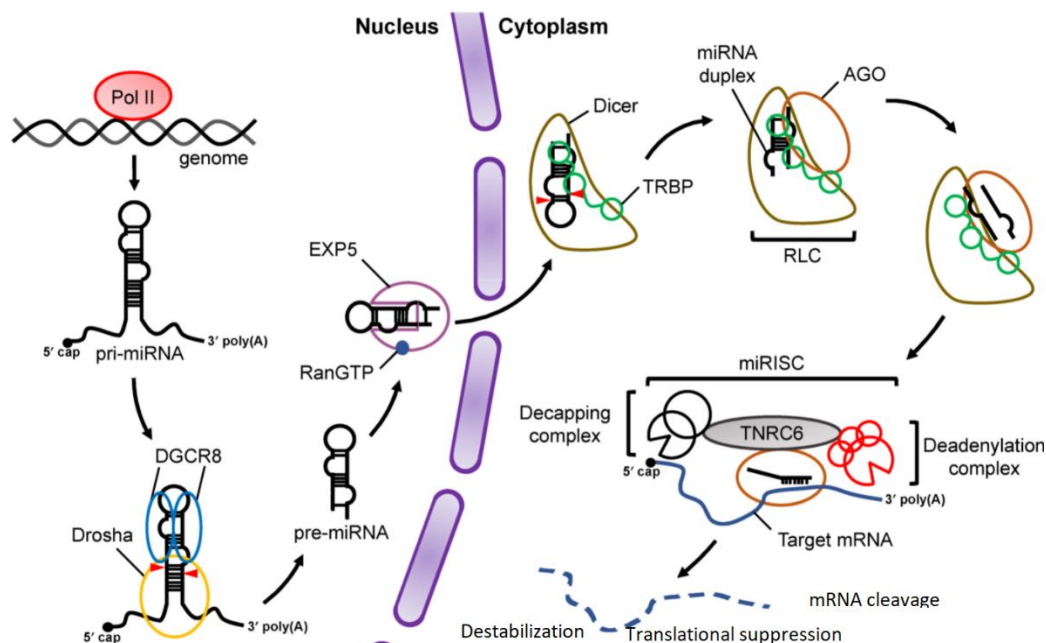


Figure 5. MicroRNA biogenesis and function. The miRNA processing pathway starts with the production of the primary miRNA transcript, the pri-miRNA. Pri-miRNA is then cleaved by the complex Drosha–DGCR8 in the nucleus. The resulting precursor miRNA (pre-miRNA) is exported from the nucleus by a complex of proteins; one of the main is Exportin-5. In the cytoplasm, the RNase enzyme Dicer, in complex with TRBP, binds the pre-miRNA hairpin and cleaves it to its mature length. The mature miRNA is then loaded together with Argonaute (Ago2) proteins into the RNA-induced silencing complex (RISC), where the functional arm of mature miRNA (guide arm) guides RISC to silence target mRNAs, whereas the passenger arm is degraded. miRNA binding to target mRNA leads to mRNA destabilization and translational suppression. Adapted from [22].

It has been demonstrated that Drosha and Dicer determine the seed sequence of miRNAs, which determines target specificity, by cleaving pri-miRNA and pre-miRNA sequences at specific sites, respectively. However, from 1881 human miRNAs documented and annotated in miRBase (version 21), only 758 showed Drosha dependence *in vitro* [23], which indicates many more factors involved in the regulation of canonical miRNA processing in relevant *in vivo* systems besides Drosha, or possibly, that other annotated molecules are not real miRNAs. Non-canonical miRNAs can encompass for example, special group of miRNAs called mirtrons, miRNA-like molecules that do not include the Drosha protein in their biogenesis are formed by splicing and unwinding of small hairpin-shaped introns. In addition to the above, some of the snoRNA (small nucleolar), tRNA (transfer) and shRNA (short hairpin) can also mature into miRNA-like molecules. Another alternative pathway of biogenesis involves the formation of miRNAs arising from the terminal portions of the siRNA hairpin precursor [24].

1.2.2. Ago preference

The duplex formed by miRNA biogenesis (containing both miR-5p/-3p), as mentioned above, is loaded into RISC, that shows a preference for small RNA duplexes with central mismatches [25]. The RISC complex consists of one of four proteins from the Argonaute protein family (Ago 1-4) and its cofactor GW182. The role of Ago proteins is to bind miRNA to the RISC complex and create a favorable conformation to recognize the target mRNA. The RISC complex retains mature miRNAs with weaker base pairing at the 5' end (guide arm), so the duplex can be efficiently unwind. In some cases, both arms can be loaded into RISC complex, suggesting that the base pairing at both 5' ends is equal [26, 27]. An additional selection for arm preference is the first nucleotide in the sequence: a miRNA having U or A in the first place will be bound up to 30-fold higher affinity than C or G because of the strong preference for U or A of Ago2 that nucleotide binding pocket exhibits [28]. The selected miRNA arm then directs the RISC complex to its target mRNA, which can be destabilized, translationally repressed or cleaved depending on the pairing with the target.

1.2.3. Function and targeting

The first few nucleotides at the 5' end of the miRNA, from nucleotide 2 – 8, also called the seed region, play an essential role in binding to the target sites. However, the length and composition of the whole sequence affect this process and play a role in determining the stability and binding to the target. First miRNA nucleotide is unable to interact with the target because of its position within the Ago in the nucleotide-binding pocket. However, it has been shown that targets are strongly repressed if A is in the first position [29]. There are a few types of seed-matched sites within mRNA targets that affect miRNA regulation efficacy by Watson-Crick matching: 6mer A1 site, which has an A across miRNA nucleotide 1 as well as almost complete seed match lacking pairing at position 7; offset 6mer site with seed match with 1 nt offset to either 5' or 3' side; 6mer site which perfectly matches 6-nt miRNA seed; 7mer-A1 site which has an A across miRNA nucleotide 1 as well as seed match; 7mer-m8 site which has a match at nucleotide 8 in addition to miRNA seed match; and 8mer site which has both A1 and m8 match together with seed match, from the minimum efficacy to the most efficient pairing, respectively. The binding of the miRNAs to the sites mentioned above makes them canonical. In addition, other possible binding models have been described, such as canonical binding with 3' supplementary site pairing, typically from nucleotides 13-16, or non-canonical binding lacking continuous 6mer pairing, however, with the compensatory pairing at the 3' end with larger stretch of paired nucleotides at 3' end from nucleotides 13-16 [21].

Using TargetScan database of evolutionary conserved miRNA binding sites for finding preferential conservation of sequence motifs, researchers found that more than 60% of human protein-coding genes contain at least one evolutionary conserved miRNA target site, which implies that miRNAs play a significant role in regulating most of the molecular processes and pathways [30]. miRNA binding sites are usually within the three prime untranslated regions (3'UTR) of mRNAs but can also be found in ORFs and 5'UTRs.

The regulatory role of miRNAs is associated with their localization within the cytoplasm. However, research by Pan et al. has shown the existence of a mechanism controlling pri-miRNA conversion to mature miRNA by ICP27, an important protein encoded by HSV-1, that mediates downregulation of *XPO5* and nuclear export of pri-miRNA during HSV-1 productive infection [31].

Many other factors can also impact the pairing by affecting the seed sequence of the miRNA. Early seed sequencing data revealed a number of miRNA sequence variants regardless of the sequencing platform used, termed isomiRs, and their importance will be described in detail below.

1.2.4. Modifications affecting miRNA stability and targeting

Many miRNAs naturally display sequence variations, i.e. isomiRs, arising from imprecise Drosha or Dicer processing, changes within the sequence, or nucleotide additions. All these differences and modifications in miRNA sequence may theoretically affect miRNA targeting, stability, or loading potential. The fact that isomiRs are detected at such high frequency argues against the claim that they could represent background noise, such as sequence artifacts or poor-quality RNA. Furthermore, isomiRs have been found to co-immunoprecipitate with Ago proteins and have been found to have a biological function in luciferase and cleavage assays *in vitro* and *in vivo* [32].

IsomiRs are usually classified as: nucleotide variants in the canonical sequence; 5' length variants; 3' length variants; templated/non-templated additions; or belonging to several of these categories simultaneously [33].

5' and 3' length variants can usually arise from the imprecise Drosha or Dicer cleavage and correspond to the sequence from which they arose (referred to as templated additions, -TA) but vary in length. Shorter template products can occur by exonucleases degrading the end of miRNA and longer by adding bases that do not match the sequence from which they arose (non-templated additions - NTA) [34]. 5' isomiRs occur less frequently compared to 3' isomiRs which occur more frequently both in number and in the abundance of miRNAs affected. More frequent occurrence of 3' isomiRs can be explained by the fact that 3' ends of miRNAs are not buried within Ago and are therefore available to the exonucleases for nucleolytic trimming to create shorter TA isomiRs. Nucleotidyl transferases are 5'-3' polymerases that catalyze the nucleotide additions at the 3' end of miRNAs to create longer isomiRs. For example, at least eight nucleotides added by uridyltransferases and adenytransferases have been shown that regulate miRNA degradation or stability, respectively. NTA sequence variations can also play a role in arm selection, resulting in arm-switching. Although the compensatory role of the 3' end of miRNA in binding to

mRNA target cannot be excluded, variations on the 5' end of miRNAs are presumed to carry more weight in targeting specificity. That way, 5' length isomiRs and isomiRs from nucleotide changes could theoretically change the impact of miRNA on their target repertoire within the seed sequence, which will be explained further.

1.2.4.1. RNA editing

One of the most important isomiRs are nucleotide variants within the seed region. Such variations can directly impact the set of target genes due to the shift or nucleotide variation in the 5' seed region, i.e., some genes will lose regulation by miRNAs, while other will gain target sites due to changes in the seed region of miRNAs. RNA modifications can have the same effect as nucleotide variants as they change the capacity to form hydrogen bonds with its complementary nucleotide. Such RNA editing mechanism is caused by deaminase enzymes include adenosine deaminases acting on RNA (ADARs), and cytidine deaminases from the AID/APOBEC protein family (activation-induced cytidine deaminases/apolipoprotein B mRNA editing enzyme cytidine deaminases. ADARs deaminate adenosine (A) to inosine (I), and are responsible for almost 90% of all editing events observed in the cell while AID/APOBEC deaminate cytidine (C) to uridine (U) [35]. This frequently occurring A-to-I editing found within the miRNAs of the host, such as miR-140, miR-301a and miR-455, miR-376 cluster (in the brain), suggests a highly conserved mechanism [36]. It has been found in four precursors of miRNAs expressed by EBV, where editing of the position +20 dramatically decreased the loading of miRNA onto Dicer, subsequently affecting virus latency [37]. In contrast, infection with HCMV impacts the increase in editing of host miR-376a, which was in turn shown to impact the downregulation of the immune modulating molecule HLA-E and renders HCMV-infected cells susceptible to elimination by NK cells [38]. For KSHV, it has been shown that its most abundant transcript in latency, K12 RNA, which produces kaposin proteins and miR-K10, is heavily edited (>60%), resulting in changed protein and miRNA seed sequence [39].

1.2.5. Viral miRNAs

Discovery of miRNAs encoded by viruses started with computational predictions and/or by sequencing of cloned small RNAs, and since then, more than 250 viral miRNAs have been discovered mostly in viruses with a DNA genome, and

over 95% of miRNAs are from the *Herpesviridae* family. A small number of miRNAs have been found in polyomaviruses and human adenoviruses. However, miRNAs have been found in a small number of RNA viruses, such as HIV [20].

One of the possible explanations why herpesviruses encode miRNAs is their ability to establish latency, where they can take advantage of the specific properties of miRNAs. miRNAs are non-immunogenic, that is, their expression is unnoticed by the host immune system and thus increases the survival of infected cells. Also, due to their small size, they take up little space in the virus genome. Furthermore, their specificity for the target miRNA can be changed with only one alteration in the sequence, particularly in the seed region. The function of most viral miRNAs is not yet fully known; however, they are thought to affect the regulation of the transition from the latent to the productive phase and vice versa and to avoid the host immune response. Avoiding an immune response is key to establishing a latent phase. Therefore, miRNAs are thought to play an important role in establishing latency by reducing the level of proteins required to establish the productive phase [20].

1.3. HSV-1 encoded miRNAs

miRNAs encoded by the herpes simplex viruses have first been computationally predicted by Pfeffer et al. [40], which was followed by the experimental identification of the first HSV-1 miRNA named miR-H1, more than 15 years ago [41], and since then, HSV-1 has been shown to encode 20 precursor miRNAs: miR-H1-H8, miR-H11-18, and miR-H26-H29 [42-48]. For HSV-2, 18 precursors have been detected [41-44, 46-53], many of which are positional homologs to HSV-1 but share limited sequence similarity. Most HSV-1 miRNAs are encoded within or near the LAT region and are antisense to the important HSV-1 genes such as ICP0 and ICP34.5 (Figure 2.). All miRNAs located in repetitive regions can be found in two copies in the genome and are among the most abundantly detected miRNAs, suggesting their importance.

Interestingly, two antisense miRNAs located upstream of the LAT region, miR-H1 and miR-H6, are miRNAs expressed at the highest levels in productive infection, miR-H1 is transcribed in the same direction as the LAT and miR-H6 is expressed at the same locus, but transcribed from the opposite strands [42]. A number of miRNAs miR-H2, -H3, -H4, -H5, -H7 and -H8, that are detected more abundantly in latent than in productive HSV-1 infection, arise from the 8.3 kb LAT transcript [44].

Peculiarly, three miRNAs, miR-H11, miR-H12 and miR-H13, arise from the palindrome sequence of oriL and oriS (i.e. miR-H11 can arise from the transcription in both directions), and miR-H12 and -H13, expressed in the opposite direction from the palindrome. The function of these miRNAs is not known but might play some role in priming DNA synthesis [42]. Some less abundant miRNAs found in both phases of infection are miR-H15, located at the 5' end of LAT close to miR-H1/H6 locus, followed by miR-H14 and miR-H27 located within the ICP0 transcript, in the same locus but in the opposite direction of miR-H2 and miR-H7, respectively. Located in short repetitive region are miR-H17, within the ICP4 transcript, and miR-H18. Others are encoded within the unique long region (miR-H28 and miR-H29, miR-H16, miR-H26) [42, 46-48].

HSV-2 shares 9 precursors representing sequence and/or positional homologs, with a high number of identical nucleotides in the seed sequence between HSV-1 and HSV-2 homologous miRNAs which also suggests conserved targets [42, 51, 54]. Although sequence and/or positional homologs can be found for most of the abundantly expressed HSV-1 miRNAs, HSV-2 does not encode a homolog of HSV-1 miR-H1, which could represent one of the molecular determinants of biological differences between two viruses.

All described miRNAs can be found in the productive phase of the infection, while only a number of miRNAs have been detected reproducibly in the latent phase such as miR-H2-miR-H8 mentioned above [42-44]. Notably, several other miRNAs were found accumulated during reactivation in mouse ganglia and include miR-H8-5p, -H15, -H17, -H18, -H26, and -H27, which may represent one of the mechanisms of regulation during reactivation [55]. The role of vast majority of miRNAs in the viral replication cycle is still unknown; only a few viral targets have been elucidated up to date.

1.3.1. HSV-1 miRNAs targeting viral transcripts

Assigning the exact function of miRNAs can be very challenging. Particularly, bearing in mind that average miRNA-target interaction produces up to a two-fold decrease in protein levels; thus, depletion of miRNAs may not have an easily observable phenotype. Furthermore, the functions that have been revealed point to the roles of HSV-1 miRNAs in the regulation of latency. However, confirming this experimentally remains challenging because latency models cannot replace all

components of latency in humans (including immunity and species specific responses and functions).

A few HSV-1 miRNAs located within the LAT region encode miRNAs antisense to important viral genes which indicates their function in targeting these genes, and are thought to play an important role in inhibiting proteins that are important for maintaining latency. For example, miR-H2, -H7, and -H8 are encoded antisense to the gene encoding ICP0; but only the miR-H2 function was associated with the ICP0 regulation. It has been shown that miR-H2 can repress ICP0 expression in co-transfection assays, and using photoactivatable ribonucleoside-enhanced crosslinking and immunoprecipitation (PAR-CLIP) assays, it has been associated with ICP0 [56]. However, a study by Pan et al. using a miR-H2-deficient mutant virus suggested that there was no significant increase in ICP0 in productively infected cells or mice infected with HSV-1 deficient for the -H2 expression compared to the wt strain [57]. Conversely, Jiang et al. have explored similar mutations and have observed somewhat increased expression of ICP0 and a significant increase in neurovirulence in the more virulent HSV-1 strain McKrae [58]. Homologous HSV-2 miR-H2 mutant virus also did not show a significant difference in the expression of ICP0 during the lytic or recurrent phase in the guinea pig model [59]. In the end, differences between studies can be attributed to the use of different models with modest impact, indicating their role as reinforcers of the specific phenotype.

In the same fashion, miR-H3 and -H4 are encoded antisense to ICP34.5; however, only miR-H4 has been shown to decrease ICP34.5 levels using transfection assays [60]. On the other hand, HSV-2 miR-H3 and -H4 mutants did not affect the virus lytic infection and its reactivation in guinea pigs [59].

For other HSV-1 miRNAs, the target is not so intuitive, and seed sequence complementarity needs to be investigated to determine possible targets; for example, it has been shown that miR-H6 seed sequence is complementary to the ICP4 and thus can repress ICP4 expression in co-transfection assays [50]. It has also been shown that the HSV-1 replicated less efficiently in the cells transfected with miR-H6 prior to the infection and that the expression of ICP4 was significantly affected in human cornea epithelial cells [61]. Furthermore, Barrozo et al. have investigated the virus having a deletion of the entire miRH1/H6 locus and have observed a reduction in reactivation of HSV-1 in mouse and rabbit models [62]. However, a doctoral thesis by Pribanić Matešić has shown that the expression of HSV-1 miR-H1 or miR-H6 is not

required for the efficient HSV-1 strain KOS replication in cultured cells. On the other hand, since miR-H1 and miR-H6 are encoded at the same locus but are antisense to each other, it is theoretically possible that they may regulate the expression of each other. Important to mention are other HSV-1 miRNA pairs encoded antisense to one another with potential for mutual regulation (miR-H11, which is transcribed in both directions, miR-H2 and -H14, miR-H7 and -H27, miR-H12, and -H13) (Figure 2).

1.3.2. HSV-1 miRNAs targeting host transcripts

Numerous studies have shown that, in addition to targeting viral transcripts, HSV-1 miRNAs target many host transcripts, the relevance of which has not been evaluated in relevant *in vivo* models. These host targets control various important pathways including apoptosis, cell cycle control, cell-signaling and immunity (summarized in Figure 6) [63].

HSV-1 miR-H1-5p and HSV-2 miR-6-5p, two miRNAs that share the identical seed sequence, in transient transfection experiments have been shown to downregulate alpha-thalassemia/mental retardation syndrome X-linked (ATRX), an important transcriptional regulator, a component of host cell defense mechanisms involved in silencing of the virus genome, however, experimental results also indicated other mechanisms, in addition to mentioned miRNAs that contribute to the regulation of ATRX [64].

The functions of miR-H1 have been further analyzed and its potential to regulate a number of host genes has been shown in cells transfected with miR-H1 mimics. Potential targets included Leukemia Inhibitory Factor Receptor Alpha (LIFR), Transforming Growth Factor Beta Receptor 1 (TGFB1), Autophagy Related 16 like 1 (ATG16L1), Sortilin 1 (SORT1), ubiquitin protein ligase E3 component n-recognin (Ubr1) and others [61, 65, 66].

Besides ATRX, other targets involved in transcriptional regulation include cellular transcriptional repressor Kelch-like 24 (KLHL24), which has been shown as a target for miR-H27 [47], another HSV-1 miRNA expressed at very low levels during the productive infection, but not detected in latency.

The effects of HSV-1 miR-H4-5p and HSV-2 miR-H4-5p, which are abundantly expressed in latency, have been shown in reporter assays on cell cycle progression; they have been found to target cyclin-dependent kinase inhibitor 2A (CDKN2A), a

negative regulator of cell-cycle and PI3K/Akt pathway [60, 67], indicating their role in the latent phase of the infection.

More challenging to investigate were the functions of miRNAs potentially involved in the regulation of different aspects of immunity. For example, using functional screen and transient transfection assays, HSV-1 miR-H8 has been found regulating the function of natural killer (NK) cells, it decreased the expression of several ligands for NK-activating receptors by targeting phosphatidylinositol glycan anchor biosynthesis class T (PIGT), a member of the protein complex involved in the glycosylphosphatidylinositol (GPI) anchoring pathway, essential for the presentation of proteins on the cell surface [45]. Furthermore, in the context of latent infection and reactivation, deletion of miR-H8 has been found to have no apparent role in establishing latency or reactivation in differentiated human neurons (Lund human mesencephalic cells - LUHMES) and mouse and rabbit models [68].

Another proposed target for miR-H2-3p besides viral transcript ICP0 was Asp-Glu-Ala-Asp (DEAD)-box helicase 41 (DDX41), a cytosolic DNA sensor of the DNA-sensing pathway, showed in miR-H2 mimic transfection experiment, but not in relevant models of HSV-1 infection [69].

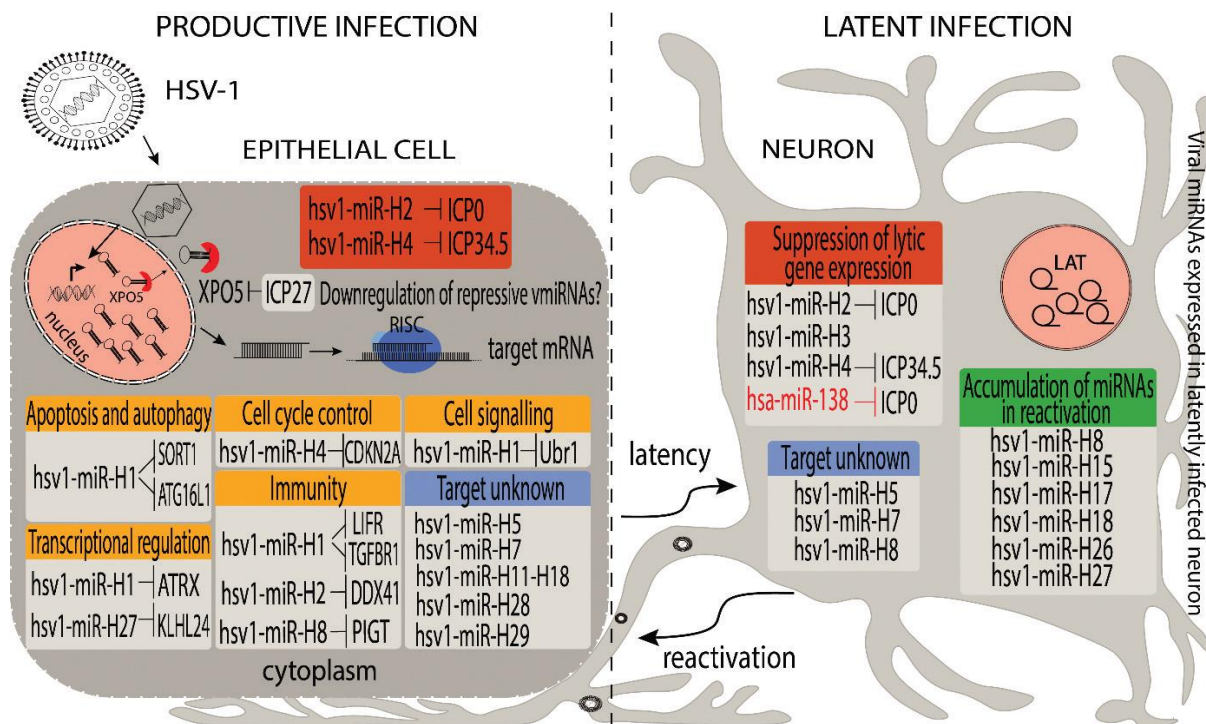


Figure 6: Schematic representation of reported HSV-1 miRNAs and their role in different phases of the infection. During the productive infection, a number of HSV-1 miRNAs have been shown to interfere with different host genes involved in apoptosis, cell cycle control, cell signaling, transcriptional regulation and immunity, depicted in orange titled boxes. During both stages of infection miR-H2 and -H4 regulate important viral proteins, ICP0 and ICP34.5, respectively, as depicted in the brown box. Viral protein ICP27 inhibits the nuclear export of pre-miRNAs late in infection. In latent phase, host miRNA, miR-138 (marked with red letters) regulates ICP0, alongside miR-H2 and -H4 (brown-titled box). Several miRNAs were found to be accumulated during reactivation (green-titled box). miRNAs detected in both phases, whose targets are unknown, are depicted in blue-titled boxes. LAT – latency associated transcript, ICP0 – infected cell polypeptide 0, ICP34.5 – infected cell polypeptide 34.5, ICP27 – infected cell polypeptide 27, XPO5 – Exportin-5, RISC – RNA induced silencing complex, LIFR – Leukemia Inhibitory Factor Receptor Alpha, TGFBR1 – Transforming Growth Factor Beta Receptor 1, ATG16L1 – Autophagy Related 16 like 1, SORT1 – Sortilin 1, CDKN2A – cyclin-dependent kinase inhibitor 2A, Ubr1 – ubiquitin-protein ligase E3 component n-recognin 1, ATRX - alpha-thalassemia/mental retardation syndrome X-linked, KLHL24 – Kelch like family member 24, DDX41 – (DEAD)-box Helicase 41, PIGT - phosphatidylinositol glycan anchor biosynthesis class T (reviewed in [63]).

1.4. HSV-1 deregulates host miRNAs

In addition to viral miRNAs targeting viral or host transcripts, it has been shown in many studies that HSV-1 has a profound impact on the host microRNA expression profile, which indicates their importance during viral infection. Although they were previously thought to play an inhibitory role in viral replication because of the

mechanism of the action to act as mRNA inhibitors, it has been shown that viruses can exploit miRNAs to enhance viral replication and persistence of the virus [70].

A deregulation of host miRNAs could represent one aspect of the host cell's innate immune responses triggered by a viral infection in inhibiting viral replication [71, 72]. On the other hand, changes in cellular miRNA expression may be specifically induced by a certain virus in order to create a more favorable environment for viral replication [73]. For example, viruses have been shown to manipulate the host cell through host miRNAs by regulating antiviral immunity, increasing the inflammatory response, and inhibiting apoptosis of the infected host cell. Additionally, increased expression of otherwise regulated levels of host miRNAs during viral infection has been linked to the development of various diseases such as Alzheimer's and Behçet's disease, encephalitis, and the angiogenesis leading to stromal keratitis.

In addition to deregulating host miRNAs, some viruses have developed miRNAs that share the target specificity of specific host miRNAs to promote their life cycle; for example, KSHV and avian Marek's disease virus 1 encode miRNAs that mimic host miRNA miR-155, miRNA frequently found upregulated in lymphomas and crucial for B-cell development [74].

Extent of such deregulation of host miRNAs is not completely understood, and, for most viruses, the exact molecular mechanism remains unknown.

miRNAs targeting host and viral transcripts that have been found deregulated in HSV-1 infection can roughly be grouped into different categories with functions in (a) regulation of apoptosis, (b) antiviral immunity, (c) inhibition of viral replication (Figure 7) [75-87].

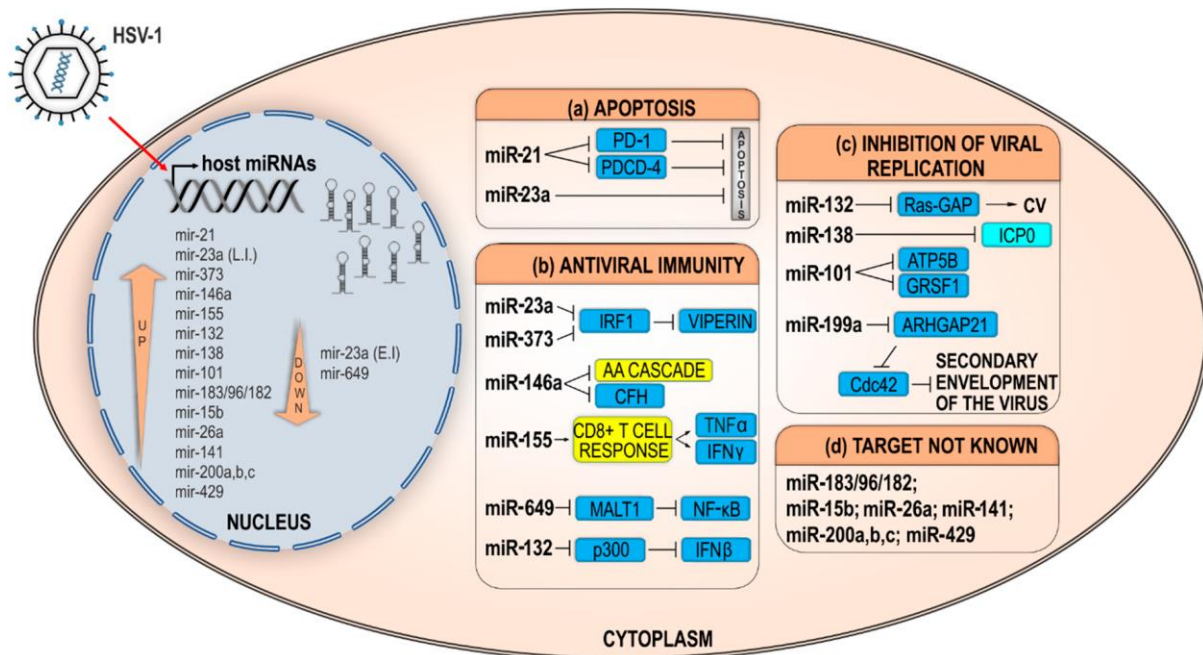


Figure 7: A schematic representation of a number of deregulated host miRNAs in HSV-1 infection. Many miRNAs have been found to be upregulated (arrow up within the nucleus) or downregulated (arrow down in the nucleus). These miRNAs regulate different host (blue boxes) or viral transcripts (light blue box) with functions in (a) regulation of apoptosis, (b) antiviral immunity, (c) inhibition of viral replication, and (d) miRNAs with targets not known depicted in separate boxes. During early infection (EI), miR-23a is downregulated, while later in the infection (LI) miR-23a is upregulated. The exact targets of miR-155 and miR-146a have not been identified; however, they regulate host immune response (yellow boxes) by regulating T-cell differentiation and the arachidonic acid cascade (AA cascade) pathway, respectively. Upregulated miR-132 activates Ras by removing Ras-GAP, leading to corneal neovascularization (CV). Neuron-specific miR-138 regulates virus protein ICP0. Arrows indicate positive regulation. PD-1: Programmed cell death protein 1; PDCD-4: Programmed cell death protein 4; IRF1: Interferon regulatory factor 1; CFH: Complement factor H; TNFα: Tumor necrosis factor alpha; IFNβ/γ: Interferon beta/gamma; MALT1: Mucosa-associated lymphoid tissue lymphoma translocation gene 1; NF-κB: Nuclear factor kappa-light-chain-enhancer of activated B cells; Ras-GAP: Ras-glyceraldehyde-3-phosphate; ICP0: Infected cell polypeptide 0; ATP5B: ATP synthase subunit beta; GRSF1: G-rich sequence factor 1; ARHGAP21: Rho GTPase-Activating Protein 21; Cdc42: Cell division control protein 42 homolog (Reviewed in [88])

1.4.1. Host miRNAs with functions in regulation of apoptosis

Few studies have shown host miRNAs to indirectly control apoptosis by targeting different genes involved in cell survival, and many such miRNAs are deregulated in cancer.

For example, highly abundant and conserved miR-21 has been linked to Behçet disease (BD) [89], a multisystem inflammatory disease. Viral infection, including HSV-

1 which was detected in patients with BD, has long been hypothesized to be one of the main factors leading to BD [90]. The study aimed to investigate differences in miRNA expression between mice infected with HSV-1 and uninfected in a model of BD found that miR-21 was upregulated in lymph nodes of BD mice. Moreover, miR-21 was also upregulated in peripheral blood mononuclear cells (PMBC) of human patients with BD. To detect target molecules for this miRNA, antagomir of miR-21 was used, and the increase in expression of potential target genes was monitored. Discovered upregulated genes were PDCD4 (Programmed cell death 4) and PD1 (Programmed cell death 1), which are known to be involved in the regulation of apoptosis. However, the relevance for HSV-1 has not been revealed [89].

Another example is miR-23a, cellular miRNA which is thought to modulate cell proliferation, survival and apoptosis during the initiation and progression of human cancers. Researchers have shown that miR-23a could regulate apoptosis in HSV-1 infected cells, assuming that miR-23a facilitates virus replication by downregulating interferon regulatory factor 1 (IRF1) to suppress viperin expression and apoptosis [75].

1.4.2. Host miRNAs with functions in antiviral immunity

In addition to regulation of apoptosis, miR-23a downregulation of IRF1 results in lower levels of radical S-adenosyl methionine domain-containing 2 (RSAD2)/viperin, suggesting its role in limiting virus infections, including HSV-1, and role in innate antiviral immunity. Viperin creates conditions that are not conducive to virus replication by inhibiting progenic viral proteins. It also plays an important role in the production of type I interferon, which is extremely important in nonspecific antiviral immunity. In addition to IRF1, increased viperin levels may also occur after interferon stimulation [91]. However, this complex interaction is not yet fully understood, and the mechanisms by which HSV-1 induces miR-23a expression are not clear [75].

In addition to miR-23a, Xie et al have shown that miR-373 was significantly upregulated in HSV-1 infected HeLa cells and patients with herpetic gingivostomatitis and that it facilitates HSV-1 replication *in vitro* by targeting IRF1 and inhibiting type I interferon pathway. Expression of ISGs was affected by miR-373 expression. Real-time PCR analyses indicated that miR-373 expression almost completely blocked the expression of ISGs, such as double-stranded RNA-dependent protein kinase (PKR), 2', 5'- oligoadenylate synthetases (OAS), and myxovirus protein A (MxA). In contrast,

miR-373 inhibition significantly increased ISG expression. These data suggest that miR-373 negatively regulates Type I IFN expression in HSV-1 infected cells. However, how the virus induces the expression of miR-373 still remains unknown and further investigation is necessary [85].

miR-146a was first identified as an immune regulator responsive to induction by IL-1 β and other proinflammatory cytokines in human monocytes. Infection of human neuronal-glial (HNG) cells in primary co-culture with HSV-1 induces irregular hypertrophy of HNG cell bodies, atrophy of neurite processes and upregulation of miR-146a. In addition, two specific members of the arachidonic acid (AA) cascade - cytosolic phospholipase A2 (cPLA₂) and the inducible prostaglandin synthase cyclooxygenase-2 (COX-2), as well as the neuroinflammatory cytokine IL-1 β are also upregulated, and, on the other hand, a known miR-146a target in the brain and an important repressor of the complement signaling cascade, complement factor H (CFH) is downregulated [80]. Although a link between HSV-1 infection and Alzheimer's disease was proposed 30 years ago, the molecular mechanisms of this association are not yet fully understood. Hill et al. suggest a role for HSV-1-induced miR-146a in the evasion of HSV-1 from the complement system and the activation of key elements of the arachidonic acid cascade known to contribute to Alzheimer-type neuropathological change [80].

HSV-1 is the most common cause of sporadic viral encephalitis, which can be lethal or result in severe neurological defects [2]. There are several possible causes of encephalitis, such as trauma, neoplasm and vascular changes, but inflammatory changes of the brain as a result of a viral infection should also be considered. In a study by Bhela et al, miR-155 has been connected with the etiology of herpes simplex encephalitis [82]. They showed that miR-155 knockout (KO) mice show heightened susceptibility to HSV ocular infection and have elevated viral titers in the brain. The infection leads to diminished CD8⁺ T cells response, allowing the virus to spread within the nervous system, subsequently causing encephalitis. Also, HSV-1 reactivated more abundantly from latency when miR-155 was not present in mice, resulting in the development of zosteriform lesions due to viral dissemination into the nervous system [82]. In addition to lower CD8⁺ T cell response, the difference in NK cell homeostasis and levels of IFN induced, which have both been implicated as providing protection in herpetic encephalitis, should be further analyzed. Currently, it is not yet clear how miR-155 influences the CD8⁺ T cell response, but there are several possibilities. It is

possible that miR-155 plays a direct role during CD8⁺ T cell differentiation, and in the absence of miR-155 they survive less well and produce less IFN γ and TNF α . The other possibility is that in the absence of miR-155, suppressor of cytokine signaling 1 (SOCS1) is upregulated and in turns it inhibits cytokine signaling necessary for complete host immunological response [82].

In addition, Majer et al analyzed global changes in miRNA expression during HSV-1 encephalitis (HSVE) using next-generation sequencing (NGS) and identified several immune-related miRNAs that were induced in HSVE-affected brain tissue, including miR-155 that was previously shown to play a role in the host response to HSV-1 infection by preventing the replication and dissemination of HSV-1 within the brain [77].

Next, study by Zhang et al. first reported the relationship between miR-649 and targeting of mucosa-associated lymphoid tissue lymphoma translocation gene 1 (MALT) important for innate and adaptive immunity. Authors showed that miR-649 facilitates HSV-1 replication through direct targeting of 3'-UTR of MALT1 in both, HeLa and Hep-2 cells. Additional experiments also confirmed that miR-649 facilitates HSV-1 replication through MALT1 in TGs. MALT1 is an essential component of nuclear factor κ B (NF- κ B) signaling initiated by T- and B-cell receptors (TCR and BCR), as well as activating natural killer (NK) cell receptors. This research showed that NF- κ B, an important signaling molecule downstream of MALT1, plays an essential role in MALT1-regulated HSV-1 replication [84]; however, in contrast to many other host miRNAs found upregulated, miR-649 was found downregulated, and further studies are necessary to confirm the significance of this mechanism in virus-host interaction.

Another example is miR-132, which was shown to be induced in HSV-1 infection of monocytes, and that potentially targets p300, a protein that associates with CREB and is an important mediator of antiviral immunity. By decreasing the levels of p300, the expression of IFN- β , ISG15, IL-1 β and IL6 is impaired, resulting in the suppression of antiviral immunity [76].

Recently, miR-24 was found upregulated in HSV-1 infection, implicating its role in the evasion of antiviral immune response. It has been known that during infection HSV-1 activates STING, an important protein required for signaling by PRRs, which may inhibit virus replication through both IFN-dependent and independent pathways. In study by Sharma et al., upregulation of miR-24 inhibited STING synthesis in HSV-1 infection by binding to its site in the 3' UTR of STING mRNA. Inhibition of STING

synthesis leads to less IFN induction and consequent enhancement of virus replication [86].

1.4.3. Host miRNAs with functions in inhibition of viral replication

Similarly to the above-mentioned study by Lagos et al, which showed upregulation of miR-132 in KSHV infection [76], Mulik et al have shown that miR-132 expression was upregulated 10- to 20-fold after ocular infection with HSV-1 [81]. HSV-1 is the cause of severe inflammation of the cornea, stromal keratitis, which occurs in the area without blood vessels. HSV-1 infection causes upregulation of vascular endothelial growth factor (VEGF-A) leading to increased expression levels of miR-132. The authors propose a model where several uninfected cell types in response to proinflammatory cytokines, such as IL-6 and IL-17A, produced by innate immune cells in initial stages and later on by CD4 Th17T cells in the cornea after HSV-1 infection increase levels of VEGF-A. VEGF-A, through VEGFR2 receptors on the blood vessel endothelial cells, upregulates miR-132 expression via CREB. miR-132 removes Ras-GAP, leading to activation of Ras and corneal neovascularization which is beneficial for HSV-1 infection. Mice that were knockouts for IL-17A receptor had lower levels of miR-132 produced compared to wt mice, which supports the importance of IL-17A in the regulation of miR-132 expression [81].

Zheng et al. have found that miR-101 is highly induced in the early stages of HSV-1 infection, and it is used by the host cells to defend against HSV-1 infection. The authors have shown that ectopic expression of miR-101 could significantly suppress HSV-1 replication and that blocking endogenous miR-101 increases viral progeny [79]. Using a bioinformatic approach, the authors found no complementary sequences of miR-101 in HSV-1 transcripts, but they identified host transcript for ATP synthase subunit beta (ATP5B) to have putative miR-101 binding site within its 3'-UTR. ATP5B is a subunit of F1 ATP synthases constitutively expressed in the inner mitochondrial membrane. Although ATP5B has not yet been reported to be involved in HSV-1 replication, it is speculated that ATP and FoF1 ATP synthase are crucial for supplying the energy required for the virus to complete its replication cycle. Infection with HSV-1 leads to an increase in the levels of miR-101 in parallel to a decrease in ATP5B expression and this interaction has an antiviral effect on HSV-1 replication; however,

the mechanism of miR-101 upregulation and its suppression of HSV-1 infection remained unknown.

Furthermore, Wang et al. have shown the molecular mechanisms underlying this interaction. They identified the HSV-1 immediate early gene infected-cell polypeptide 4 (ICP4) to directly bind to the miR-101-2 promoter on chromosome 9, and induce the expression of miR-101. To elucidate the mechanism of miR-101 regulation of HSV-1 replication, the authors, similarly to their previous study [79], used bioinformatics to identify the target genes of miR-101 and RNA-binding protein G-rich sequence factor (GRSF1) was identified as a novel target of miR-101. The proposed molecular mechanism is that the immediate early viral protein ICP4 directly binds to and activates the promoter of miR-101. Consequently, miR-101 represses the expression of GRSF1 leading to the reduction of p40 mRNA translation and subsequently to the inhibition of HSV-1 replication. In that way, the host cell could maintain a permissive environment for viral replication by preventing lytic cell death [83].

Kobayashi et al found miR-199a to impair the secondary envelopment of HSV-1 by suppressing ARHGAP21, a Golgi-localized GTPase-activating protein for Cdc42 [92]. Expression of miR-199a did not affect the expression levels of immediate early, early or late HSV-1 genes suggesting that this miRNA inhibits the later stages of viral replication such as capsid assembly, nuclear egress, and secondary envelopment and exocytosis of infective particles. However, several pieces of evidence are still lacking to explain the impact of miR-199a on HSV-1 infection completely. There are several possibilities: disturbance of secondary envelopment may be due to low efficiency of trans-Golgi cisternae during HSV-1 infection, transport of some HSV-1 protein essential for virion maturation or disturbance of some unknown mechanism important for HSV-1 secondary envelopment. Precise mechanism remains unknown, and further investigation is necessary to elucidate how and if the virus induces miR-199a.

1.4.4. Other host miRNAs with unknown targets

A number of host miRNAs have been shown to be upregulated in massive screens in the context of HSV-1; however, for many miRNAs found deregulated targets were unknown.

For example, a recent study by Kim et al. in which the authors analyzed the miRNA expression in tears of patients with herpes epithelial keratitis and found that among many, miR-182 and miR-183 were upregulated, supporting the idea that the activation of miR-183/96/182 represents the innate antiviral response to HSV-1 infection [87].

In a previously mentioned study by Majer et al, they also observed the upregulation of several miRNAs belonging to the related and often co-transcribed miRNA-200 family (miR-200a,b,c/miR-141/miR-429) and miRNA-182 cluster (miR-182/miR-183). Further understanding of the role of these miRNAs during HSV-1 infection is still required for a better understanding of the mechanism of upregulation [77].

Many previous studies were limited to the analysis on just one cell line where miRNAs were detected up or down-regulated during productive infection, but a few studies have gone further and tried to explain the mechanism of that deregulation. For example, Lutz et al. have described the mechanism of upregulation of a subset of miRNAs transcribed as a single pri-miRNA transcript, miR-183/96/182, which depends on the expression of viral IE protein ICP0 which is responsible for directing host protein ZEB for ubiquitin-dependent proteasomal degradation and in that way de-represses the miR-183/96/182 cluster. However, in the end, targets of the co-expressed miR-183, miR-96, and miR-182 are unknown [78].

1.4.5. Relationship between HSV-1 latency and miR-138

Some deregulated miRNAs have been found to impact the expression of viral transcripts directly. For example, miR-138, a neuronal-enriched miRNA, decreases the expression of ICP0, reduces the expression of the lytic gene and promotes host survival and viral latency in mice [77, 93].

miR-138 is a neuron-specific miRNA abundantly expressed in the brain and neuroblastoma cell lines. Because HSV-1 latent infection occurs in neurons and miR-138 has been found highly represented in trigeminal ganglia of latently infected mice [50], Pan et al. tested the possibility that miR-138 might repress lytic gene expression. Indeed, authors computationally identified two miR-138 binding sites in the 3'-UTR of viral infected cell protein 0 (ICP0) mRNA and showed that miR-138 represses its expression in both transfected and HSV-1-infected cells. Mutations in miR-138 target sites result in increased expression of ICP0 and other lytic genes and increase host

morbidity and mortality. Given that repression of lytic genes is a hallmark of HSV-1 latency, miR-138 could be regarded as a neuronal host factor contributing to establishing and maintaining latency. Moreover, there is a possibility that miR-138 may act synergistically with virus-encoded miRNAs, such as miR-H2, that targets ICP0 [93].

Additionally, miR-138 has been found to decrease the expression of host genes important for HSV-1 replication to create a favorable environment for latent infection. Transcription factors Oct-1 and FoxC1 have been downregulated, which is important for HSV-1 replication in neuronal cells. Role for Oct-1 has been shown in initiation of HSV transcription. On the other hand, FoxC1 was not known to affect HSV-1; however, its overexpression promoted HSV-1 replication in murine neurons and ganglia [94].

These results implicate that HSV-1 has evolved to utilize miR-138 to establish latency and represents the ability of a virus to spread throughout the population without killing the host cell.

1.5. Potential targets of host miR-183/96/182

The study by Lutz et al., mentioned above, showed that HSV-1 selectively and reproducibly induces the transcription of three cellular miRNAs: miRNA-183, miRNA-96, and miRNA-182, during productive infection in primary fibroblasts and neurons [78]. Increased expression of these miRNAs has also been observed in HCMV [95] and EBV infections [96]. These clustered miRNAs are located on human chromosome 7, transcribed as a single pri-miRNA transcript, and further processed as separate miRNA molecules. However, their function and impact on HSV-1 infection are not fully known.

Therefore, to determine the biological function of these miRNAs, we performed bioinformatics analysis of their gene targets using TargetScan 7.1 [97] and miRDB [98]. Interestingly, three members from the Forkhead Box O (FoxO) subfamily were high on the list of potential targets: FoxO1, FoxO3 and FoxO4, and will be described below.

1.5.1. FoxO transcriptional factors

FoxO proteins are a subgroup of the Forkhead transcription factor (TF) family. The term forkhead comes from the fork head (fkh) gene, first identified in the *Drosophila melanogaster*, which has a fork-headed appearance if that gene is mutated

[99]. The characteristics of all Forkhead TFs is a well-preserved DNA-binding domain, the so-called forkhead box, which, by binding of DNA of interest, determines the activity of a number of different genes involved in important cellular processes such as differentiation, proliferation, cell growth, and longevity. The family has more than 100 members, classified from A to S, based on the similarity of the forkhead box sequence. Members of the "O" class have been evolutionarily preserved from *C. elegans* to mammals and share similarities in structure and function. Mammals have four FoxO genes: FoxO1, FoxO3, FoxO4, and FoxO6, which play an important biological role in cell signaling and life cycle as promoters of cell survival and longevity [100, 101]. Also, they play a role in the development and differentiation of immune cells, and in pro-inflammatory cytokine secretion [102, 103], and because of that role, their function in numerous infections and disorders is interesting to investigate.

1.5.2. The role of TF FoxO in the antiviral response of the cell

In recent years, research has shown that FoxO proteins play an important role in the innate antiviral response of the cell [104, 105]. Investigating the effect of poly(I:C), a mimic of foreign double-stranded RNA (dsRNA) present in certain viral infections, which binds to toll-like receptors 3 (TLR3) and stimulates an antiviral response of the cell, on the regulation of the antiviral response through the FoxO proteins, it was found that FoxO1 and FoxO3 act as negative regulators of antiviral defense by reducing interferon beta (IFN- β) production. It has been shown that, in response to infectious stimuli, FoxO1 and FoxO3 inhibit transcription or mediate the degradation of IRF3 and IRF7 proteins by reducing IFN- β expression. In contrast, large amounts of IFN- β inhibit the action of FoxO proteins by stimulating the transcription and stabilization of IRF3/IRF7 proteins to stimulate self-production [104, 105]. Given the importance of FoxO proteins in regulating the antiviral response, it is logical to assume that they are also a target for manipulation of the HSV-1 virus.

In EBV, KSHV, and HCMV infection, individual FoxO protein roles have been shown. For example, it has been shown that in EBV-positive advanced nasopharyngeal carcinoma cells, which exhibit type II latency, EBV LMP1 modulates the PI3K/AKT/FoxO3 pathway, resulting in the accumulation of FoxO3 phosphorylation. This inactivation of FoxO3 led to the induction of miR-21, which in turn downregulated programmed cell death 4 (PDCD4) and Fas ligand and reduced

apoptosis [106]. In addition, Liu et al. showed that in EBV-associated gastric cancer cells that showed type I/II latency, the FoxO1, FoxO3, and FoxO4 protein levels were significantly lower when compared to the control cells. Interestingly, FoxO1 mRNA was downregulated, but not FoxO3 or FoxO4 mRNAs, which might suggest diverse regulatory mechanisms by various EBV latent genes [107]. Similarly, FoxO1 has been shown to sufficiently suppress Kaposi's sarcoma-associated herpesvirus (KSHV) lytic replication and maintain latency by controlling the levels of reactive oxygen species (ROS), since the disruption of FoxO1 could trigger KSHV reactivation and induce lytic infection by increasing the cellular ROS level [108]. On the other hand, a recent study investigating human cytomegalovirus (HCMV) has shown that FoxO1 and FoxO3 positively regulate virus lytic gene expression by activating alternative major immediate-early gene promoters and promoting IE re-expression and virus reactivation [109]. To elucidate the roles of the FoxO protein family in HSV-1 infection, more research, and an adequate in vitro latency model, is needed to understand their roles in HSV-1 latency.

2. RESEARCH AIMS

Two general aims of this study were, first, to investigate miRNAs, regulatory molecules of the host in HSV-1 infection, and second, miRNAs encoded by HSV-1. In order to present these two aims - analysis of host miRNAs and HSV-1 in more detail, the research is divided into two parts, and each general aim has several specific aims.

In Part 1, we aim to show that only a subset of miRNAs is upregulated reproducibly in multiple cells infected with HSV-1 and to show their biological relevance in infection. For that reason, we hypothesize that, first, a set of specific host miRNAs is deregulated upon HSV-1 infection, and second, deregulated host miRNAs confer a biological relevance for the virus infection.

Based on the set hypotheses, we set the specific aims of the study:

- a) determine deregulated host miRNAs during productive HSV-1 infection
- b) determine targets of deregulated host miRNA
- c) determine the function of deregulated host miRNA target genes in productive virus infection

In Part 2, we outline how studies on HSV-1 miRNA led to numerous discrepancies and inconsistencies that hinder the basic understanding of HSV-1 biology. Therefore, we hypothesize that, first, some reported HSV-1 miRNAs do not satisfy stringent criteria for miRNAs; second, that the exact sequence of HSV-1 miRNA can be determined if a comprehensive analysis is applied; third, that HSV-1 miRNAs depend on the canonical miRNA biogenesis pathway, and fourth, that difference in miRNA sequence might be related to the difference in pathogenesis and virulence of different strains.

Based on the set hypotheses, we set the specific aims of the study:

- a) to develop an algorithm and a scoring system for HSV-1 miRNAs to evaluate all previously and newly discovered HSV-1 miRNAs.
- b) to determine the exact sequence of HSV-1 miRNAs by comparing different data sets
- c) to determine the miRNA sequence conservation of HSV-1 miRNAs between different clinical isolates and common laboratory strains

- d) to determine the pattern of HSV-1 miRNAs expressed in the relevant latently infected human tissues
- e) to determine the dependence of HSV-1 miRNA on the canonical pathway
- f) to determine the frequency of isomiRs

To complete specified aims, we applied techniques such as massively parallel sequencing of small RNAs derived from cells infected with HSV-1 and their bioinformatics analysis, formed criteria for viral miRNAs (vmiRNAs) selection, cloning, performed reporter assays, etc.

3. MATERIALS AND METHODS

3.1. Materials

3.1.1. Cell lines

The following cells were used in this research:

- Human Embryonic Kidney cells containing the SV40 large T-antigen (HEK-293T, ATCC CRL-3216).
- Epithelial cells of the African green monkey kidney (Vero, ATCC CCL-81).
- Human neuroblastoma cells (SH-SY5Y, ATCC CRL-2266).
- Human retinal pigment epithelial cells immortalized with hTERT (hTERT RPE-1, ATCC CRL-4000)
- Primary human foreskin fibroblast cells (HFF), kindly provided by Professor Stipan Jonjić, Center for Proteomics, Faculty of Medicine, University of Rijeka.
- Human Lung Fibroblast diploid cell lines derived from embryonic human lung (WI-38, ATCC CCL-75)
- Bone Marrow-Derived Macrophages (BMDM), kindly provided by Professor Ivana Munitić, Department of Biotechnology, University of Rijeka, Croatia.
- Mouse Embryonic Fibroblast (MEF), kindly provided by Professor Ivana Munitić, Department of Biotechnology, University of Rijeka, Croatia.
- SH-SY5Y cells with the FOXO 1 / FOXO3 / FOXO4 gene ^{-/-} were created by CRISPR/Cas9 tool via lentiviral delivery.

3.1.2. Cell culture media

All media that were used for this research are based on the commercially available DMEM (PAN-Biotech), MEM (Capricorn) or RPMI-1640 (Lonza), and to complete media, the following supplements listed in Table 1 were added.

Table 1: Complete media used in the cell culture

Cells maintained in complete media	Base medium/type	Supplements	Concentration
- HEK-293	Dulbecco's	- Fetal bovine serum (PAN-Biotech)	10%
- Vero	Modified Eagle	- L-glutamine (Capricorn)	2 mM
- HFF	Medium	- Penicillin/Streptomycin (Capricorn)	100 µg/µl
- MEF	(DMEM)	- Sodium Pyruvate (Capricorn)	1 mM
- WI-38			
- SH-SY5Y	Minimum	- Fetal bovine serum (PAN-Biotech)	15%
- SH-SY5Y	Essential	- L-glutamine (Capricorn)	2 mM
FoxO KO	Medium (MEM) with Earle's Salts	- Penicillin/Streptomycin (Capricorn)	100 µg/µl
		- Sodium Pyruvate (Capricorn)	0,5 mM
- RPE-1	Minimum	- Fetal bovine serum (PAN-Biotech)	10%
	Essential	- L-glutamine (Capricorn)	2 mM
	Medium (MEM) with Earle's Salts	- Penicillin/Streptomycin (Capricorn)	2 mM
		- Sodium Pyruvate (Capricorn)	0.5 mM
		- 4- (2-hydroxyethyl) -1- piperazineethanesulfonic acid - HEPES (Capricorn)	15 mM
		- Hygromycin B (Invitrogen)	10 µg/ml
- BMDM	RPMI-1640	- Fetal bovine serum (PAN-Biotech)	10%
		- L-glutamine (Capricorn)	2 mM
		- Penicillin/Streptomycin (Capricorn)	100 µg/µl
		- Sodium Pyruvate (Capricorn)	1 mM
- All	Methylcellulose medium	- Fetal bovine serum (PAN-Biotech)	3%
		- Penicillin/Streptomycin (Capricorn)	2 mM
		- Sodium Pyruvate (Capricorn)	1 mM
- All	Freezing medium	- Fetal bovine serum (PAN-Biotech)	90%
		- DMSO (Wvr)	10%

3.1.3. Viruses

- Wild-type HSV-1 laboratory strain KOS (kindly provided by Professor Donald M. Cohen, Harvard Medical School, Boston, USA) was prepared in Vero cells and stored at -80°C.

- Mouse cytomegalovirus (MCMV), strain C3X (MCMV BAC pSM3fr cloned from MCMV Smith strain, ATCC VR-1399; kindly provided by Stipan Jonjić, Faculty of Medicine, University of Rijeka, Croatia) was prepared in MEF cells and infections were performed using centrifugal enhancement as previously described [110].

3.1.4. Reagents – buffers, solutions and kits

3.1.4.1. Buffers for plasmid preparation and gel electrophoresis of nucleic acids

Table 2: Complete buffers used for the nucleic acid handling

Alkaline Lysis Solution I (resuspension buffer)	Tris (pH 8.0) (Carl Roth) EDTA (pH 8.0) (Carl Roth)	50 mM 10 mM
Alkaline Lysis Solution II (lysis buffer)	NaOH (Carl Roth) SDS (Carl Roth)	200 mM 1% (w/v)
Alkaline Lysis Solution III (neutralization buffer)	Potassium acetate (Carl Roth) Glacial acetic acid (adjusted to pH 5.5)	3 M
Tris-acetate (TAE) buffer, 50X	Tris (Carl Roth) Glacial acetic acid EDTA (pH 8.0) (Carl Roth)	2 M 1 M 50 mM
TE buffer	Tris (pH 8.0) (Carl Roth) EDTA (pH 8.0) (Carl Roth) RNase A (Macherey-Nagel)	10 mM 1 mM 10 µg/mL
DNA loading buffer	Bromophenol-blue (MilliporeSigma) Xylene cyanol (MilliporeSigma) Glycerol (Carl Roth)	2.5 g/L 2.5 g/L 1 mL
agarose gel	Agarose (Carl Roth) 1x TAE buffer	0.8-3%

Note: All buffers were made by dissolving the ingredients in double distilled water and were then sterilized by filtration if needed.

3.1.4.2. Buffers for protein isolation, SDS-PAGE and Western Blot

Table 3. Complete buffers used for the protein handling

RIPA (Radioimmunoprecipitation assay) lysis buffer	NaCl (Carl Roth) NP-40 (Thermo Scientific) Na deoxycholate (Carl Roth) SDS (Carl Roth) Tris (pH 8.0) (Carl Roth) Protease inhibitors (Roche)	150 mM 1% (v/v) 0.5% (w/v) 0.1% (w/v) 50 mM
NP-40 lysis buffer	Tris NaCl NP-40 Protease inhibitors (Roche)	0.5 M 5 M 1%
Separating Gel Buffer	Tris (pH 8.8) (Carl Roth)	1.5 M
Stacking Gel Buffer	Tris (pH 6.8) (Carl Roth)	1 M
SDS-PAGE Electrophoresis Running Buffer (10x)	Tris (Carl Roth) Glycine (Carl Roth)	25 mM 192 mM

	SDS (Carl Roth)	0.1% (w/v)
Transfer Buffer (10x)	Tris (Carl Roth)	25 mM
	Glycine (Carl Roth)	192 mM
Transfer buffer (1x)	1x transfer buffer	
	Methanol (Carl Roth)	20%
Tris-Buffered Saline (TBS) 10x (pH 7.6)	Tris (Carl Roth)	10 mM
	NaCl (Carl Roth)	150 mM
TBS-T	1x TBS	
	Tween-20 (Carl Roth)	0.05% (v/v)
Ponceau S	Ponceau S (Carl Roth)	0.1% (w/v)
	Glacial acetic acid (Carl Roth)	1% (v/v)
Milk blocking buffer	Milk powder (Carl Roth)	5% (w/v)
	1x TBS	

Note: All buffers were made by dissolving the ingredients in double distilled water and were then sterilized by filtration if needed.

3.1.4.3. Buffers for immunofluorescence

Table 4. Complete buffers used for immunofluorescence

Formaldehyde solution	Paraformaldehyde (Carl Roth)	4% (w/v)
	NaOH (Carl Roth) 1x PBS	1N
	1x PBS	
Permeabilization buffer	Triton-X-100 (MilliporeSigma)	
	1x PBS	0.5% (v/v)
Bovine serum albumin (BSA) blocking buffer	BSA (Capricorn)	3% (w/v)
	Triton-X-100	0.2% (v/v)
	1x PBS	

3.1.4.4. Plaque assay solutions

Table 5. Complete buffers used for plaque assay

2x methylcellulose	Methylcellulose (MilliporeSigma)	2.4% (w/v)
	FBS (PNA-Biotech)	3% (v/v)
	1x DMEM (Lonza)	
	Penicillin/Streptomycin (Capricorn)	2 mM
	Sodium Pyruvate (Capricorn)	0.5 mM
5x DMEM (pH 7.0)	DMEM powder (Gibco)	
	Sodium hydrogen carbonate (Carl Roth)	1.85 % (w/v)
Fixation buffer	Methanol (Carl Roth)	5% (v/v)

	Glacial acetic acid 1x PBS	10% (v/v)
Staining buffer	Giemsa (Carl Roth) 1x PBS	5%

3.1.4.5. Kits and other materials and reagents

The following kits and reagents were used according to the manufacturer's instructions. Reagents used for cell treatment in the experiments were added 30 minutes before the infection and maintained during the time course of the infection.

- GelStar Nucleic Acid Gel Stain 10,000x (Lonza) diluted in DMSO 1:100
- Gel Loading Dye (6x) (New England Biolabs)
- Quick-Load Purple 2-Log DNA Ladder (0.1-10.0 kb) (New England Biolabs)
- NucleoSpin Gel and PCR Clean-Up Kit (Macherey-Nagel)
- NucleoSpin Plasmid, Mini kit for plasmid DNA (Macherey-Nagel)
- NucleoBond PC 100, Midi kit for transfection-grade plasmid DNA (Macherey-Nagel)
- Restriction endonucleases (BsmBI, EcoRI, BamHI, PmeI) (New England Biolabs)
- Antibiotics Ampicillin, Kanamycin (Carl Roth)
- Lipofectamine 3000 (ThermoFisher Scientific)
- Polybrene (MilliporeSigma) - 8 µg/mL
- Puromycin (Carl Roth) - 1 µg/mL
- Chloroform (Carl Roth)
- Isopropanol (Macron)
- TRIreagent (Ambion)
- RNase ZAP (Ambion)
- miRNeasy Micro Kit (Qiagen)
- 4',6-diamidino-2-phenylindole (DAPI) stain (10 000x) (MilliporeSigma)
- 10x Phosphate Buffer Saline (PBS) (Carl Roth)
- Nitrocellulose membrane (Santa Cruz Biotech)
- Enhanced Chemiluminescence (ECL) Detection System (GE Healthcare)
- SuperSignal West Femto Maximum Sensitivity Substrate (ThermoFisher)
- High molecular weight polyinosinic:polycytidylic acid (Poly[I:C]) (Invivogen) - 100 µg / ml

- rIFN- β (PBL Biomedical Laboratories) - 1 U / μ l
- MG132 (MilliporeSigma) 20 μ M
- Acyclovir (ACV) (MilliporeSigma) 100 μ M
- Cycloheximide (MilliporeSigma) 100 μ g/ml
- Actinomycin D (MilliporeSigma) 1 μ g/ml
- Microscope slides (Carl Roth)
- Coverslips (Carl Roth)
- Mounting medium (VWR)
- High Capacity cDNA Reverse Transcription Kit (Applied Biosystems)
- FastStart Essential DNA Green Master (Roche)
- TaqMan microRNA Reverse Transcription Kit (Applied Biosystems)
- TagMan Universal PCR Master Mix (Applied Biosystems)
- Dynabeads Protein G immunoprecipitation kit (Life Technologies)

3.1.5. Bacterial strains and medium

Escherichia coli XL1 BLUE was used to prepare chemically competent cells stored at -80°C and used for the transformation. Luria Broth (LB) medium and LB agar (Carl Roth) plates were used for cultivation.

Ampicillin (100 μ g/mL) and Kanamycin (100 μ g/mL) were used when needed for the selection of transformed cells.

3.1.6. Plasmids

The following plasmids were used:

- pRS-1-ICP0 – containing entire ICP0 gene ¹ [111]
- pcDNA-1-ICP4 – containing entire ICP4 gene ¹ [112]
- pEGFP-N1 – Vector for fusing EGFP to the C-terminus of a partner protein (Clontech)
- lentiCRISPR v2 – 3rd generation lentiviral backbone (Addgene, plasmid #52961)
- psPAX2 - 2nd generation lentiviral packaging plasmid (Addgene, plasmid #12260)
- pMD2.G - VSV-G envelope expressing plasmid (Addgene, plasmid #12259)

¹ Plasmids kindly provided by Dongli Pan, Department of Medical Microbiology and Parasitology, Zhejiang University School of Medicine, Hangzhou, China

3.1.7. CRISPR/Cas9 constructs

Table 6. Oligonucleotides used for cloning of the vectors for CRISPR/Cas9 genome editing of mammalian cells.

Name	Sequence	Vector
FOXO1-KO-1-F	CACCGTAGCATTTGAGCTAGTTCTGA	pLenti-hFOXO1-KO1
FOXO1-KO-1-R	AAACTCGAACTAGCTCAAATGCTAC	
FOXO1-KO-2-F	CACCGGTGGCGCAAACGAGTAGCA	pLenti-hFOXO1-KO2
FOXO1-KO-2-R	AAACTGCTACTCGTTTGCGCCACC	
FOXO1-KO-3-F	CACCGGAGTTTATGCCAGTCCAACT	pLenti-hFOXO1-KO3
FOXO1-KO-3-R	AAACAGTTGGACTGGCTAAACTCC	
FOXO3-KO-1-F	CACCGCCTGCCATATCAGTCAGCCG	pLenti-hFOXO3-KO1
FOXO3-KO-1-R	AAACCGGCTGACTGATATGGCAGGC	
FOXO3-KO-2-F	CACCGCAGAGTGAGCCGTTTGTCCG	pLenti-hFOXO3-KO2
FOXO3-KO-2-R	AAACCGGACAAACGGCTCACTCTGC	
FOXO3-KO-3-F	CACCGAACAAGTATACCAAGAGCCG	pLenti-hFOXO3-KO3
FOXO3-KO-3-R	AAACCGGCTCTTGGTATACTTGTTT	
FOXO4-KO-1-F	CACCGTTCATCAAGGTTCAACAACG	pLenti-hFOXO4-KO1
FOXO4-KO-1-R	AAACCGTTGTGAACCTTGATGAAC	
FOXO4-KO-2-F	CACCGAGACCACTCCGAGATAGCA	pLenti-hFOXO4-KO2
FOXO4-KO-2-R	AAACTGCTATCTCGGAGTGGTCTC	
FOXO4-KO-3-F	CACCGCACTTGCCCAGATCTACGAG	pLenti-hFOXO4-KO3
FOXO4-KO-3-R	AAACCTCGTAGATCTGGGCAAGTGC	
FOXO6-KO-1-F	CACCGCCTTGAAGTAGGGCACGTAA	pLenti-hFOXO6-KO1
FOXO6-KO-1-R	AAACTTACGTGCCCTACTTCAAGGC	
FOXO6-KO-2-F	CACCGAGGCTTGGGCCGACTTCCG	pLenti-hFOXO6-KO2
FOXO6-KO-2-R	AAACCGGAAGTCGGCCCAAGCCTC	
FOXO6-KO-3-F	CACCGGAAAGCGAAGAGCTCTCGG	pLenti-hFOXO6-KO3
FOXO6-KO-3-R	AAACCCGAGAGCTCTTCGCTTTCC	
NC1_CRISPR-Cas9-F	CACCGATATACCGACTTAACACGGA	pLenti-NC1
NC1_CRISPR-Cas9-R	AAACTCCGTGTTAAGTCGGTATATC	

3.1.8. Antibodies used for Western Blot and Immunofluorescence

Table 7. Specific antibodies used for Western Blot and immunofluorescence

Antibody	Company	Catalog No.	Dilution WB	Dilution IF
Actin	Millipore	2691430	1:10 000	
HSV-1 ICP0	Abcam	ab6513	1:2000	1:10 000
HSV-1 ICP4	Abcam	ab6514	1:2000	
HSV-1 gC	Abcam	ab6509	1:2000	1:500
FoxO1	Cell Signaling	2880P	1:1000	1:100
FoxO3	Cell Signaling	12829S	1:1000	1:800
FoxO4	Santa Cruz Biotech.	sc-373877	1:100	1:50
P-FoxO1/3	Cell Signaling	9464P	1:1000	1:500
P-FoxO3	Cell Signaling	9465T	1:1000	
GFP	Millipore	MAB1083	1:2000	
GM130	BD Transduction Laboratories	610822		1:100
MCMV m123 *	Capri	HR-MCMV-12		1:100
Mouse-hrp	Cell Signaling	7076S	1:2000	
Rabbit hrp	Cell Signaling	7074S	1:2000	
Goat anti mouse Alexa 555	Life Technologies	A21425		1:1000
Goat anti rabbit – alexa 488	Life Technologies	A11070		1:1000

* kindly provided by Professor Stipan Jonjić, Center for Proteomics, Faculty of Medicine, University of Rijeka

3.1.9. siRNA

4392420 - siRNA DROSHA, Pre-designed, 5 nmol (Invitrogen)

4390843 - Silencer Select Negative Control No. 1 siRNA 5 nmol (Invitrogen)

3.1.10. PCR Primers

Primers for sequencing mir-H2 locus region:

- miR-H2-F2 – 5' - CCC CCG GGG CGG AGC CGG C-3'
- miR-H2-R3 - 5' - GGA GGG CCC GTG CCC ACC CT-3'

qRT-PCR primers:

- FoxO1-F1 - 5' –GCT TCC CAC ACA GTG TCA AGA C-3';
- FoxO1-R1 - 5' –CCT GCT GTC AGA CAA TCT GAA GTA C-3';
- FoxO3-F1 - 5' -GGGGAAGTTCCTGCTGCTGCTA-3';
- FoxO3-R1 - 5'- TGTCCACTTGCTGAGAGCAG-3'
- 18S rRNA-F1 - 5' –GTAACCCGTTGAACCCCAT-3';
- 18S rRNA-R1 - 5' –CCATCCAATCGGTAGTAGCG-3'

- GAPDH-mouse – F1 - 5' –GGTGCTGAGTATGTCGTGGA-3';
- GAPDH-mouse – R1 - 5' –GTGGTTCACACCCATCACAA-3'.

All primers listed were ordered from Metabion.

miRNA assays:

- hsa-miR-183-5p – Assay ID 002269
- hsa-miR-96-5p – Assay ID 000186
- hsa-miR-182 – Assay ID 002334
- hsa-miR-23a – Assay ID 000399
- hsa-miR-101 – Assay ID 002253
- hsa-miR-132-3p – Assay ID 000457
- hsa-miR-138-5p – Assay ID 002284
- let-7a-5p – Assay ID 000377
- miR-H6-3p – Assay ID 197219_mat

All miRNA assays listed were ordered from Applied Biosystems.

3.1.11. Data sets collected from databases obtained by massively parallel sequencing of HSV-1 or HSV-2 infected samples

Table 8: Samples infected with HSV-1 or transfected with HSV-1 fragments

HSV-1 infected small RNA sequencing data sets that were considered a single experiment are shaded light gray, or white, if it is a single sample, and separated by a line. Transfected samples are shaded in light blue, and discarded samples are shaded in dark gray.

	Samples	sRDS	Species	Replicates	Infection/strain	Condition	Length of the reads	Sequencer	Adapter	Publication	Total No. of USABLE reads ^{1,*}	miRNAs [*]	% of miRNAs	HSV-1 miRNA RC [*]
EXP 1	1	1	Human TG_1 ²	/	HSV-1; VZV clinical sample	latency <i>in vivo</i>	36	Solexa/Illumina sequencer	TCGTATGCCGTCTTCTG	[44]	3,222,391	2,856,170	88.64%	432
	2	2	Human TG_2 ²	/	HSV-1; VZV clinical sample	latency <i>in vivo</i>	36	Solexa/Illumina sequencer	TCGTATGCCGTCTTCTG	[44]	9,571,984	8,994,500	93.97%	3,906
EXP2	3	3	Human TG_3 ²	/	HSV-1; VZV clinical sample	latency <i>in vivo</i>	1x75	Illumina NextSeq	AGATCGGAAGAGCACACGTCTG	[113]	14,016,692	11,423,933	81.50%	25,783
EXP 3	4	4	Human TG_4 ²	/	HSV-1; VZV clinical sample	latency <i>in vivo</i>	36	Illumina miniSeq sequencer	TGGAATTCTCGGGTGCC AAGGG	[114]	871,532	332,841	38.19%	114
	5	5	Human TG_5 ²	/	HSV-1; VZV clinical sample	latency <i>in vivo</i>	36	Illumina miniSeq sequencer	TGGAATTCTCGGGTGCC AAGGG	[114]	981,060	284,754	29.03%	84
EXP 4	6	6	Human ARPE1 cells	/	HSV-1 F	productive inf. 24hpi MOI=1	1x75	Illumina NextSeq	AGATCGGAAGAGCACACGTCTG	[113]	4,400,767	2,016,851	45.83%	116,742
EXP 5	7	7	Human HEK293 cells	biological replicates	HSV-1 KOS	productive inf. - 12hpi <i>in vitro</i> + siRNA NC	36	Illumina miniSeq sequencer	TGGAATTCTCGGGTGCC AAGGG	Unpublished ³	1,175,103	530,709	45.16%	9,758

	10 11 12	8	Human HEK293 cells	biological replicates	HSV-1 KOS	productive inf. - 12hpi <i>in vitro</i> + siRNA DROSHA	36	Illumina miniSeq sequencer	TGGAATTCTCGGGTGCC AAGGG	Unpublished ³	1,169,459	543,473	46.47%	5,192
EXP 6	13 14 15 16 17	9	Human HFF cells	biological replicates	/	uninfected	50	Illumina HiSeq 2500 sequencer	AGATCGGAAGAGCACAC GTCTGAACT	Unpublished ⁴	38,462,280	20,571,104	53.48%	uninfected (92)
	18 19 20 21	10	Human HFF cells	biological replicates	HSV-1 KOS	productive inf. - 8hpi <i>in vitro</i>	50	Illumina HiSeq 2500 sequencer	AGATCGGAAGAGCACAC GTCTGAACT	Unpublished ⁴	48,711,853	32,490,553	66.70%	74,695
	22 23 24	11	Human HFF cells	biological replicates	HSV-1 KOS	productive inf. - 18hpi <i>in vitro</i>	50	Illumina HiSeq 2500 sequencer	AGATCGGAAGAGCACAC GTCTGAACT	Unpublished ⁴	40,134,384	27,140,685	67.62%	181,395
EXP 7	25	12	Primary neurons derived from rat SCG	/	HSV-1 Patton GFP-Us11	productive inf. - 24hpi <i>in vitro</i>	50	Illumina HiSeq 2000 sequencer	TGGAATTCTCGGGTGCC AAGGG	Unpublished ⁵	42,103,748	34,481,658	81.90%	78,189
	26	13	Primary neurons derived from rat SCG	/	HSV-1 Patton GFP-Us11	productive - 48hpi <i>in vitro</i>	50	Illumina HiSeq 2000 sequencer	TGGAATTCTCGGGTGCC AAGGG	Unpublished ⁵	33,713,196	27,994,795	83.04%	44,174
	27	14	Primary neurons derived from rat SCG	/	HSV-1 Patton GFP-Us11	latency model - 7dpi <i>in vitro</i>	50	Illumina HiSeq 2000 sequencer	TGGAATTCTCGGGTGCC AAGGG	[49]	28,566,874	23,575,187	82.53%	20,005
EXP 8	28	15	Human HEK293 cells	/	HSV-1 KOS	productive inf. - 18hpi <i>in vitro</i>	36	Illumina Genome analyzer II	TCGTATGCCGTCTTCTG	[42]	172,718	122,238	70.77%	3,189

EXP 9	29	16	Mouse TG_1 ²	/	strain KOS	latency – 30dpi <i>in vivo</i>	~55	454 Roche Sequencer	5' (first 17 nt) and 3' CTGTAGGCACCATCAAT	[50]	232,278	208,309	89.68%	151
EXP 10	30	17	Mouse TG_2 ²	/	HSV-1 KOS	latency - 30dpi <i>in vivo</i>	36	Illumina Genome analyzer II	TCGTATGCCGTCTTCTG	[42]	2,820,516	2,456,209	87.08%	411
EXP 11	31	18	Human HFFF2 cells	/	in1374 ⁶	latency model - 1,5hpi <i>in vitro</i>	36	Illumina HiSeq 2000 sequencer	TCGTATGCCGTCTTCTG	[49]	2,460,200	2,187,762	88.93%	279
	32	19	Human HFFF2 cells	/	in1374 ⁶	latency model - 16hpi <i>in vitro</i>	40	Illumina HiSeq 2000 sequencer	TCGTATGCCGTCTTCTG	[49]	15,897,353	13,163,080	82.80%	439
	33	20	Human HFFF2 cells	/	in1374 ⁶	latency model - 8dpi <i>in vitro</i>	40	Illumina HiSeq 2000 sequencer	TCGTATGCCGTCTTCTG	[49]	2,460,200	2,187,762	88.93%	475
EXP 12	34	21	Human HFF cells	/	HSV-1 KOS	latency model – 72hpi <i>in vitro</i>	50	Illumina HiSeq 2000 sequencer	TGGAATTCTCGGGTGCC AAGGG	[49]	41,477,444	38,025,175	91.68%	1,154
	35	22	Human HFF cells	/	/	uninfected	50	Illumina HiSeq 2000 sequencer	TGGAATTCTCGGGTGCC AAGGG	Unpublished ⁷	9,282,110	8,342,455	89.88%	uninfected (34)

EXP 13	36	23	Human HFF cells	/	HSV1 KOS	productive inf. - 10hpi <i>in vitro</i>	50	Illumina HiSeq 2000 sequencer	TGGAATTCTCGGGTGCC AAGGG	Unpublished ⁷	7,123,289	6,684,913	93.85%	1,594
	37	24	Human HFF cells	/	HSV1 KOS	productive inf. - 24hpi <i>in vitro</i>	50	Illumina HiSeq 2000 sequencer	TGGAATTCTCGGGTGCC AAGGG	Unpublished ⁷	8,122,322	7,617,876	93.79%	4,071
EXP 14	38	25	Human HeLa cells	/	/	uninfected	51	Illumina HiSeq 2000 sequencer	TGGAATTCTCGGGTGCC AAGG	[115]	19,475,637	7,092,140	36.42%	Uninfected (3)
	39	26	Human HeLa cells	/	HSV-1 KOS	productive inf. - 8hpi <i>in vitro</i>	51	Illumina HiSeq 2000 sequencer	TGGAATTCTCGGGTGCC AAGG	[115]	14,550,106	10,449,369	71.82%	15,675
EXP 15	40	27	Human KMB17 cells	biological replicates	/	uninfected	50	Illumina HiSeq 2500 sequencer	TGGAATTCTCGGGTGCC AAGG	[116]	50,350,789	40,235,772	79.91%	uninfected (65)
	41													
	42	28	Human KMB17 cells	biological replicates	HSV-1 17	productive inf. - 48hpi <i>in vitro</i>	50	Illumina HiSeq 2500 sequencer	TGGAATTCTCGGGTGCC AAGG	[116]	46,954,177	44,058,106	93.83%	101
	43													
EXP 16	44	29	Human HFF cells	biological replicates	HSV-1 KOS	12 hpi –input	50	Illumina NextSeq 500 sequencer	TGGAATTCTCGGGTGCC AAGG	Unpublished ⁸	9,266,846	10,215	12.77%	10,215
	45													
	46	30	Human HFF cells	biological replicates	HSV-1 KOS	12 hpi GFP pulldown	50	Illumina NextSeq 500 sequencer	TGGAATTCTCGGGTGCC AAGG	Unpublished ⁸	7,332,330	2114	0.29%	2,114
	47													
	48	31	Human HEK293 cells	biological replicates	HSV-1 KOS	12 hpi Ago pulldown	50	Illumina NextSeq 500 sequencer	TGGAATTCTCGGGTGCC AAGG	Unpublished ⁸	34,285,575	36,557	45.40%	36,557
	49													
	50													
	51	31	Human HEK293 cells	biological replicates	HSV-1 KOS	12 hpi Ago pulldown	50	Illumina NextSeq 500 sequencer	TGGAATTCTCGGGTGCC AAGG	Unpublished ⁸	34,285,575	36,557	45.40%	36,557
	52													
	53	31	Human HEK293 cells	biological replicates	HSV-1 KOS	12 hpi Ago pulldown	50	Illumina NextSeq 500 sequencer	TGGAATTCTCGGGTGCC AAGG	Unpublished ⁸	34,285,575	36,557	45.40%	36,557
	54													

EXP 17	55	32	Human HEK293 cells	/	pcDNA3/LAT expresses a 10.8 kb fragment, derived from the KOS	transfection	~55	454 Roche Sequencer	5' (first 17 nt) and 3' CTGTAGGCACCATCAAT	[50]	189,502	150,241	79.28%	651
EXP 18	56	33	Human HEK293 cells	/	pcDNA3/ICP34.5 plasmid	transfection	50	Illumina HiSeq 2000 sequencer	TGGAATTCTCGGGTGCC AAGGG	Unpublished ⁹	15,794,652	11,066,378	70.06%	47,921
EXP 19	57	34	Human HEK293 cells	/	HSV-1 KOS	productive INF pooled 2, 4, 6, 8, 10, 12, 16, 20, and 24 hpi	~36	Illumina Genome Analyzer IIe	5' (first 19 nt) and 3' (ACCTTGGTGC) adapter	[46]	5,770,491	111,113	1.93%	48,151
EXP 20	58	35	Human TG_6 ₂	/	HSV-1; VZV clinical sample	latency <i>in vivo</i>	2x35	Illumina NextSeq	AGATCGGAAGAGCACACGT CTG	[113]	6,130	1,403	22.89%	3
	59	36	Human TG_7 ₂	/	HSV-1; VZV clinical sample	latency <i>in vivo</i>	2x35	Illumina NextSeq	AGATCGGAAGAGCACACGT CTG	[113]	4,803	1,460	30.40%	3
	60	37	Human TG_8 ₂	/	HSV-1; VZV clinical sample	latency <i>in vivo</i>	2x35	Illumina NextSeq	AGATCGGAAGAGCACACGT CTG	[113]	2,747	1,307	47.58%	1
	61	38	Human TG_9 ₂	/	HSV-1; VZV clinical sample	latency <i>in vivo</i>	2x35	Illumina NextSeq	AGATCGGAAGAGCACACGT CTG	[113]	2,529	902	35.67%	0
EXP 21	62	39	Mouse cornea	/	HSV-1 KOS clinical sample	productive inf.	50	Illumina HiSeq 2000 sequencer	TGGAATTCTCGGGTGCCAA GGG	Unpublished ¹⁰	6,792,616	1,802,418	26.53%	20

¹ Pre-processed reads that enter the analysis with removed adapters that satisfied parameters for length and quality of reads

* Expressed in read counts (RC)

² Trigeminal ganglia

- ³ HEK293 cells were transfected with negative control (siRNA NC) and siRNA that targets DROSHA (siRNA DROSHA) and, after 48 hours, infected with HSV-1. RNA was extracted, and a small RNA library was prepared according to the TruSeq Small RNA Library Prep Guide, Illumina. Biological replicates numbered 7, 8 and 9 belong to the sRDS 7, while 8, 9 and 10 belong to the sRDS 8.
- ⁴ HFF cells were infected with HSV-1, RNA was extracted at indicated time points, and a small RNA library was prepared according to protocol. Biological replicates 13-16 belong to the sRDS 9, 17-20 to sRDS 10, and 21-24 to sRDS 11
- ⁵ Primary neurons were infected with HSV-1 Patton strain GFP-Us11 at an MOI of 1 in the presence of acyclovir (ACV) and nerve growth factor (NGF). These samples are part of the same experiment as sample 27
- ⁶ in1374 – virus mutant derived from HSV-1 strain 17syn+ that carries mutations in genes encoding VP16, ICP0 and ICP4
- ⁷ HFF cells were infected with HSV-1, RNA was extracted at indicated time points without replicates, and a small RNA library was prepared according to protocol.
- ⁸ AGO-IP was performed according to the immunoprecipitation protocol using DynabeadsProtein G and a small RNA library prepared according to the TruSeq Small RNA Library Prep Guide, Illumina
- ⁹ HEK293 cells were transfected with a plasmid expressing ICP34.5
- ¹⁰ Mouse corneas were infected with HSV-1 KOS strain KOS

Table 9: Samples infected with HSV-2

Samples	sRDS	Species	Replicates	Infection/strain	Condition	Length of the reads	Sequencer	Adapter	Publication	Total No. of USABLE reads ^{1,*}	miRNAs [*]	% of miRNAs	HSV-1 miRNA RC [*]
1	1	Mouse TG ²	/	HSV-2 186ΔKpn ³	latency - 30dpi in vivo	36	Genome analyzer II (Illumina)	TCGTATGCCGTCTTCTG	[42]	3,662,148	3,101,445	84.69%	283
2	2	Human HEK293 cells	/	HSV-2 186ΔKpn ³	productive inf. - 18hpi in vitro	36	Genome analyzer II (Illumina)	TCGTATGCCGTCTTCTG	[42]	1,193,969	702,305	58.82%	1,699

¹ Pre-processed reads that enter the analysis with removed adapters that satisfied parameters for length and quality of reads

^{*} Expressed in read counts (RC)

² Trigeminal ganglia

³ 186ΔKpn, a TK-negative mutant virus that can establish latent infection in TGs without lethality in mice

3.2. Methods

3.2.1. Culturing of the cells

All cell lines were grown in a cell incubator in an atmosphere with 5% CO₂ at 37 °C. Cell growth was monitored daily under a microscope. Cells were passaged when they reached 70%-90% density - the old medium was first removed, the cells were washed with PBS, and incubated in trypsin. Cells were washed with nutrient medium and seeded on new plates in fresh medium.

Cryopreservation was performed by transferring the cells collected from the plate to the freezing medium after centrifugation, transferring them to cryotubes and storing them in liquid nitrogen.

Frozen cells were rapidly thawed by immersion in a water bath at 37 °C and transferred to a new tube with 10 mL of appropriate nutrient medium, then centrifuged for 5 minutes at 1500 RPM, after which the supernatant was discarded, and new, fresh medium was added to the cells and transferred to a dish.

The number of cells was determined by counting in a Neubauer chamber. The total number of cells was obtained by multiplying the mean value of the number of cells per quadrant of the chamber by a correction factor of 10000 and the total sample volume.

3.2.2. Infection

Cells were seeded on the dish or plate the day before the experiment. If indicated, specific inhibitors or reagents were added 30 min before infection and maintained during the infection. Cells were infected with HSV-1 or MCMV at the indicated MOI (multiplicity of infection) or mock-infected (uninfected). One hour after infection, the infectious medium was replaced with a fresh growth medium. Samples were collected at specified hours post-infection (hpi) by removing the medium, washing with PBS, trypsinizing and collecting in fresh medium.

3.2.3. Determination of viral titer using plaque assay

Virus titers were determined as previously described [78]. Briefly, confluent monolayers of Vero cells in 6-well plates were infected with 1 mL of serial 10-fold dilutions of the supernatant sampled from the HSV-1-infected cells and incubated with the infectious media for 1 h at 37 °C. The infectious medium was removed, the cells overlaid with a methylcellulose solution, and incubated in 5% CO₂ at 37 °C for 3 days.

Cells were then fixed using 5% methanol and 10% acetic acid solution for 60 min and stained using 5% Giemsa stain for 60 min. The number of plaques was counted in each well, and the viral titers were determined as the number of plaque-forming units (PFU)/mL.

3.2.4. Plasmid isolation and bacterial transformation

The bacterial suspension was prepared by inoculating a single transformed colony in appropriate antibiotic and incubated at 37°C, 250 rpm in a shaker for 24h. The bacterial suspension was then centrifuged, the supernatant was decanted, and plasmids were isolated using the Plasmid purification mini kit (Macherey-Nagel) according to the manufacturer's instructions. The concentration and the quality of isolated plasmids were measured using UV/VIS spectrophotometer (BioDrop μ LITE, UK).

Chemically competent *E. coli* XL1 cells were used for the transformation. Briefly, bacteria were kept on ice, together with the desired plasmids or ligation reactions. For heat shock transformation of bacteria, aliquots of chemically competent bacteria (50 μ l) were used to which a small amount of plasmid or half of the ligation reaction was added and incubated on ice for 10 minutes. Then, the suspension was incubated for 45 seconds at 42 °C in a Cube Dry Bath Incubator (Clever Scientific) and returned to the ice for another 5 minutes. 500 μ l of LB medium was added to the suspension of transformed bacteria, transferred to bacterial tubes and incubated for 1 hour at 37°C and 250 rpm in a bacterial shaker. After incubation, bacteria were plated on the LB plates with the appropriate antibiotic and incubated at 37 °C overnight. The next day, bacterial colonies were selected and inoculated into 2 ml of LB medium with the addition of an appropriate antibiotic. They were incubated at 37 °C overnight in a bacterial shaker (250 rpm). Plasmid DNA was isolated from the obtained bacterial cultures. 500 μ l of bacterial culture of positive clones was mixed with 500 μ l of 50% glycerol and stored at -80 °C.

3.2.5. Transfection of mimics and siRNA molecules

Transfection of the siRNAs/mimics was performed using Lipofectamine 3000 according to the manufacturer's instructions. The final concentration of the mimics was

30 nM. After 24 hours, transfected cells were infected, and samples were extracted for analysis at indicated timepoints.

3.2.6. RNA extraction and quantitative RT-PCR (RT-qPCR)

Total RNA was extracted from mock and HSV-1 infected cells using TRI Reagent solution, according to the manufacturer's instructions. Total RNA samples were transcribed with the High Capacity cDNA Reverse Transcription Kit and levels of the transcripts were determined by RT-q-PCR using FastStart Essential DNA Green Master according to the manufacturer's instructions. The results were normalized to the expression of the 18S ribosomal RNA or mouse glyceraldehyde 3-phosphate dehydrogenase (GAPDH) and presented as the relative mRNA expression compared to 18S rRNA.

For the analysis of miRNAs, total RNA was transcribed using TaqMan microRNA Reverse Transcription Kit (Applied Biosystems) according to the manufacturer's instructions and used as a template in following RT-q-PCR reactions using TaqMan Universal PCR Master Mix (Applied Biosystems). Specific TaqMan miRNA assays were used to detect human miR-23a-3p, miR-101-3p, miR-132-3p, miR-138-5p, miR-183-5p, miR-96-5p, miR-182-5p, let-7a-5p, and HSV-1 vmiR-H6-3p. All reactions were performed in biological triplicates using LightCycler 96 (Roche).

RNA concentration and quality were measured using an UV/VIS spectrophotometer (BioDrop μ LITE, UK).

3.2.7. Protein extraction and Western Blot

To extract proteins, cells were lysed in RIPA buffer and protease inhibitors, mixed with 2x Laemmli buffer with β -mercaptoethanol and denatured for 6 minutes at 95 °C. Proteins were separated in 10% SDS–PAGE gels and transferred onto a nitrocellulose membrane. Membranes were blocked in 5% w/v nonfat dry milk in 1× Tris-buffered saline (TBS) for 30 minutes at room temperature and incubated with the specified primary antibodies at 4 °C with gentle rotation overnight. Blots were washed for 30 minutes with TBS-Tween 20 (TBS-T), and primary antibodies were detected using horseradish peroxidase-conjugated goat α -rabbit or α -mouse secondary antibodies and incubated at room temperature for 1h. Blots were again washed for 30

minutes and visualized using Amersham ECL reagent or SuperSignal West Femto Maximum Sensitivity Substrate and ChemiDoc MP (Bio-Rad).

3.2.8. Immunofluorescence

Cells were seeded in 24-well plates in which sterile microscopy coverslips were previously placed. Cells were infected with HSV-1 at a given MOI, washed in PBS and fixed for 10 min at room temperature at indicated time points. Cells were permeabilized for up to 7 minutes and left for 30 minutes in a blocking solution at room temperature. Cell slides were incubated with primary antibodies in a blocking solution. After incubation, cells were washed 3 times and incubated in a mixture of secondary, anti-mouse and anti-rabbit antibodies conjugated with fluorescent dyes Alexa 555 (red) and Alexa 488 (green) for 1 h. Cells were incubated with DAPI for 5 minutes to stain their nuclei. After incubation, the slides were washed 3 times with PBS and once with sterile water. The coverslips were mounted to the slides. Images were obtained using an Olympus fluorescent microscope IX83.

3.2.9. Crispr-Cas9 constructs and validation of knockout ($^{-/-}$) cells

Three guideRNA constructs per one gene were generated using the GPP sgRNA Designer tool (Broad Institute) [117, 118] based on the human reference GRCh38. A list of all constructs can be found in supplemental table 1. gRNA oligonucleotides for each gene were cloned into pLentiCRISPRv2 (kindly provided by Professor Oliver Vugrek, Ruđer Bošković institute, Zagreb, Croatia). Briefly, pLentiCRISPRv2 was digested with BsmBI restriction enzyme and gRNA oligonucleotides were subsequently ligated with T4 ligase. Sequences of cloned constructs were confirmed by Sanger sequencing at GATC Services. HEK293 cells were transfected with generated constructs and packaging plasmids psPAX2 and pMD2.G (kindly provided by Professor Oliver Vugrek, Ruđer Bošković institute, Zagreb, Croatia), using Lipofectamine 2000 (ThermoFisher, Germany) according to the manufacturer's protocol. Created lentiviral vectors with guide RNAs for the same gene were collected from the samples, pooled, filtered, and added to the SH-SY5Y cells. Transduced cells were incubated for 24 h and selected with puromycin at 1 $\mu\text{g/mL}$. The efficacy of knockouts was confirmed by Western Blot analysis.

3.2.10. Ago immunoprecipitation

Immunoprecipitation of RNA bound to Argonaute (Ago) proteins was performed according to the Dynabeads Protein G protocol. Briefly, Dynabeads were incubated with the 10 µg of α -Ago antibody (Millipore), or α -GFP (Millipore) that acted as a negative control, diluted in PBS with 0,1% Tween20 overnight at 4°C. After incubation, the supernatant was removed using a magnet, and beads were washed with PBS with 0,1% Tween20. HFF samples were collected 12 hpi in triplicates using NP-40 lysis buffer, and supernatant from cell lysis was added to the beads-Antibody complex and incubated overnight at 4°C. After incubation, beads were washed and resuspended in TriReagent solution.

3.2.11. Small RNA sequencing and data analysis

To comprehensively analyze the differential expression of host miRNAs during the HSV-1 productive infection, we performed massively parallel sequencing of small-RNA libraries. HFF cells were infected with HSV-1 and collected 8hpi and 18 hpi. In addition, HEK293 cells transfected with Drosha siRNA and infected were collected at 12 hpi. Furthermore, Ago immunoprecipitation samples were prepared following 12 hpi infection in HFFs. All samples mentioned above were used to prepare libraries according to the TruSeq Small RNA Sample Preparation Guide for sequencing. Size selection was performed on cDNA libraries, and species from 15 to 30 nt were isolated. cDNA libraries were then sequenced by single read sequencing (50 nt) in Illumina HiSeq 2500 sequencer. The total number of aligned sequence reads (read count) for each host and viral miRNA was normalized using read counts for human let-7a, whose expression does not change during HSV-1 infection or to the size of the library (RPM value). Sequence reads were analyzed with sRNAbench [119, 120], a collection of tools for small RNA analysis. After adapter trimming and removal of short reads (< 15 nt), the program uses Bowtie1 for mapping the clean reads against a user provided reference annotation, which in our case consists of the miRBase entries for HSV-1 [121], and to that reference database, we also added newly reported HSV-1 miRNAs miR-H28 and miR-H29 [48]. Only alignments within the first 19 nucleotides with 2 mismatches allowed are considered. Only reads detected at least once in any condition were used to determine differential expression.

3.2.12. Transcriptome sequencing and analysis

For whole transcriptome sequencing, samples were prepared for sequencing following the TruSeq Stranded Total RNA Sample Preparation Guide (Illumina). Briefly, samples were rRNA depleted and fragmented, primed for first and second-strand cDNA synthesis, adenylated 3' ends, adapters were ligated, and DNA fragments were enriched. The libraries were validated, using the Agilent Bioanalyzer and sequenced on NextSeq 500 Illumina platform at Ruđer Bošković Institute, Zagreb, Croatia. Following sequencing, obtained reads were assessed for quality using the FastQC quality control tool. Reads were then mapped to the reference HSV-1 genome, strain KOS (GenBank accession number JQ673480.1), Homo sapiens (human) genome assembly GRCh38 (hg38) from Genome Reference Consortium, using TopHat. Mapped reads were then visualized using Integrative Genomics Viewer (IGV). Finally, Cufflinks was used for differential expression, and normalized expression levels were reported in FPKM (Fragments Per Kilobase Of Exon Per Million Fragments Mapped).

3.2.13. Statistical analysis

To analyze statistical significance, Student's t-test was used (GraphPad Prism software). A level of $p \leq 0.05$ was considered statistically significant. Statistical significance levels are marked with asterisks: *** $p \leq 0.001$; ** $p \leq 0.01$; * $p \leq 0.05$. Statistically non-significant samples were not highlighted on the graphs.

4. RESULTS

Since the first discovery of miRNAs, the number of miRNA sequences deposited in miRBase (the principal miRNA registry) has increased enormously, including miRNAs encoded by viruses. However, due to a lack of established universal criteria for their annotation, the identification of genuine miRNAs remains a challenging task. For example, only about 26% of miRNAs found in humans are considered high-confidence miRNAs [122]. Similarly, one third of annotated mouse miRNAs is considered non-authentic [123].

Furthermore, over a decade after discovering that HSV-1 also expresses numerous miRNAs in infected cells, their basic biological properties and roles in infection remain largely unknown. In addition, HSV-1 infection leads to massive deregulation of host miRNAs, the consequences of which are also poorly understood. In our study, we addressed these two critical aspects of HSV-1 biology. In the first part, we investigated host miRNAs deregulated in HSV-1 infection to address possible consequences of such deregulation for efficient virus replication. In the second part of the study, we comprehensively examined HSV-1 miRNAs reported in previously published small RNA sequencing datasets and critically addressed the authenticity of reported miRNAs. In addition, we investigated some post-transcriptional modifications that might influence the function of miRNAs.

Each of these parts will be described in detail below.

4.1. Comprehensive analysis of host miRNAs in HSV-1 infection

4.1.1. A number of host miRNAs are deregulated during HSV-1 infection

To comprehensively investigate the deregulation of host miRNAs during productive HSV-1 infection and their potential biological functions, we compared two independent miRNA sequencing datasets. First, we infected the primary HFFs at an MOI of 5 in four replicates, extracted RNAs from mock-infected cells and cells infected with HSV-1 strain KOS at 8 and 18 h post-infection (hpi), and analyzed miRNA expression by massively parallel sequencing. The sequences obtained were analyzed using sRNAtoolbox. In each experiment, we detected about 1500 human miRNA expressed at a wide abundance range (i.e., from 0.02—279,598 reads per million (RPM)). On the other hand, HSV-1 encoded miRNAs represented only a minor fraction of the total miRNA in the sample (i.e., 0.24% and 0.68% at 8 and 18 hpi, respectively)

(Figure S1), which is in accordance with similar previous studies. Our differential expression analysis showed significant deregulation (fold change ≥ 2) of 134 human miRNAs at 18 hpi (Figure 8A), however, only a small fraction of miRNAs was deregulated with a fold change ≥ 3 . As expected, at 8 hpi, we did not observe significant deregulation of miRNAs compared to the mock; nonetheless, a slight trend in the deregulation of the same miRNAs that were significantly deregulated at 18 hpi can be observed. The second experiment represented one of our previous sequencing efforts, which was performed similarly (i.e., using the identical virus strain (KOS) infecting the matching cell type (HFFs)) under similar conditions (10 and 24 hpi) and the same sequencing platform. The overall sequencing quality was comparable (i.e., the total number of reads, the HSV-1 miRNA pattern, and the relative quantity). By comparing two unrelated sequencing experiments, we hypothesized that we would be able to identify the reproducibly deregulated miRNAs in HSV-1 infections. Surprisingly, the overlap between these two experiments was rather limited (i.e., only four miRNAs (miR-182, -183, -96, and -375) were reproducibly upregulated, and two miRNAs were downregulated (miR-29 and -27a) under all experimental conditions) (Figure S2). The fold change in the reproducibly deregulated miRNAs is shown in Figure 8B. These results suggest a strong dependence on the cells used in the experiments and may explain the observed discrepancies between different studies. Nonetheless, miRNAs expressed from a single transcriptional cluster, miR-183, -96, and -182 were reproducibly upregulated and showed the highest level of deregulation, indicating their importance. In contrast, a number of miRNAs were found deregulated in other experimental settings could not be confirmed deregulated by this experiment, such as miR-101, miR-138, miR-132 [75, 76, 79, 81, 93, 94].

The same cluster was upregulated in a study on two in vitro HSV-1 latency models (rat superior cervical ganglia derived neurons quiescently infected with HSV-1 GFP-US11 (Patton strain) and HFF quiescently infected with HSV-1 KOS strain) [49], but also in cells infected with other herpesviruses [95, 96]. Importantly, we detected only minor fluctuations ($<1.5\times$) in the expression levels for several miRNAs that had previously been shown to be significantly deregulated in HSV-1 infected cells [75-87]. As mentioned above, the use of different viruses, different cells, and conditions could explain this discrepancy.

Heatmap was also generated and using the most informative microRNAs, a perfect clustering pattern can be observed, i.e., mock-infected in one cluster and infected 8 hpi and 18 hpi in the others (supplemental data – Figure S3).

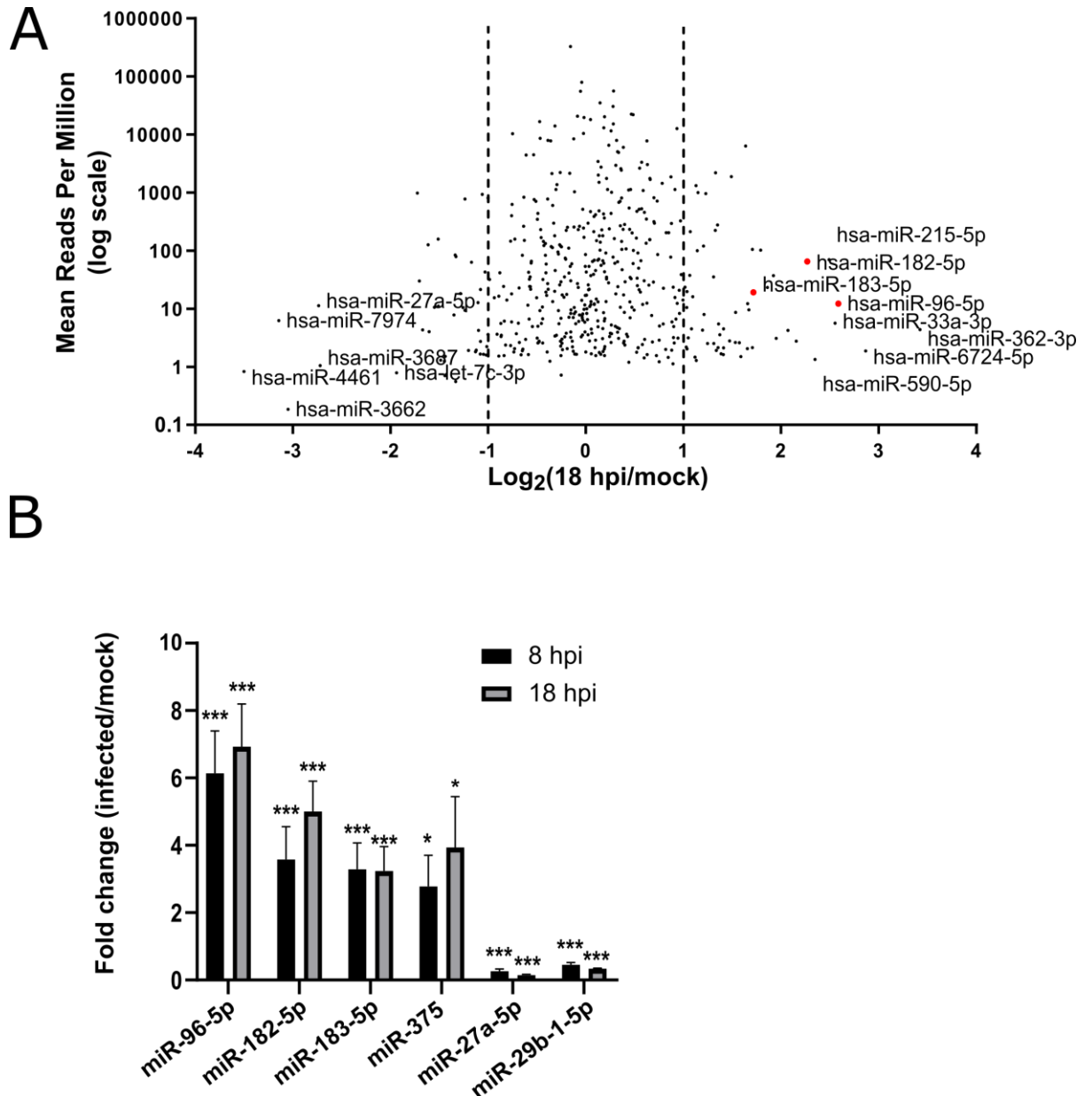


Figure 8: The host miRNAs are deregulated in HSV-1 infection. (A) MA-plot of log₂ transformed fold-change values (18 h after infection divided by uninfected (mock-infected)) vs. the mean of reads per million (RPM) expression values. The most deregulated miRNAs are indicated, and the miRNAs of the miR-183/96/182 cluster are indicated with red dots. (B) Fold change of miRNA expression at 8 (black bars) and 18 (gray bars) hours after infection over the mock-infected cells. Student's t-test was used to calculate statistical significance, and statistical significance is indicated with asterisks (* p < 0.05, *** p < 0.001).

4.1.2. miR-183/96/182 cluster is upregulated in HSV-1 infected primary HFF and WI38 cells

To additionally test the reproducibility of our sequencing results and to address the upregulation of the miR-183/96/182 cluster in different cells, we infected two primary cell types (i.e., human foreskin fibroblasts HFFs and mouse bone marrow-derived macrophages BMDM), human lung fibroblasts WI38 cells, and two widely used transformed cell lines (i.e., human embryonic kidney cells HEK293 and human neuroblastoma cells SH-SY5Y), and analyzed the miRNA expression by the stem-loop-RT-qPCR at 8 and 18 or 24 hpi. In the analysis, we included four additional host miRNAs, miR-23a-3p, miR-101-3p, miR-132-3p, and miR-138-5p, previously reported as deregulated and/or important for HSV-1 infection [75, 76, 79, 81, 93, 94]. Of note, the expression of the HSV-1 late gene product, miR-H6, served as the indicator of late viral gene expression. Surprisingly, only miR-182, miR-96, and miR-183 were upregulated more than >2x in both the fibroblast cells (HFFs and WI38; ~10x) (Figure 9 A, C) but not in other cells (Figure 9, B, D, E). Moreover, we observed only minor statistically significant deregulation for all other miRNAs tested, previously reported as deregulated. Thus, we selected miR-183/96/182 as the primary target for further functional analysis.

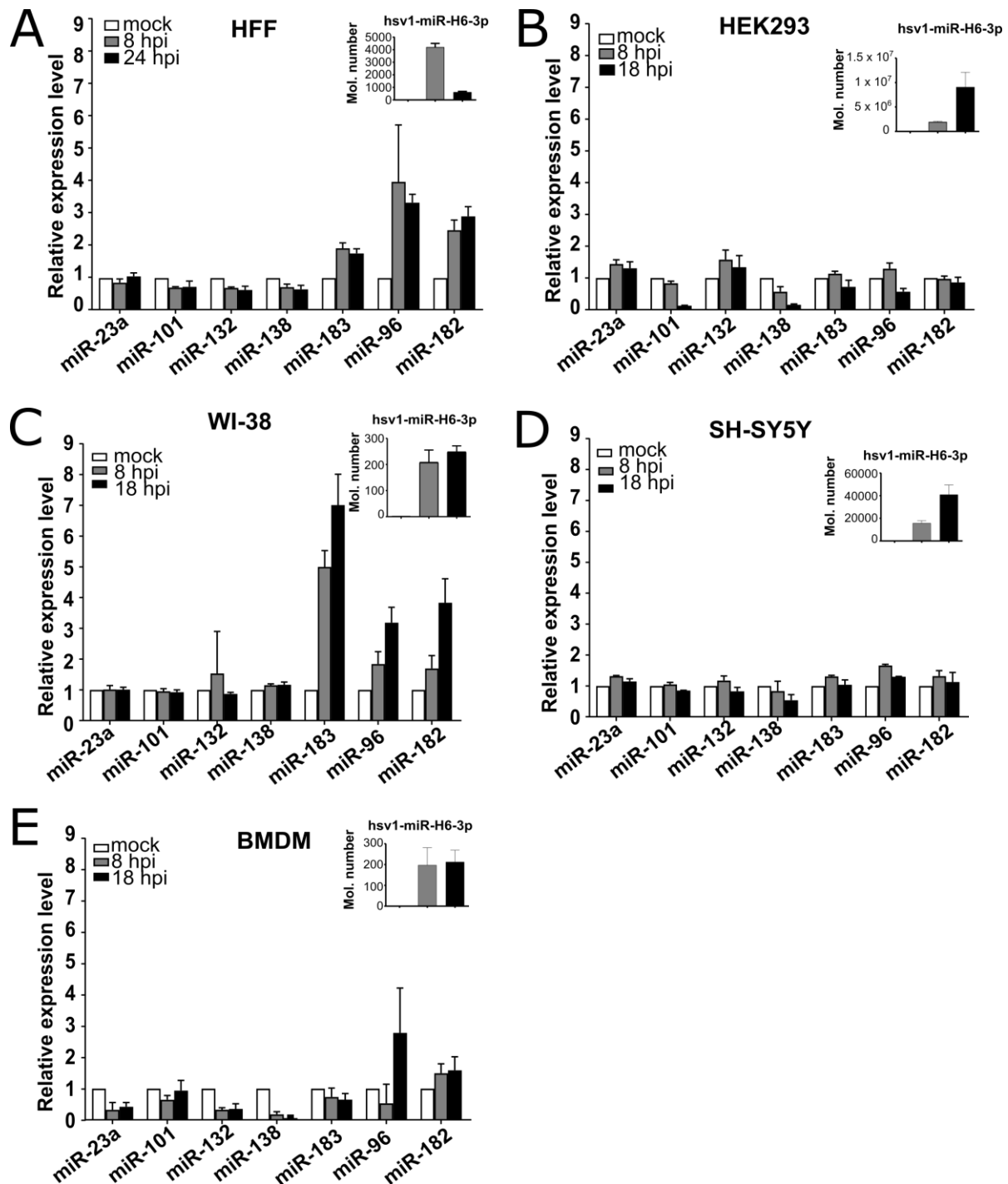


Figure 9.: A host miRNA cluster miR-183/-96/-182 is upregulated in human foreskin fibroblasts (HFFs) and human lung fibroblast (WI-38) cell lines. (A) HFF, (B) HEK293, (C) WI-38, (D) SH-SY5Y and (E) BMDM cells were infected with HSV-1 at an MOI of 10, and total RNA was extracted at the indicated time points. Results were normalized to let-7a expression. Relative expression levels are based on absolute quantification using standard curves based on serial dilutions of synthetic RNA oligonucleotides. The expression of virus-encoded miR-H6, as an indicator of the progression of a viral expression, is shown in the upper right corner of each graph.

4.2. Upregulated host miRNAs miR-183, -96 and -182 regulate 33 common targets

To determine the biological importance of the observed miRNA upregulation, we searched for the common targets of all three miRNAs-183/96/182 with TargetScan 7.1 and miRDB, two widely used algorithms that predict mRNA targets [97, 98]. The prediction revealed many highly conserved potential targets for each of these miRNAs (between 300 and 778 targets found by both prediction tools for each of the miRNAs; examples of TargetScan and miRDB search are shown in Tables S1 and S2, respectively). Notably, only 33 potential targets were identified as shared by all three miRNAs, and these, according to the Enrichr web tool [124], largely represent genes encoding proteins involved in regulating gene expression (Figure 10 and Table S3). Among these, *FoxO1* was identified as a potential target for all three miRNAs, and two other members of the Forkhead box protein family, *FoxO3* and *FoxO4*, were found as potential targets for miR-182 and miR-96, and solely miR-96, respectively (Figure 10). The binding sites for each miRNA of the cluster predicted by TargetScan are shown in Figure S4.

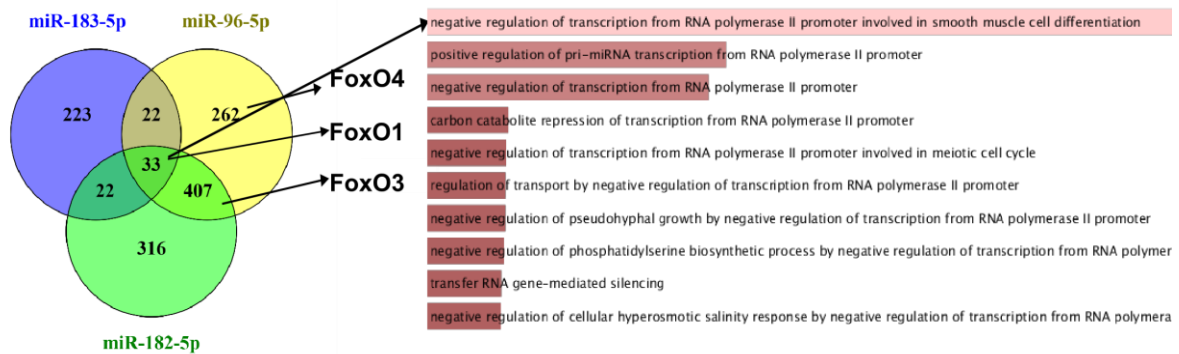


Figure 10. Overexpressed miRNAs miR-183, -96 and -182 potentially regulate 33 common targets. The members of the FoxO family are the predicted targets of miRNAs of the miR-183/96/182 cluster and are induced during productive HSV-1 infection. (A) The Venn diagram shows the number of conserved targets for miR-183 (blue circle), miR-96 (yellow circle), and miR-182 (green circle). The predicted targets of the FoxO family are indicated with arrows. Gene Ontology was determined by the Enrichr Gene Ontology analysis tool (Ma'ayan Lab, Icahn School of Medicine at Mount Sinai, NY, USA) [124]. The length of the bar and the color indicate the significance of gene sets in the different functional categories, i.e., the longer the bar and lighter the color, the term is more significant.

4.3. Members of the FoxO protein family as potential targets of miR-182/-96/-183

4.3.1. HSV-1 productive infection induces FoxO1 and FoxO3 expression

Based on the target prediction (Figure 10), we hypothesized that the increase in miRNAs miR-96, -182, and -183 would consequently lead to decreased levels of the FoxO family members. To address this, we infected various cells with HSV-1 at an MOI of 1 and collected samples for the Western blot and RNA analysis at different time points after infection. We observed an initial increase in the FoxO1 and FoxO3 levels between 1 hpi and 12 hpi and a slight decrease later in infection (Figures 11 and S5), which could be explained by the increase in miRNAs late in infection (Figure 9). FoxO4 levels steadily increased through the time of infection (Figure 11). Of note, the same dynamic pattern of the FoxO proteins (first upregulation followed by downregulation) was observed in all cell lines tested (HEK293, RPE-1, HFF, SH-SY5Y; Figure 11 and Figure S5). However, surprisingly, we observed FoxO1 and FoxO3 downregulation in cells in which we did not observe upregulated levels of miR-183/96/182 during the time course of infection (e.g., HEK293 (Figure S5A)), indicating additional mechanisms other than miRNAs for the depletion of FoxO family members late in infection.

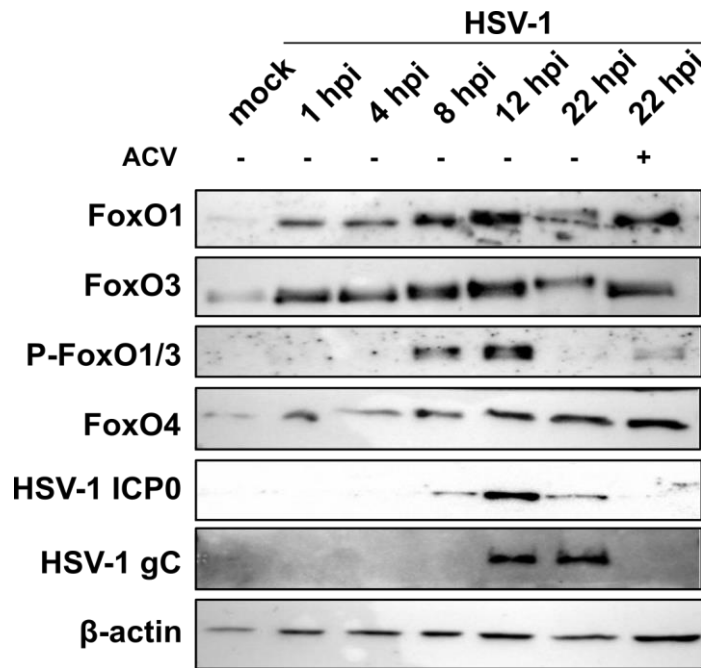


Figure 11. Protein levels of FoxO family members are increased during productive HSV-1 infection. The RPE-1 cells were mock-infected (mock), infected with HSV-1 (wt), or infected and treated with acyclovir (ACV), collected at indicated time points, and analyzed by Western blot. ICP0, immediate-early viral gene, and gC, late viral gene.

Moreover, in cells infected and treated with different inhibitors, including cycloheximide (CHX, protein synthesis inhibitor) and actinomycin D (ActD, RNA synthesis inhibitor), or in cells infected with UV inactivated virus, we did not observe the downregulation of FoxO proteins (Figure 12). These results indicate that IE/E viral gene expression may be required for the depletion of FoxO proteins. Interestingly, the depletion was not fully achieved during infection in the presence of acyclovir (i.e., a condition that allows for the expression of IE but prevents the expression of L proteins) (Figure 11). On the other hand, the addition of the proteasome inhibitor MG132 30 min prior to infection (*), but not 2 hpi (**), successfully prevented the depletion (Figure 12). These results may point to the role of the IE protein ICP0 in the depletion of FoxO, a well-characterized ubiquitin ligase, and additional mechanisms such as miRNAs and late viral functions.

Furthermore, by carefully analyzing the expression of FoxO protein members by Western blot, we observed the appearance of double bands (i.e., a shift of a few kilodaltons (kDa) during the time course of infection (Figure 11)), which might represent phosphorylated forms of proteins (i.e., inactive forms). Notably, this phenomenon was observed in most of the cell lines tested, but was particularly

apparent in RPE-1 cells (Figure 11 and Figure S5). Indeed, using phospho-specific antibodies, we confirmed the phosphorylation of FoxO1 and FoxO3. Interestingly, the addition of acyclovir, an inhibitor of viral DNA replication and late gene expression, prevented the shift of FoxO proteins (Figure 11). The observed phosphorylation is consistent with the previous study by Chuluunbaatar et al., who found that FoxO1 can be phosphorylated by Akt kinase and viral kinase Us3 [125] expressed as a late gene.

Taken together, we show that the virus is equipped with multiple mechanisms to control the expression and function of FoxO proteins and that miRNAs might have only a minor contribution to observed depletion of FoxO.

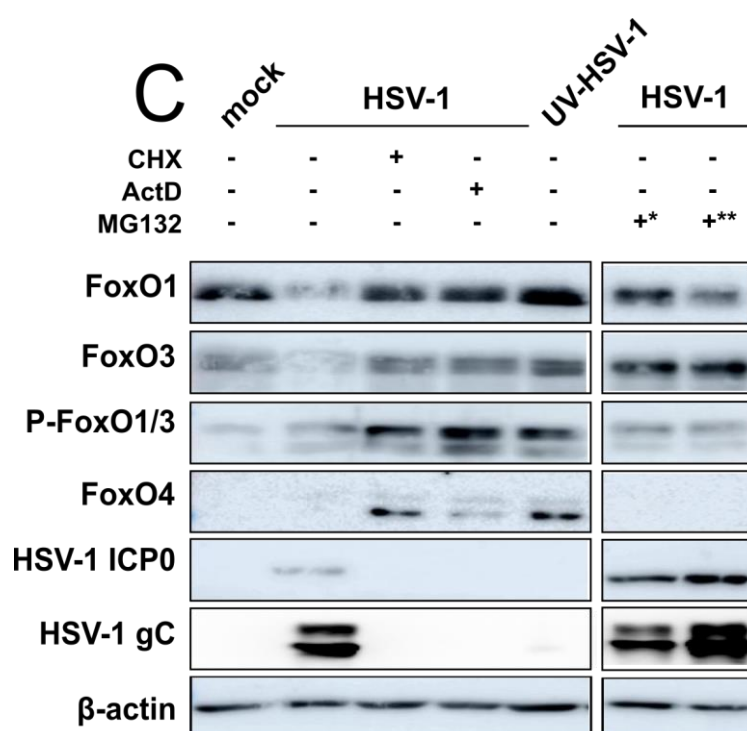


Figure 12: Other mechanisms in addition to miRNAs, impact the downregulation of FoxO members. HEK293 cells were mock-infected (mock), infected with HSV-1 (wt), or infected and pretreated with indicated inhibitors: cycloheximide (CHX), actinomycin D (ActD), proteasome inhibitor MG132 (*) 30 min before infection, or (**) 2 h post-infection; or infected with UV-inactivated HSV-1 (UV-HSV-1). Proteins for the Western blot were collected at 12 hpi.

4.3.1.1. FoxO1 and FoxO3 transcripts are induced after HSV-1 infection

We were intrigued by the increased levels of proteins of the FoxO family in cells infected with HSV-1, which indicates the possible transcriptional activation of FoxO genes. To address this, we analyzed the transcriptome of HSV-1-infected cells. Briefly, we infected HEK293 cells with strain KOS at MOI 10 and collected the total RNA at 1, 4, 8, and 12 hpi from two biological replicates for each time point. The sequencing

libraries were prepared using the TruSeq Stranded Total RNA Sample Preparation Kit (Illumina) and sequenced on the NextSeq 500 Illumina platform. The transcriptome analysis showed an increase in FoxO1 and FoxO3 mRNAs (Figure 13A) early in infection (4 hpi). However, the results were inconclusive for the FoxO4 transcript due to the low number of reads (not shown). The transcriptional activation of the FoxO family was additionally confirmed in a time-course experiment (Figure 13B) using RT-qPCR for FoxO1 and FoxO3. Similar to the sequencing results, we observed an increase early after infection and a sharp drop in mRNA levels after 8 hpi.

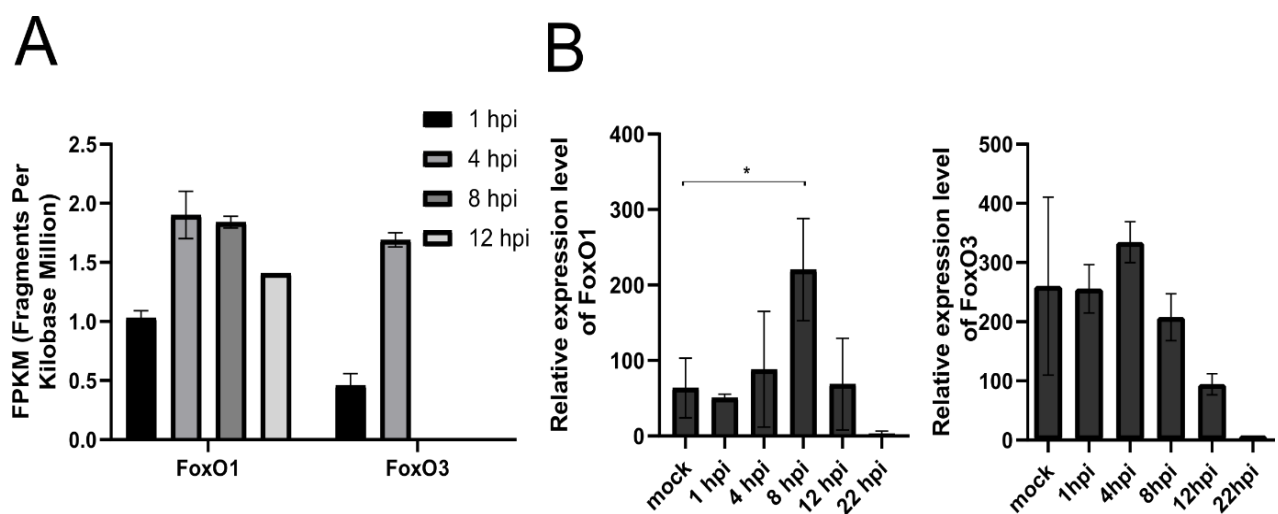


Figure 13: The members of the FoxO family are induced and then downregulated during productive HSV-1 infection on the mRNA level. (A) Levels of the FoxO1 and FoxO3 transcripts were obtained by the RNA-seq and subsequent bioinformatics analysis. Results were normalized for the sequencing depth and gene length and reported in fragments per kilobase million (FPKM). (B) The expression levels of the FoxO1 mRNAs were determined by RT-qPCR and normalized to 18S rRNA expression. Student's t-test was used to calculate statistical significance, and statistical significance is indicated with asterisks (* $p < 0.05$).

4.3.2. FoxO family of proteins is upregulated during MCMV infection

To further investigate whether the FoxO family induction is limited to HSV-1 infection or if it might represent a conserved host–response mechanism to infection with other herpesviruses, we studied the expression of FoxO members in cells infected with murine cytomegalovirus (MCMV). Briefly, primary mouse embryonic fibroblasts (MEFs) were infected with the MCMV strain C3X, and samples for protein and RNA

analysis were collected at different times post-infection. Interestingly, we observed a strong upregulation of all tested members of the FoxO protein family (Figure 14A) during MCMV infection. Moreover, the analysis of RNA confirmed the transcriptional activation of FoxO genes (Figure 14B), similar to HSV-1. It is important to note that although we observed an apparent increase in the phosphorylation of FoxO proteins compared to the HSV-1 infected human cells, we did not observe an apparent size shift detected in Figure 11. We cannot explain this difference at this point, but it might be related to the specificity of the antibodies or different activities of the virus and/or cellular kinases.

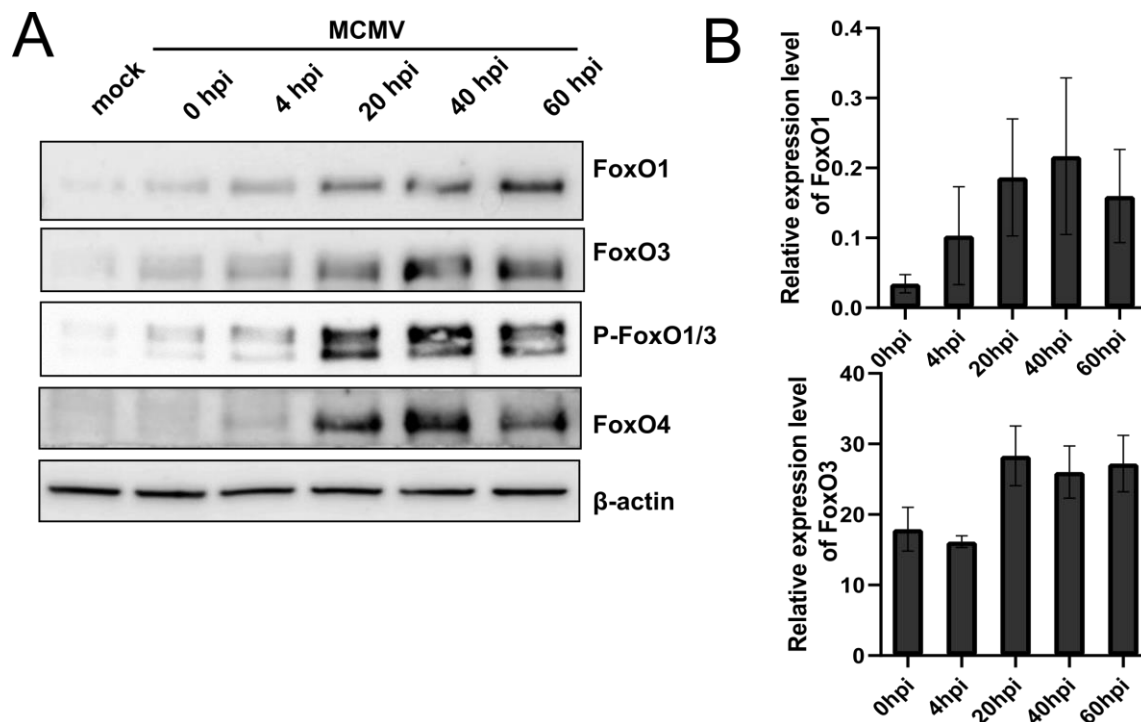


Figure 14: MCMV infection induces the FoxO family on protein and mRNA levels. (A) Mouse embryonal fibroblasts (MEF) were mock-infected or infected with MCMV, and samples for protein analysis were collected at the indicated time points after infection (hpi). (B) Cells were infected as in (A), and RNA samples were collected. The expression levels of FoxO1 and FoxO3 mRNAs were determined by RT-qPCR and normalized to 18S rRNA expression. The experiment was performed in triplicate, and the standard deviations are indicated.

4.3.3. FoxO family of proteins gets induced after IFN- β or poly(I:C) stimulation

These results led us to hypothesize that FoxO family members might be involved in intrinsic antiviral response and triggered in response to virus infection. For example, it has been found that FoxO1 promotes the degradation of IRF3 and limits IRF7 transcription [104], while FoxO3 has been found to target IRF7 and, thus, negatively regulate virus-induced type I interferon (IFN) expression [105]. To test this hypothesis, we analyzed the expression of FoxO1 and FoxO3 in response to the immunostimulants poly (I:C) and IFN- β , which mimic viral infection and elicit an antiviral response, respectively (Figure 15). Indeed, the stimulation of RPE-1 cells with poly (I:C) resulted in the gradual induction of both the FoxO protein levels, with a peak protein expression at 6 h post-stimulation. On the other hand, stimulation with IFN resulted in a sharp but very transient increase in FoxO1 and FoxO3 immediately after stimulation. The observed drop in the FoxO protein levels 3 h or 6 h after stimulation with IFN- β is in agreement with the work of Litvak et al., showing that IFN-I limits the

transcription of FoxO3, which is responsible for targeting IRF7, and thus increases the transcription of IRF7 for the maximum antiviral response [105]. Regardless, the results indicate that FoxO family proteins are induced as a result of an immune response to viral infection.

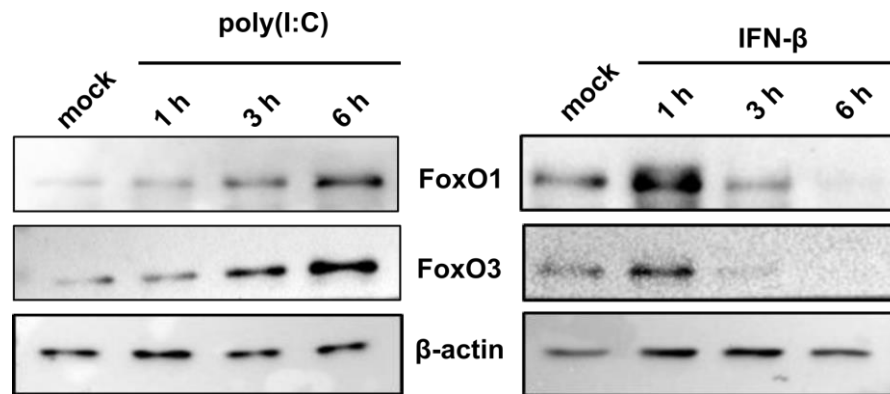


Figure 15. IFN and poly (I: C) induce the FoxO family of proteins. Protein samples were collected from untreated RPE-1 (mock) or cells treated with poly (I:C) (left panel) or IFN-β (right panel) at the indicated time points after treatment and analyzed by Western blot.

4.3.4. Induction of FoxO1 and FoxO3 expression is dependent on MOI

Several studies have shown that there is a specific limit on the number of viral particles per cell above which the function of the ICP0 protein loses significance and is surpassed by viral load. Therefore, we hypothesized that the optimal MOI values would contribute to more efficient virus replication in the cell, while extremely high MOI values cause poor replication. To investigate whether the induction phenomenon of FoxO1 and FoxO3 protein expression in HSV-1 infection depends on MOI, RPE-1 cells were infected with different MOI values and samples were collected at two time points, 2 and 8 hpi (Figure 16). The results show that the induction of FoxO1 protein is most pronounced at the lowest MOI value and decreases with increasing value. In contrast, phosphorylation accompanied by declining protein levels is faster at higher MOI values. The same pattern is seen with the FoxO3 protein.

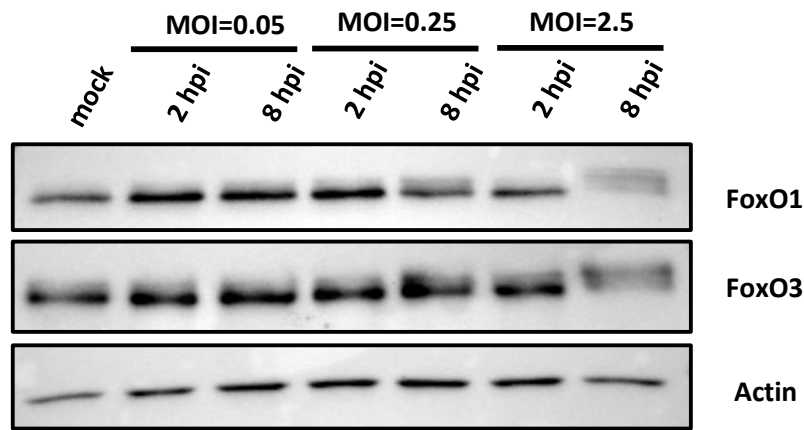


Figure 16. FoxO1 and FoxO3 protein levels are dependent on MOI infection with HSV-1. RPE-1 cells were mock-infected or infected with the WT virus with different MOIs (0.05, 0.25, and 2.5), and for each MOI, two samples were collected, 2h and 8h after infection. Mock-infected sample was collected with samples 2 h after infection. Protein levels in the samples were analyzed by the WB method. β -actin was used as an endogenous control.

4.3.5. FoxO1 re-localizes during herpesvirus infection

After investigating the expression profile of FoxO1 and FoxO3 proteins, we wanted to determine whether there is a change in their localization in the cell during productive HSV-1 infection. Results show that FoxO1 change of localization and accumulation can be observed at 4hpi (Figure 17A), and they are formed earlier than other FoxO family member aggregates (not shown). During the later phase of infection, when HSV-1 gC can be detected, strong FoxO1 protein accumulation can be observed in the cytoplasm next to the nucleus. The results of several studies have shown that, during viral infection, the Golgi apparatus and the ER are the sites of accumulation of certain cellular proteins, and for that reason, we hypothesized that FoxO1 accumulates in the Golgi apparatus. Indeed, we show that accumulated FoxO1 proteins overlap with GM130, a marker for the cis Golgi apparatus (Figure 17B).

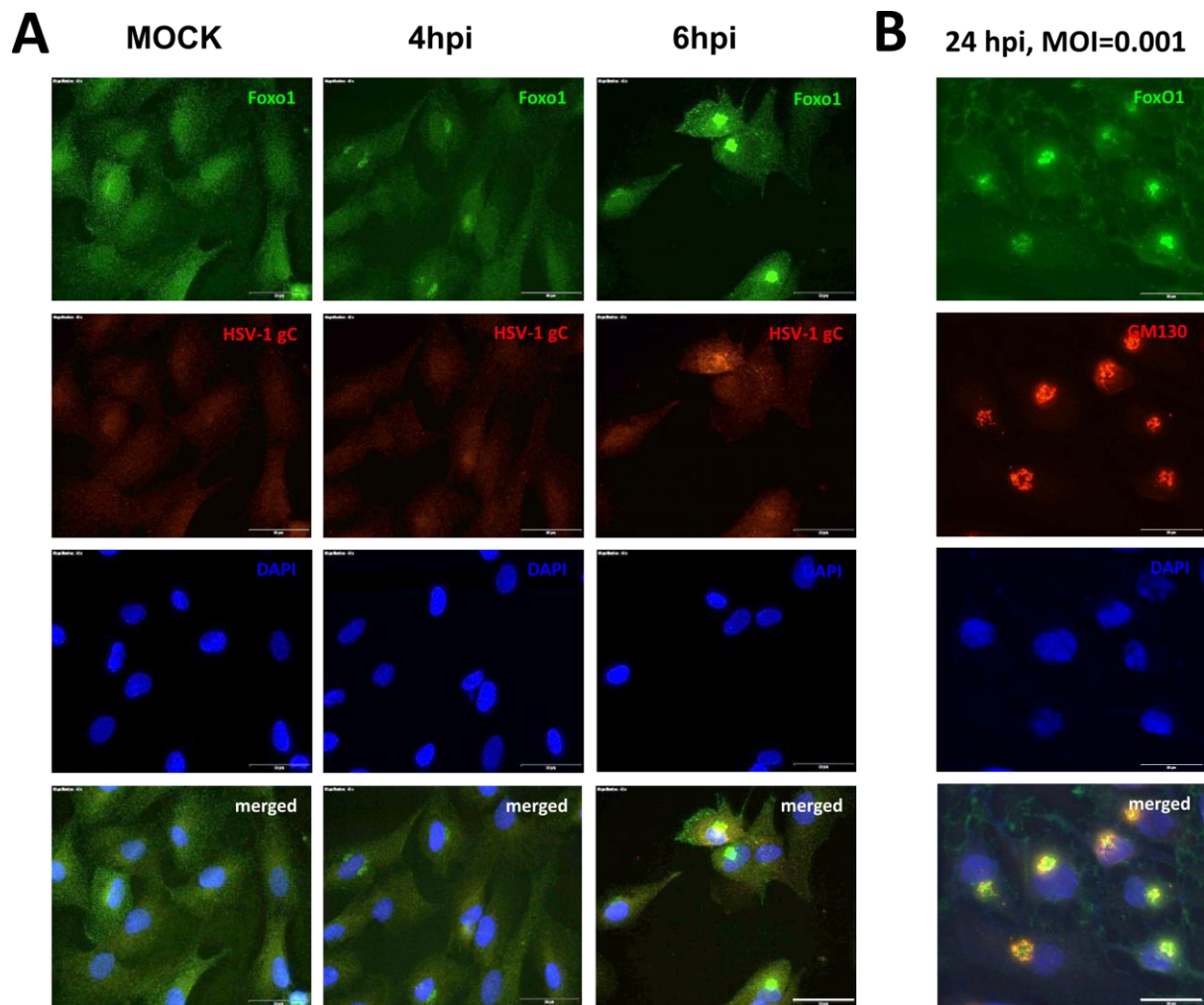


Figure 17. Foxo1 aggregates are formed early in the infection (A), and it localizes in perinuclear aggregates that overlap with the Golgi apparatus protein late in the infection (B). RPE-1 cells were mock-infected or infected at low multiplicity of infection (MOI) for 24 hours, and FoxO1 (green) and HSV-1 protein gC (red) were detected using fluorescent antibodies. Cell nuclei and cis Golgi were stained with DAPI (blue) and GM130, respectively, and observed by fluorescent microscopy. Scale bar - 50 μm.

To investigate whether the same accumulation can also be observed in the MCMV infection, we investigated FoxO1 localization in MCMV-infected samples. Surprisingly, during MCMV infection, we did not observe perinuclear aggregates as in HSV-1 infection. Nonetheless, we can still observe a change in localization to the cytoplasm during the infection in the form of diffused staining (Figure 18).

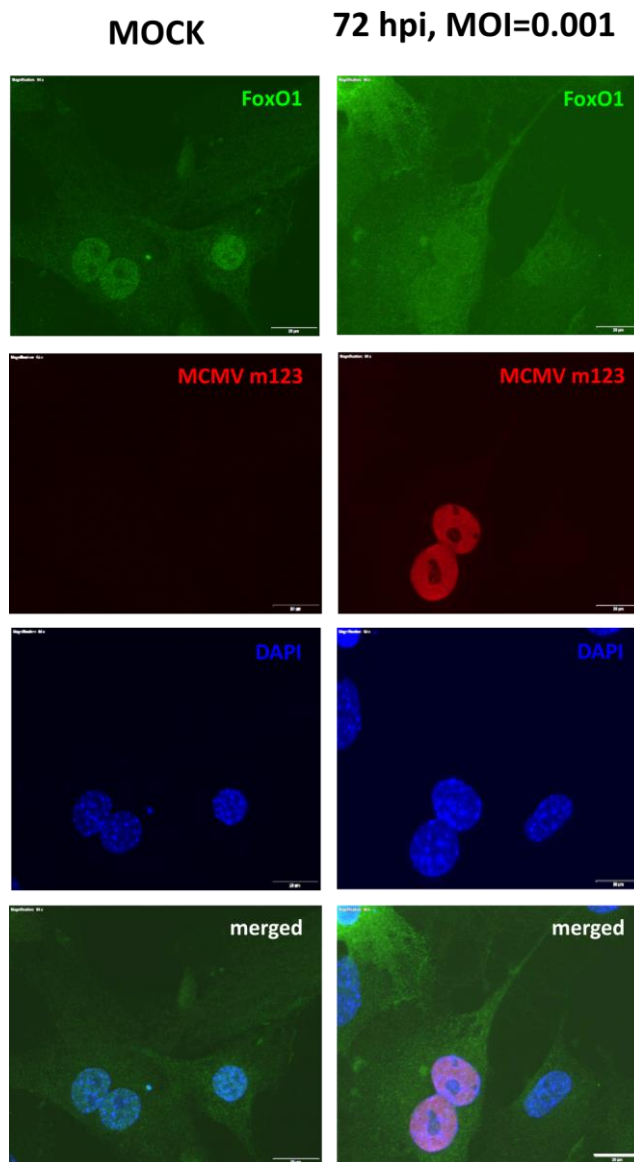


Figure 18. Diffused cytoplasmic distribution of FoxO1 during MCMV infection. Mouse embryonal fibroblasts (MEF) were mock-infected or infected for 72 hours and observed by fluorescent microscopy for FoxO1 (green), MCMV m123 red, DAPI- nuclei (blue). Scale bar - 20 μ m.

4.3.6. FoxO1 or FoxO3 are not required for efficient HSV-1 replication in SH-SY5Y cells

Finally, to address the biological relevance of the miR-183/96/182 cluster upregulation in HSV-1 infection on the one hand and the upregulation of FoxO family members on the other, we performed several functional assays. First, we asked whether the increased levels of miRNAs of the miR-183/96/182 cluster affected the virus replication. To test this, we transfected HFFs with mimics of miR-96, miR-182, and miR-183 or negative control mimics (NC), and 24 post-transfection, we infected

cells with HSV-1 at an MOI of 5 (Figure 19A) and 0.001 (Figure 19B). Surprisingly, we observed no noticeable difference in virus replication (Figures 19A and B). Similarly, these miRNAs only had minor effects on viral infection in Neuro-2a cells using a high throughput assay in which cells were transfected with individual miRNAs and infected with HSV-1-luciferase-reporter virus (Pan et al., not published; personal communication). These results led us to the conclusion that the upregulation of the miR-183/96/182 cluster has, at best, a minor role in HSV-1 replication in cultured cells.

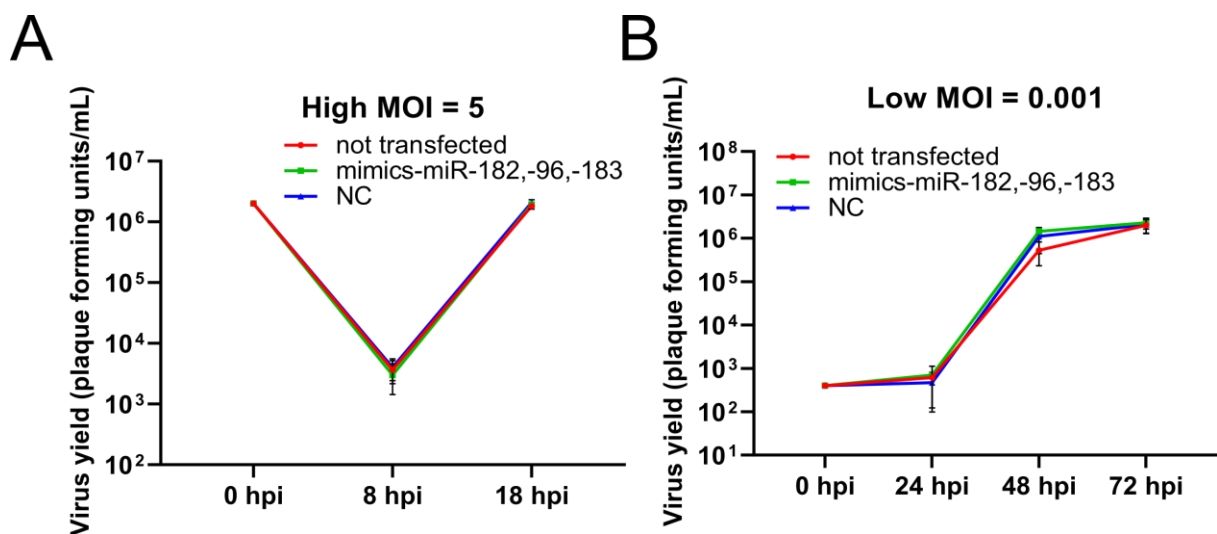


Figure 19: miR-183/96/182 cluster has no impact on the HSV-1 replication in cultured cells. (A) HFFs were transfected with miR-182, -96, and -183 mimics or the negative control mimic (NC) and, after 24h, infected with HSV-1 at an MOI of 5 (A) and 0.001 (B).

Next, to investigate the role of FoxO proteins in HSV-1 infection, we inactivated the FoxO1, Foxo3, and FoxO4 (FoxO1 $-/-$, FoxO3 $-/-$, FoxO4 $-/-$) genes in the SH-SY5Y cell using CRISPR-Cas9 technology. Briefly, we generated guides using the GPP sgRNA Designer Tool [117, 118] and selected the top three different candidate guides to target each of the genes. Several individual clones were analyzed for the expression of targeted genes, and only the complete knock-down cells were used in further experiments. We successfully knocked out FoxO1 and FoxO3 proteins (Figure 20); however, we were not able to generate FoxO4 deficient cells or cells deficient for all FoxO proteins (not shown).

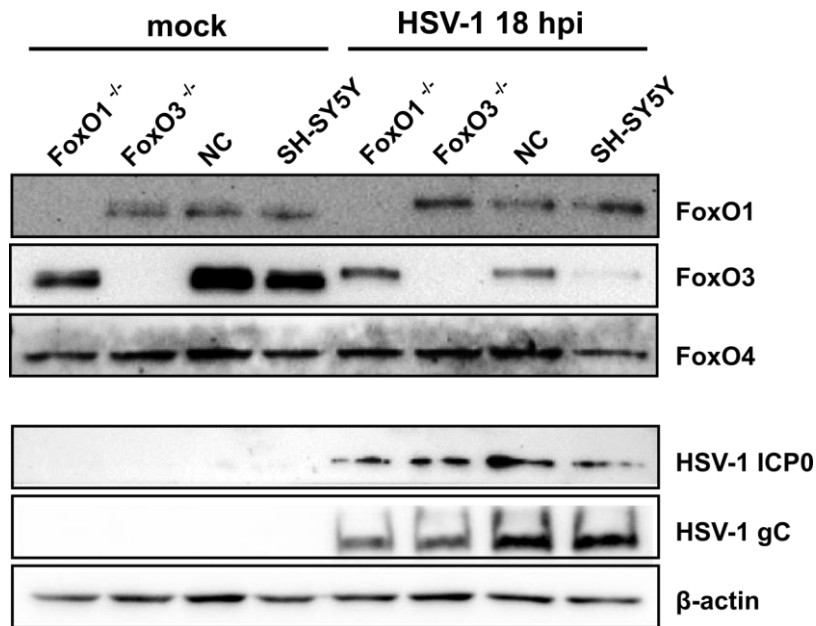


Figure 20: Successful generation of FoxO1 and FoxO3^{-/-} clones in SH-SY5Y cells using CRISPR-Cas9. Cells were mock-infected (mock) or infected with HSV-1 at an MOI of 5, and proteins were extracted at 18 hpi for Western blot analysis. SH-SY5Y—parental cells, NC- negative control gRNA, FoxO1^{-/-}, and FoxO3^{-/-} cells.

Next, FoxO1 and FoxO3 deficient cells were infected at high and low MOIs, and virus replication was monitored through the time course of infection. Interestingly, we observed a slight decrease in ICP0 and gC expression in a high MOI experiment (Figure 20) at 18 hpi. However, we observed, at best minor, a difference in virus yield between the individual FoxO deficient cells and the negative control at high (Figure 21A) and low (Figure 21B) MOIs. These results led us to conclude that individual FoxO proteins are not required for efficient HSV-1 infection. The FoxO family protein members may have, at least to some extent, redundant functions and compensate for individual depletion.

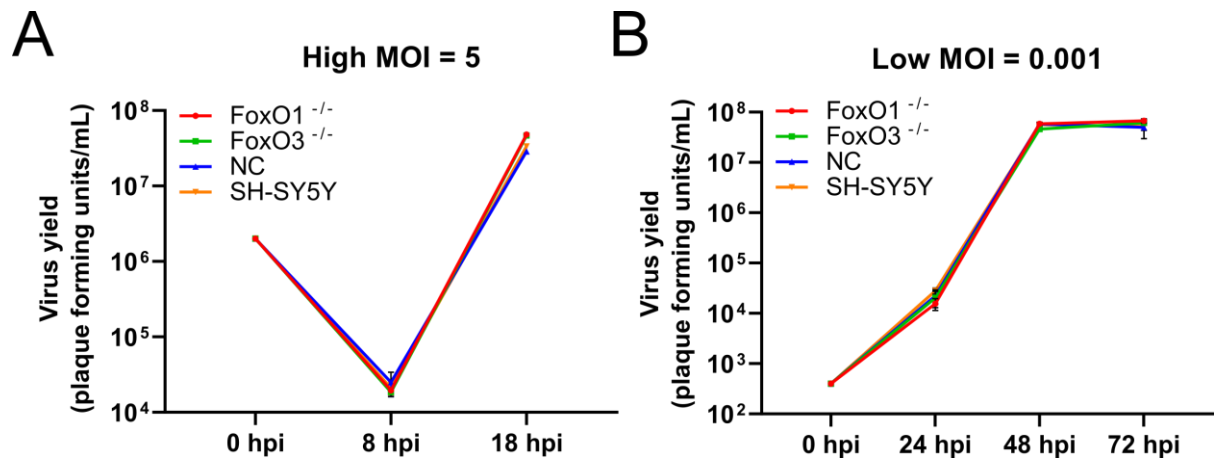


Figure 21. FoxO proteins are not required for HSV-1 replication. (A) Cells were infected at an MOI of 5, and 0.001 MOI (B), and the supernatants were collected at the indicated time points after infection (hpi). The virus titer was determined by titration on Vero cells and shown as plaque-forming units per mL (PFU/mL). 0 hpi corresponds to the virus titer in the infectious medium. SH-SY5Y—parental cells, NC—negative control gRNA, FoxO1^{-/-}, and FoxO3^{-/-} cells.

4.4. Comprehensive analysis of HSV-1 encoded miRNAs

4.4.1. HSV-1 microRNA profiling using deep sequencing data sets

To comprehensively investigate and validate miRNAs expressed by HSV-1, we collected and analyzed 21 experiments, with 39 data sets, referred to as small-RNA sequencing data sets (sRDS), composed of 62 samples. In addition, we analyzed two HSV-2 miRNA experiments (2 data sets). HSV-2 sequencing data sets served as a control of sample re-analysis. A detailed list of experiments, samples and DATA sets is given in Tables 8 and 9 of Materials and methods chapter 3.1.

Briefly, our collection of the samples included experiments on productive and latent HSV-1 infection; experiments using a variety of different animal and *in vitro* models of latency; studies involving four HSV-1 strains; samples containing HSV-2 productive and latent infection; the samples of human tissue latently infected with HSV-1, and samples of cells transfected with fragments derived from HSV-1. First, we analyzed the sequencing quality of the samples using a standard FastQC protocol, which were then processed using a versatile miRNA-analyzing collection of programs sRNAtoolbox (version 1.5 (6/2018) [120]; details below). To discriminate between good-quality data sets, at least one of two conditions had to be satisfied: all data sets with less than 25 mapped reads to the HSV-1 miRNA library (except for mock-infected samples) or samples with less than 25% of total reads mapped to miRNAs were discarded (i.e. 6 of 62 samples). The only exception were functional experiments such as silencing of Drosha, or Ago pulldown (immunoprecipitation of Ago-bound RNA and small RNA sequencing), because of the expected lower number of miRNA reads. After initial quality analysis, six samples, shaded with dark gray in Table 8, were discarded. The resulting analysis was conducted with the remaining 18 experiments with 33 data sets and 56 samples with more than 550×10^6 adapter trimmed sequence reads. miRNAs expressed from all previously reported HSV-1 miRNAs precursors were found in our analysis of the productively infected samples. However, we detected only a fraction of these miRNAs in latently infected samples (described below).

Importantly, by analyzing the individual samples of one experiment, we did not observe large differences between the biological replicates. As we did not expect technical/biological replicates to fluctuate, to facilitate a more efficient analysis and increase statistical power, the experimental replicates were pooled into one sRDS. Notably, the sequencing experiments from different laboratories were performed using different platforms and protocols (454 Roche Sequencer, NextSeq, miniSeq, HiSeq

2000/2500, Genome analyzer Illumina), and thus the number of reads and miRNAs between different data sets vary significantly.

4.4.1.1. Establishing selective criteria and defining the confidence score for HSV-1 miRNAs

With the emergence of high throughput technologies, a lot of small RNA sequencing data was generated, and thus, many novel small RNA sequences were annotated in miRBase, the most relevant database for miRNA annotation [126, 127]. It is important to note that, in earlier experiments, less advanced sequencing technologies were used, and bioinformatic methods were not as advanced. On the other hand, newer technologies offer sensitivity to one miRNA molecule in the sample that is impossible to confirm by different techniques. This resulted in several annotated small RNA sequencing reads that might be falsely classified as miRNAs and represent various degradation products. That sequences were deposited in miRBase, database which did not implement unified annotation criteria [127]. On the other hand, MirGeneDB, manually curated miRNA database, implements set criteria [128, 129] that take into account miRNA biogenesis and evolutionary signatures of miRNAs for annotation.

To address the issue of potentially falsely classified reads, recent studies re-addressed the evaluation of annotated miRNAs by applying stricter, biogenesis and evolutionary biased criteria [128]. Along with a basic uniform system for miRNA annotation [130], recent studies have determined criteria for plant [126, 131] and vertebrate miRNAs. For example, mature human miRNAs have surpassed 2600 entries in miRBase, and a recent study confirmed only 519 miRNAs as genuine miRNAs [129].

Regarding virus-encoded miRNAs, the annotation problem is even more severe because of the limited number of researchers in the field. Most of the annotated HSV-1 encoded miRNAs in miRBase are based on only one data set, and not all reported miRNAs are deposited in miRBase. Moreover, our own preliminary work indicated that the second arm of the miRNA duplex was not detected for several annotated HSV-1 miRNAs, which is one of the main criteria for miRNA annotation; and observed HSV-1 miRNAs, mir-H28 and mir-H29 are not yet introduced to the database. Therefore, in this study, we aimed to comprehensively address various aspects of HSV-1 miRNAs,

from determining exact sequences to the detection of putative RNA modification events.

The current, widely accepted, criteria for annotating and determining miRNA authenticity [130] served as guidelines for establishing selective criteria for the HSV-1 miRNAs. To improve stringency and based on our experience and preliminary results, we added a few criteria specific to viral miRNAs (see below). Challenges we encountered while setting these criteria centered around the fact that the viral miRNAs could be more variable in structure, so the criterion regarding consistent 5' terminus were less strict compared to cellular miRNAs. However, at the same time, this criterion represents one of the most important criteria to differentiate between true miRNAs and frequent degradation products. In total, eight criteria were defined, based on their importance and their value if the criteria were satisfied (Table 10). In brief, two criteria were selected as the most important and fundamental criteria to determine miRNA authenticity: a) **the pre-miRNA folding criterion** (Satisfactory hairpin folding with no big irregular bulges larger than 5 nt in the area of mature miRNA sequence and with minimum free energy less than ΔG -0.2 kcal/mol per nt (Figure S6, S7, S8)); and b) **5' homogeneity criterion** (Criterion is satisfied if a fraction of reads start at the same position as canonical (or most dominant) read at a minimum of 20% homogeneity (0.2), i.e., if 5' isomiRs do not exceed 80%. If the homogeneity of sequences is lower than 20%, sequences are discarded as putative miRNAs (Figure S9)). Those two criteria, if satisfied, scored 3 points each. The other six criteria are more adapted for the evaluation of HSV-1 miRNAs and included: c) **length of the miRNA** (i.e., the number of sequences in the analysis was limited by discarding sequences shorter than 18 or larger than 27, to still detect unusual additions, but to eliminate other sRNA species), d) **the number of reads** (i.e., read count (RC), arms of mature miRNAs with reads lower than 10 detected in any phase of HSV-1 infection were not considered), e) **reproducibility of the sequences in different hosts** (i.e., we searched for the same sequence within different hosts – human, mouse or rat species), f) **complementarity within the hairpin** (i.e., at least 13 nt complementarity), g) **Drosha/Dicer dependence** (i.e., detection of 2 arms that make duplex with overhangs), and h) **evolutionary conservation** (i.e., detection of positional homologs in HSV-2).

Table 10: criteria for calculating confidence score of HSV-1 miRNAs

Criteria	Explanation	Score
- Pre-miRNA folding	no irregular bulges and ΔG -0.2 kcal/mol/nt ¹	3
- 5' homogeneity	> 0,2 ²	3
- Length of miRNA	between 18-27 nt ³	1
- Number of reads	RC >10 in the productive or latent phase, both arms ⁴	1
- Reproducibility in different hosts	detected the same sequence in different host species ⁵	1
- Complementarity within hairpin	≥ 13 ⁶	1
- Drosha/Dicer dependence	0-4 nt overhangs ⁷	1
- Evolutionary conservation	detected in HSV-2 ⁸	1
		total 12

¹ pre-miRNA sequence extracted from miRBase was analyzed using the default settings of RNAfold for minimum free energy fold algorithm, and hairpins with large internal bulges larger than 5 nt and with minimum free energy less than -0.2 kcal/mol/nt were not considered.

² 5' end isomiRs have been detected in different cell types at a lower rate than 3' isomiRs suggesting evolutionary pressure to preserve the seed sequence at around 15%, i.e. at 85% homogeneity [32]. For vmiRNAs which tend to express higher variability, we aimed to allow much more variability within 5' end, and thus we set variability at 5' end to a minimum of 80%, or 20% homogeneity (0.2), i.e. if homogeneity of sequences is lower than 20%, sequences are not scored.

³ Mammalian machinery for miRNA biogenesis creates mature miRNAs of typical length ~ 21-22 nt, for which many NTA modifications at the 3' end of the sequence have been observed [132]. Therefore, we limited the amount of sequences in analysis by discarding sequences shorter than 18 or larger than 27, to still detect unusual additions, but to eliminate other sRNA species.

⁴ Any of both arms of mature miRNAs with a low number of reads (RC lower than 10) detected in any phase of HSV-1 infection were not considered

⁵ Reproducibility of the miRNA was challenged by searching for the same sequence within different hosts – human, mouse or rat species

⁶ To preserve to a degree shape of a hairpin, we propose that complementarity within a hairpin has to be at least 13 nt complementary

⁷ Drosha and Dicer usually create 2 nt overhangs, however, it has been shown that their deviation from perfect 2nt overhang cut is not random, and many factors besides main RNase III enzymes are involved in the process of canonical biogenesis, creating overhangs in the range from 0-4. Therefore, all sequences with more than 4 nt overhang were not considered

⁸ Sequences that have a sequence or positional homolog detected in HSV-2 were scored.

4.4.1.1.1. Analysis

Pre-miRNA folding. Analysis of almost all HSV-1 pre-miRNA showed minimum free energy per nucleotide lower than the set threshold. However, pre-miRNAs for miR-H17, miR-H26, miR-H28 and miR-H29 showed uncharacteristic hairpin structures.

5' homogeneity. For some HSV-1 miRNAs, at least one arm had 5' homogeneity lower than 0,2, i.e. did not satisfy the criterion, and these are miR-H12, miR-H26 and miR-H28-miR-H29. Consequently, these miRNAs were classified into a lower-ranking group (Table 13).

Length of miRNA. Among less important criteria selected to differentiate between other small RNA molecules, such as piRNA and siRNA, and improve miRNA annotation, the length criterion is the simplest way to cut off other small RNAs and focus further analysis on molecules ~22 nt long. For most HSV-1 miRNAs, their length corresponded to the length of typical human miRNAs 21-24 nt, but for some, most dominant sequences were either too short and not specific only for the HSV-1 genome (e.g. miR-H15-5p arm with size 14 nt) or too long and not typical for miRNAs (e.g. miR-H26-3p arm with size 30 nt). Furthermore, smaller reads that were found to map to the HSV-1 pre-miRNAs did not match already annotated miRNAs or the second arm product. For miR-H18, miR-H26, miR-H27, miR-H28 and miR-H29, reads were inconsistent between different samples, and usually very short (~15 nt) or too long (~30 nt). Therefore, we limited our annotation to miRNAs between 19 and 27 nt. This would also include regular-size miRNAs with non-templated nucleotide additions [132]. In brief, miR-H18-5p, miR-H26-5 and -3p, miR-H28-3p and miR-H29-5p did not satisfy this criterion (Table 13).

Number of reads. We sought to detect second arms of annotated miRNAs and set the threshold of the detection of both arms to at least 10 detected RC, i.e., considering such an abundant number of available sequences, we expect we will be able to detect another arm of annotated miRNA in at least one of datasets. For that reason, we hypothesize that all miRNAs for which we can detect only one arm cannot be called true miRNAs at this point, but they may represent miRNAs in evolutionary formation. It is important to note that shorter sequences of significantly lower G/C content are likely to be overrepresented [133], and accordingly, we cannot exclude the role of this bias regarding some underrepresented sequences. For most of the sequences, we detected sufficient RC for both arms, except for the passenger arms of the miR-H12, miR-H13, miR-H15, miR-H16, miR-H17, miR-H18, miR-H26, miR-H28 and miR-H29.

Reproducibility in different hosts. It has been shown that miRNAs generated from different cells and organs show length variations of the most abundant read [132]. Therefore, to extensively analyze HSV-1 miRNAs and to determine their consistency, we determined following factors. We searched for the most dominant sequences determined by the most frequent nucleotides found at each position, and consequently the correct sequence of the seed, by aligning it to the database sequence. We determined if sequences can be detected in different hosts, comparing the most dominant sequences generated in different cells and in different species. Starting hypothesis was that the identical dominant sequence represents more robust evidence in favor of these miRNAs. Results showed that miR-H12, miR-H14, miR-H15, miR-H17, miR-H18, miR-H26, miR-H28 and miR-H29 could not be detected in mouse or rat hosts (Table 13). Important to note, not all HSV-1 miRNAs can be detected in both phases of the infection, and mouse or rat datasets included in the analysis were mostly used as the models of latent infection, i.e., we did not have many productively infected mouse or rat cells.

Complementarity within hairpin. Complementarity within hairpin strongly depends on the existence of the mismatches and bulges around mature miRNA. Considering the higher variability of viral miRNAs, we set complementarity between two arms to a minimum of 13 bp. A number of miRNAs (miR-H14 – miR-H29) did not satisfy this criterion (Table 13, Figures S7 and S8). On the example of *bona fide* host miRNA mir-let-7a differences in hairpin structures of miRNAs that did not satisfy this criterion can be observed (Figure S10).

Drosha/Dicer dependence. To accurately distinguish passenger arm of already annotated miRNAs from other sequences mapped to the pre-miRNA, we introduced other predicted arms of the miRNAs (Table S4) to the database with 2 nt overhangs usually created on the 3' end of miRNAs. It has been implicated that some other elements like RNA sequence and not only the structural features of pre-miRNAs determine Dicer-dependent cleavage precision. Therefore, we also considered the heterogeneity of elements generated by Dicer and the most dominant molecules were evaluated for 0-4 nt overhangs [134]. For most of the miRNAs passenger arms that fit these criteria were found, but for some miRNAs, no molecules with sufficient RC were found, such as miR-H13-miR-H26, miR-H28 and miR-H29. Precursors for many of these HSV-1 miRNAs have not been identified or experimentally validated, though the general belief is that they arise through canonical biogenesis pathway. However, it has

been shown that miRNAs encoded by another herpesvirus, murine γ -herpesvirus 68 (MHV68), go through other non-canonical biogenesis pathways by being processed by tRNase Z instead of Drosha [135]. For that reason, in addition to this *in silico* pre-miRNA folding and analysis, we generated Drosha knock-out cells to detect candidates for non-canonical biogenesis. Cells were transfected with siRNA targeting Drosha and infected after validation of transfection (Figure S11A). Sequencing results were normalized based on total library size because the total pool of host miRNAs was not abundantly affected (the number of usable reads can be found in Table 8). The set of miRNAs showed statistically significant Drosha dependence, and miRNA expression in siRNA Drosha transfected samples was 2 times lower than in samples transfected with negative control scrambled sequence (Figure S11C). miR-H1-3p, miR-H2-3p, miR-H4-3p, miR-H6-3p were most significantly affected compared to cells transfected with negative control, which corresponds to the scores obtained in Table 12. On the other hand, miR-H12 – miR-29 (except miR-H13, -H16 and -H27) were not affected (which doesn't entirely correspond to the scores given in Table 13), indicating a concern regarding the confidence score and/or alternative biogenesis pathways.

Evolutionary conservation. HSV-1 miRNAs are considered well-conserved between different strains [136]. However, to validate this, we analyzed the sequences of 26 publicly available strains of HSV-1 and found that pre-miRNA sequences are 100% or with a maximum 1-2 nt mismatch conserved among all analyzed HSV-1 strains (Figure S12). Curiously, we found a few consistent mismatches in four analyzed pre-miRNA sequences from miRBase, compared to HSV-1 strains, including sequences for pre-miRNAs miR-H8, miR-H17, miR-H28 and miR-H29, and that indicated that these pre-miRNA sequences are not annotated correctly. Therefore, we suggest a change in the reference sequences to avoid incorrect mapping of small RNA reads (Figure S13).

In contrast to conservation between HSV-1 strains, there is limited conservation between HSV-1 and HSV-2. It has been shown that only 9 out of 29 precursors of miRNAs were conserved between HSV-1 and HSV-2 as positional homologs, and some of these share the similarity within the seed sequence [42]. It can be hypothesized that miRNAs preserved across species are inherited from a common virus ancestor and have important roles for viruses' infection, and it is a very strong indicator of genuine miRNAs. Therefore, for these miRNAs with their counterpart positional homologs detected in HSV-2, such as miR-H2, miR-H3, miR-H4, miR-H5,

miR-H6, miR-H7, miR-H11, miR-H12 and miR-H13, one additional point has been added (Tables 12 and 13).

Taking together, miRNAs that satisfy all listed criteria score 12 points, and important to note if the two arms of an HSV-1 miRNA fit into different groups, that miRNA was classified into a lower-ranking group.

Based on the confidence score, we divided miRNAs into three groups shown in Table 11: -A) **high confidence miRNAs** (score 10-12), which satisfy most of the criteria, including the two most important ones, B) **tentative miRNAs** (score 5-9)– miRNAs that do not satisfy all criteria. In most cases, the 5' homogeneity criterion and 2nd arm is usually not detected or was below the threshold and C) **low confidence miRNAs** –miRNAs which did not satisfy most of the criteria, most importantly, their hairpin is uncharacteristically folded with large bulges >5 nt long, and they do not have mature 5' homogeneity.

Table 11: Scoring system for confidence score of each HSV-1 miRNA.

Points	Group
10-12	A – high confidence miRNAs
5-9	B - tentative miRNAs
0-4	C – low confidence miRNAs

4.4.1.2. Final score for all HSV-1 miRNAs

Table 12: List of HSV-1 miRNAs grouped into “high confidence miRNAs”

vmiRNA	Pre-miRNA folding	5' homogeneity	Length of miRNA	Number of reads	Reproducibility in different hosts	Complementarity within hairpin	Drosha/Dicer dependence	Evolutionary conservation	Confidence level or score	Group
miR-H1-5p	+	0.52	22	16845	+	13	+	-	11/12	HIGH
miR-H1-3p	+	0.89	22	4872	+	13	+	-	11/12	HIGH
miR-H2-5p	+	0.79	22	9058	+	17	+	-	11/12	HIGH
miR-H2-3p	+	0.40	24	127592	+	17	+	+	12/12	HIGH
miR-H3-5p	+	0.49	22	1153	+	18	+	-	11/12	HIGH
miR-H3-3p	+	0.78	22	5823	+	18	+	+	12/12	HIGH
miR-H4-5p	+	0.45	22	2708	+	18	+	-	11/12	HIGH
miR-H4-3p	+	0.61	22	31888	+	18	+	+	12/12	HIGH
miR-H5-5p	+	0.22	24	104	+	17	+	+	12/12	HIGH
miR-H5-3p	+	0.27	23	87	+	17	+	-	11/12	HIGH
miR-H6-5p	+	0.45	21	2202	+	18	+	+	12/12	HIGH
miR-H6-3p	+	0.69	22	228611	+	18	+	-	11/12	HIGH
miR-H7-5p	+	0.52	22	930	+	13	+	-	11/12	HIGH
miR-H7-3p	+	0.95	22	8537	+	13	+	-	11/12	HIGH
miR-H8-5p	+	0.54	22	641	+	15	+	-	11/12	HIGH
miR-H8-3p	+	0.91	22	1722	+	15	+	-	11/12	HIGH

Table 13: List of HSV-1 miRNAs grouped into “tentative miRNAs” and “low confidence miRNAs”

vmiRNA	Pre-miRNA folding	5' homogeneity	Length of miRNA	Number of reads	Reproducibility in different hosts	Complementarity within hairpin	Drosha/Dicer dependence	Evolutionary conservation	Confidence level or score	Group
miR-H11-5p	+	-1.00	22	0	-	20	-	-	5/12	TENTATIVE
miR-H11-3p	+	0.44	22	1903	+	20	-	-	10/12	HIGH
miR-H12-5p	+	-1.00	25	0	-	19	+	-	6/12	TENTATIVE
miR-H12-3p	+	0.16	22	432	-	19	+	-	7/12	TENTATIVE
miR-H13-5p	+	0.00	23	0	+	18	-	-	6/12	TENTATIVE
miR-H13-3p	+	0.58	22	168	+	18	-	-	10/12	HIGH
miR-H14-5p	+	0.08	19	335	-	12	-	-	5/12	TENTATIVE
miR-H14-3p	+	0.30	22	124	-	12	-	-	8/12	TENTATIVE
miR-H15-5p	+	0.44	14	0	-	-	-	-	6/12	TENTATIVE
miR-H15-3p	+	-1.00	23	8	-	-	-	-	4/12	LOW
miR-H16-5p	+	0.41	29	250	+	-	-	-	9/12	TENTATIVE
miR-H16-3p	+	-1.00	20	0	+	-	-	-	5/12	TENTATIVE
miR-H17-5p	-	-1.00	22	0	-	-	-	-	1/12	LOW
miR-H17-3p	-	-1.00	20	14	-	-	-	-	2/12	LOW
miR-H18-5p	+	-1.00	18	22	-	-	-	-	4/12	LOW
miR-H18-3p	+	-1.00	19	0	-	-	-	-	4/12	LOW
miR-H26-5p	-	-1.00	30	0	-	-	-	-	0/12	LOW
miR-H26-3p	-	0.42	30	266	-	-	-	-	4/12	LOW
miR-H27-5p	+	-1.00	22	0	+	14	+	-	7/12	TENTATIVE
miR-H27-3p	+	-1.00	22	236	+	14	+	-	8/12	TENTATIVE
miR-H28-5p	-	0.11	20	66	-	-	-	-	2/12	LOW
miR-H28-3p	-	0.11	18	0	-	-	-	-	0/12	LOW
miR-H29-5p	-	0.03	30	0	-	-	-	-	0/12	LOW
miR-H29-3p	-	0.03	21	100	-	-	-	-	2/12	LOW

The miRNA scores show that the profile of miRNAs described as “high confidence miRNAs” (Table 12) largely follows the pattern of Drosha-dependent miRNAs (Figure S11), including miRNAs miR-H1-miR-H8, which represents experimental proof of the bioinformatic sequence analysis. The main feature of miRNAs in this group is that they have satisfied most important general criteria and satisfied most of the criteria specific to HSV-1 miRNAs. On the other hand, one or both arms of miRNAs that fit into the “tentative miRNAs” group based on the score have not satisfied one of the two main criteria, such as miR-H11-miR-H14, miR-H16 and miR-H27. The last group consists of “low confidence” miRNAs, for which we suggest the need for additional evidence. They have not satisfied the main criteria or more specific ones. We identified miR-H15, miR-H17 -miR-H26 and miR-H28 – miR-H29 (Table 13). It is important to note that for some HSV-1 miRNAs, the second arm is not present, or the dominant sequence found in the hairpin region is different from annotation, and for that reason, these scores refer to the sequences annotated in miRBase.

4.4.1.3. High frequency of HSV-1 isomiRs and their true sequence

Earlier studies using next-generation sequencing have reported a high frequency of sequence variations for the majority of miRNAs. Lots of publications confirmed the detection of isomiRs, especially regarding viral miRNAs. In other words, despite intensive research in the field, there is no consensus on the exact sequence for the majority of HSV-1 miRNAs, which is essential for functional studies. On the other hand, the size and abundance of miRNAs can significantly vary between different stages of HSV-1 infection [42], [49]. To address these issues, we performed a focused analysis on all small RNAs mapped to the HSV-1 pre-miRNA sequences. First, to facilitate the discovery of potential differences, we grouped samples in several categories, including a) all latently infected human trigeminal ganglia (hTGs) samples, b) all mouse productively and latently infected TGs, and c) all cell culture models of quiescent and latent infection and all productive infection samples infected with HSV-1. The number of reads used in the analysis is given in Table 8. We focused on the first two most abundant isomiRs to determine the most dominant sequence for each HSV-1 miRNA (Table S5).

For every HSV-1 miRNA first two isomiRs were categorized and labeled for the productive infection and transfected samples and latency (Figure S14). The observed sequence variations can be divided into a few categories: (I) canonical miRNAs (green), (II) substitution isomiRs (violet), (III) 3' end isomiRs (blue), which are further divided as 3' deletion and 3' addition isomiRs, (IV) 5' end isomiRs (orange) -5' deletion and 5' addition-isomiRs. Addition-isomiRs can be further divided into templated additions (TA) or non-templated additions (NTA). All other less abundant sequences are labeled with grey.

In our analysis, we confirmed that most HSV-1 miRNAs have a high percentage of isomiRs, and for some of them, the sequence annotated in the miRBase is not among the first 2 most dominant isomiRs, such as miR-H1-5p, miR-H3-5p, miR-H5-5p, miR-H5-3p, miR-H6-3p, miR-H8-3p, miR-H11-3p, miR-H13-3p, miR-H14-3p, miR-H15-3p, miR-H16-5p, miR-H17-3p, miR-H18-5p, miR-H26-3p, miR-H27-3p, miR-H28-5p and miR-H29-3p. Sequence variations showed different profiles in different phases and conditions, and for that reason, only consistent variations and a high percentage of variation were considered as accurate indicators of sequences that need to be updated. Most dominant sequences showed a variation of 3' end for many miRNAs, which represents various TA and NTA. Nonetheless, a smaller number of sequences consistently varied at the 5' end. Thus, based on the significance of variations of the 5' end, this strongly indicates that sequences of miR-H1-5p, miR-H8-3p and miR-H27-3p are not annotated correctly (Table 14).

Table 14: miRNAs with consistent 5' end variations

miR-H1	miRBase 5p arm	GATGGAAGGACGGGAAGTGGGA	miRBase 3p arm	TACACCCCCTGCCTTCCACCCT
	dominant sequence	ATGGAAGGACGGGAAGTGGGA AAG	dominant sequence	TACACCCCCTGCCTTCCACCC
miR-H8	miRBase 5p arm	TATATAGGGTCAGGGGGTTC	miRBase 3p arm	GCCCCCGGTCCTGTATATA
	dominant sequence	TATATAGGGTCAGGGGGTTC CG	dominant sequence	CGCCCCCGGTCCTGTATATAT
miR-H27	miRBase 5p arm	AAGAGGGGTCGGGATCCAAAGG	miRBase 3p arm	CAGACCCCTTCTCCCC CTCTT
	dominant sequence	AAGAGGGGTCGGGATCCAAAGG	dominant sequence	TTTGTTG CAGACCCCTTCTC

* nt marked bold represent changes in the sequences

4.4.1.4. miRNAs detected in infected samples show higher variability than in transfected cells

Additionally, in order to test the hypothesis that the increase in sequence variation of HSV-1 miRNAs is the property of the virus and not some intrinsic property of the miRNAs, we compared three conditions: first, sequences obtained from samples transfected with fragments and regions most prevalent in the latent phase of the infection; second, samples infected during productive, and third, latent infection.

We did not observe major changes in isomiR profiles, i.e. impact on miRNA processing between productive/latent infection or transfection. However, only a few miRNAs can be detected abundantly during latency, and only fragments and not all miRNA loci were actually transfected. Generally, the percentage of isomiRs in transfected samples is lower than in infected samples, especially compared to the productive infection. That indicates that more abundant HSV-1 isomiR expression is the outcome of the HSV-1 infection and not miRNA sequences themselves. (Figure S14).

On the other hand, miR-H2-3p showed the highest frequency of isomiRs during latent infection compared to the transfected cells or the productively infected samples, which could indicate a more important role during that phase of infection. However, to confirm this result and investigate other sequences, we would need samples transfected with fragments containing various HSV-1 pri-miRNAs, other than the ones included in these transfection assays, with deep sequencing yield.

4.4.1.5. Arm bias of viral miRNAs fluctuates between 5p and 3p in latent hTGs

After miRNA processing that yields duplex miRNAs, only one arm gets incorporated into the RNA-induced silencing complex (RISC), while the passenger arm usually gets degraded. Many miRNAs have strongly established the preferred selection of one arm over the other – arm bias. Studies analyzing the arm bias of the another herpesvirus belonging to the *Gammaherpesvirinae* subfamily, Epstein-Barr virus (EBV) miRNAs compared to host have shown that host miRNAs show strong arm bias (i.e., preferred selection of one arm), while the observed phenomenon was much weaker for EBV-expressed miRNAs [137].

To obtain a comprehensive profile and to determine if samples infected with HSV-1 show arm bias between two arms comparing different phases of the infection,

we determined the most dominant arm by observing deep sequencing data from hTGs, mTGs, HFF latency models, rat latency models, productive infection and transfection with HSV-1 fragments (Figure 22 A-F).

Important to note, due to a small number of reads for some vmiRNAs expressed and detected in our HSV-1 infected samples, arm bias for HSV-1 miRNAs could be misleading for *in vitro* latency models and latently infected hTGs. Comparing arm bias between samples, we noticed that main profiles are similar between different conditions. However, we cannot explain some fluctuations between dominant arms (e.g., in hTGs, there is a switch between dominant arms for miR-H4 and miR-H7 in some samples, Figure 22A). As these samples have been prepared in different laboratories, using different protocols for library preparation, and sequenced on various sequencing machines, there is a possibility that this fluctuation is a direct result of these differences and represents an artifact. However, we cannot exclude the possibility that this could also be one of the virus mechanisms for precise tuning of and control of latency (Figure 22). Interestingly, we did not observe a strong change in arm bias for the host miRNAs (not shown).

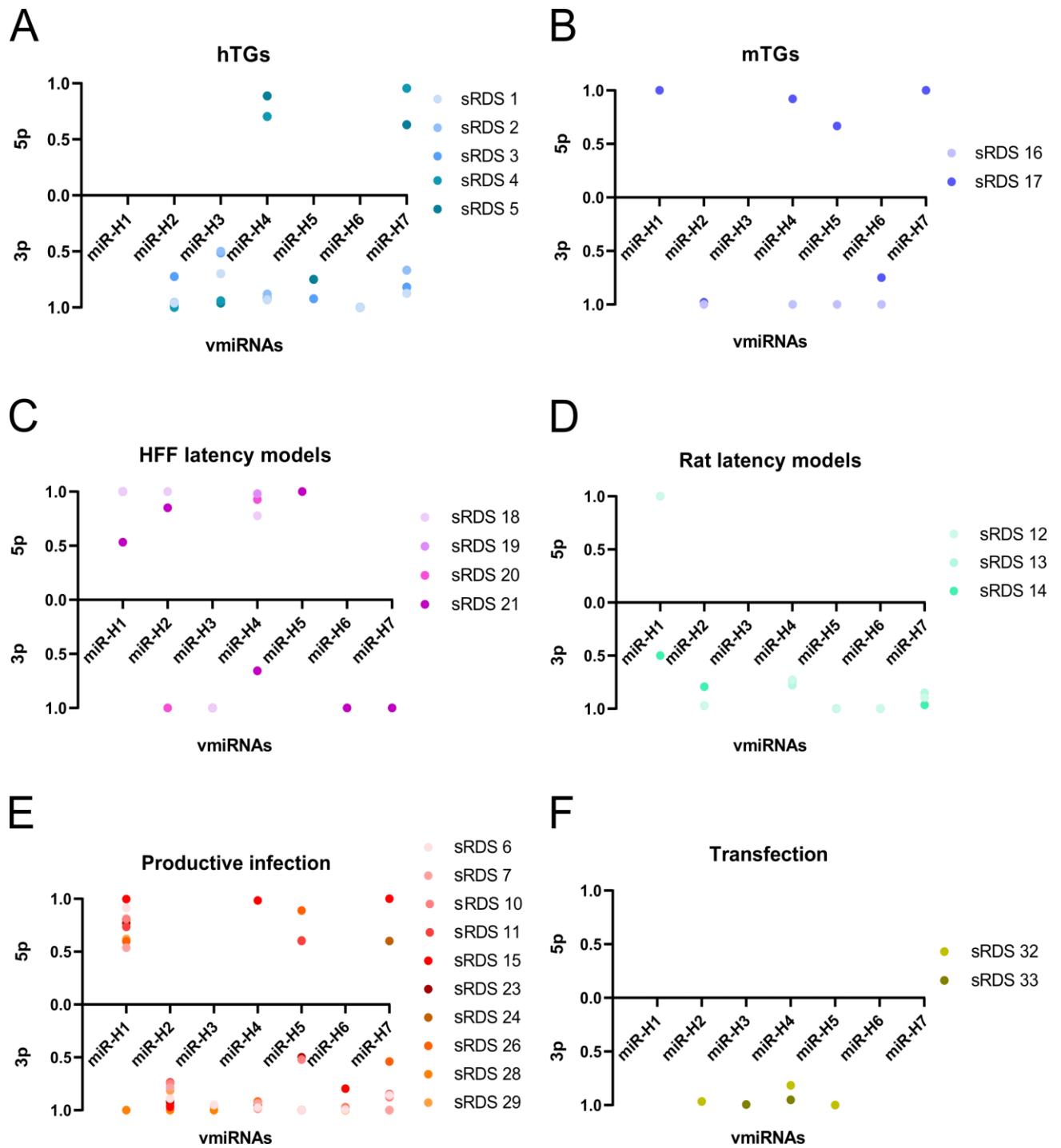


Figure 22: Fluctuating arm bias among detected arms of HSV-1 miRNAs. The fraction of the most dominant arm was calculated for HSV-1 miRNAs found in multiple samples with different conditions from miR-H1 to miR-H8. Arm bias is visible in A) latently infected hTG samples, B) latently infected mTG samples, C) HFF latency models, D) Rat DRG latency models, E) Productively infected samples, F) HSV-1 fragment transfection

4.4.2. Posttranscriptional modification detected in human trigeminal ganglia samples

4.4.2.1. HSV-1 miR-H2 seed sequence is significantly edited in neurons

In our analysis, we have observed a remarkably high frequency of changes in the seed sequence of miR-H2-3p but not in other HSV-1 miRNAs. It is well established that members of the ADAR protein family (ADARs) bind pri-miRNAs, and that, consequently, this miRNA editing plays an important role in miRNA regulation and function [138]. ADARs are predominantly nuclear enzymes responsible for A-to-I editing. Inosine (I) is structurally similar to guanosine (G) which causes I to cytidine (C) binding, and in the end, is recognized as G by the translation machinery. For that reason, we looked for all A to G changes in miRNAs throughout our samples.

HSV-1 miR-H2-3p showed a pattern of A-to-I editing within the seed predominantly at position 5, and to a lesser extent, at position 9. In latently infected hTGs, miR-H2-3p displayed more than 20% of editing at position 5, and in animal models percentage of edited cells is around 10%, while in productively infected cells, it was not detectable, or it reached a maximum of 13% in the later phase of productive infection (Figure 23). These events could represent a mechanism of the virus to increase HSV-1 miR-H2 repertoire to target and promote latency.

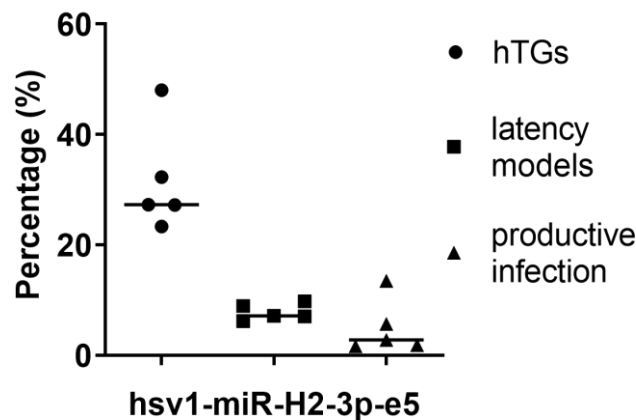


Figure 23: Percentage of edited HSV-1 miR-H2 reads on position 5 in the hairpin. Percentage of A>G changes was calculated for hTG samples (circles), latency models (squares) and productive infection samples (triangles). HSV-1 miR-H2 gets edited more frequently in human trigeminal ganglia than in other latency models or productively infected cells.

To show that these changes are actual post-transcriptional editing events, genomic sequences from HSV-1-BAC and most relevant samples prepared in our laboratory, human TG 4 and 5 that show 48% and 27.27% edited sequences,

respectively, were amplified and sequenced. Sequencing results show the wt sequence in the DNA of miR-H2 locus on positions where we can strongly detect a pattern of seed editing event, which strongly indicates the post-transcriptional editing event of this sequence (Figure S15).

Sequence variations of miR-H2-3p represent predominantly editing events, therefore, to analyze the impact of miR-H2-3p editing of the seed sequence (up to 40%) at position 5 in the hairpin, we focused on their potential targets (Figure 24A). Both TargetScan [97] and miRDB [98] analyses show that in the human genome, the putative targets of canonical and edited sequence are different compared to a higher overlap of the targets of the same sequence but between two tools, which indicates that this nt change had an impact on the targetome of miR-H2-3p (Figure 24B). Mapping of the first 15 nt from the miR-H2-3p-wt and miR-H2-3p-e5 to the HSV-1 strain KOS genome (JQ673480.1) using Bowtie alignment tool showed that only a smaller number of targets was shared between sequences (Figure 24C). A complete list of predicted targets is shown in Table S6. This could indicate that with this post-transcriptional modification, miR-H2-3p could potentially expand the target repertoire and target another HSV-1 immediate-early gene, ICP4.

A

CCUGAGCCAGGGACGAGUGCGACU - hsv1-miR-H2-3p-wt
 ..CCUGGGCCAGGGACGAGUGCGACU - hsv1-miR-H2-3p-e5
 ..CCUGAGCCGGGGACGAGUGCGACU - hsv1-miR-H2-3p-e9
 ..CCUGGGCCGGGGACGAGUGCGACU - hsv1-miR-H2-3p-e5-9

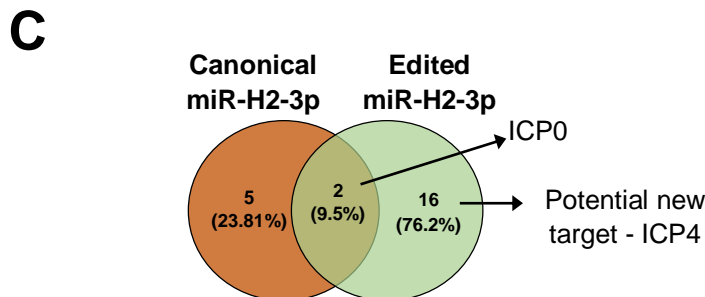
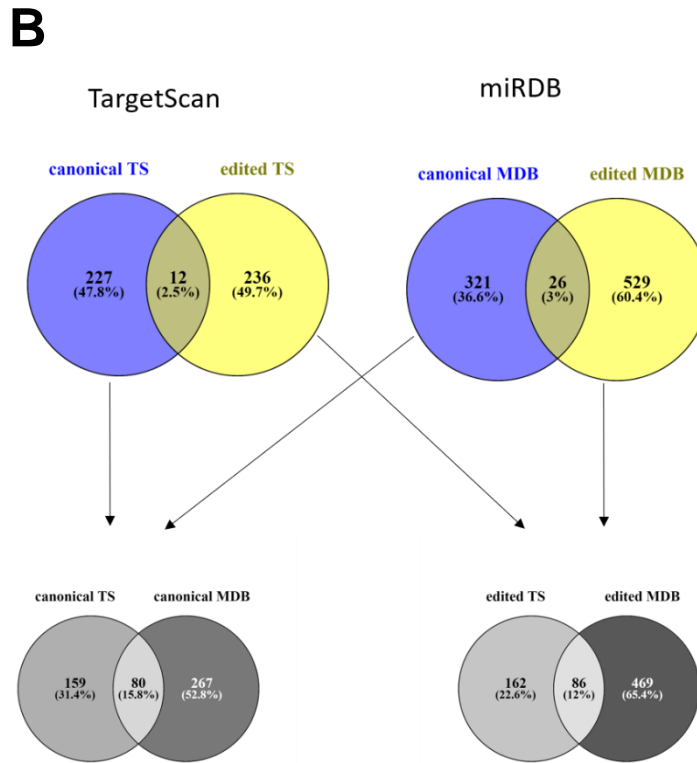


Figure 24: Editing position of miR-H2 and its change in targeting potential. A) Sequences of hsv1-miR-H2-3p-wt and edited sequences are shown with red letters at indicated positions –e5, e9, or both –e5-9. The seed sequence is marked within the yellow box. B) Predicted human targets of canonical (blue) miR-H2-3p and edited miR-H2-3p (yellow) using TargetScan (light gray) and miRDB (dark gray). C) Predicted HSV-1 targets of the wt (brown) and edited (green) miR-H2-3p sequence using Bowtie alignment tool by mapping the first 15 nt from the miR-H2-3p-wt and miR-H2-3p-e5 to the HSV-1 strain KOS genome (JQ673480.1).

4.4.3. Functional analysis of edited miR-H2-3p

4.4.3.1. *HSV-1 miR-H2-3p-wt and miR-H2-3p-e5 target both ICP0 and ICP4.*

To examine whether miR-H2-3p edited on positions 5 and/or 9 could affect ICP0 or ICP4 protein levels, we transfected HEK293 cells with a wild-type ICP0 or ICP4 expression plasmid together with pEGFP plasmid. Plasmids were co-transfected with microRNA mimics: canonical miR-H2-3p (miR-H2-3p-wt), a mutated seed sequence of the miR-H2-3p (miR-H2-3p-mut), negative control mimic, edited miR-H2-3p on position 5 and/or 9 in mature miR-H2-3p miRNA (miR-H2-3p-e5, miR-H2-3p-e5, miR-H2-3p-e5-9). As shown in Figure 25, the canonical miR-H2-3p reduced both ICP0 and ICP4 protein levels. The same strong effect was detected using miR-H2-3p-e5. Reduction of both ICP0 and ICP4 was observed, to a lesser degree, with miR-H2-3p-e9 mimic, indicating that these edited molecules also contribute to downregulating the analyzed targets. However, we observed the same level of ICP0 and ICP4 reduction with a co-transfected miR-H2-3p-e5-9 mimic (edited at both positions 5 and 9) as with miR-H2-3p-e9 mimic. The level of these proteins was unaffected by the miR-H2-3p-mut and negative control mimic.

The reduction of ICP4 by miR-H2-3p-wt was inconsistent with previously shown data [50]. Mapping miR-H2-3p-wt and edited sequences to the sequence of ICP0 or ICP4 using RNAhybrid [139], we observed a number of potential loci with seed pairing and low minimum free energy (Table S7).

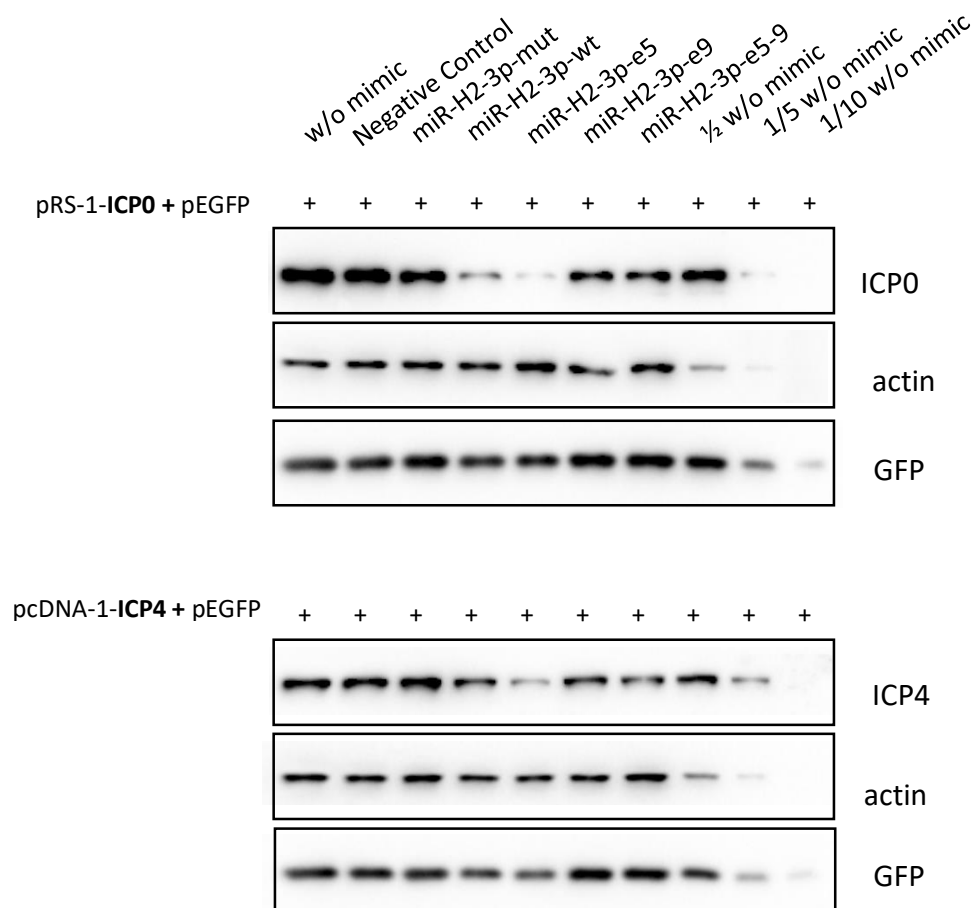


Figure 25: Downregulation of ICP0 and ICP4 protein level by HSV-1 miR-H2-3p-wt, edited at position 5 (miR-H2-3p-e5). HEK293 cells were transfected with pEGFP expression plasmid and either ICP0 or ICP4 expression construct. Samples were co-transfected with canonical or edited mimics of miR-H2-3p. Proteins were isolated and observed by Western blot.

4.4.1.3.1. Most relevant isomiR miR-H1-5p variations and the effect of sequence variation on its predicted function

To examine extensive sequence variations of miR-H1-5p, one of the miRNAs most abundantly expressed during the productive phase and of miR-H2-3p, profusely edited during the latent infection, we employed bioinformatic analysis to search for their targets. The importance of these sequence variations is the impact on their seed sequence and, consequently, their target. Therefore, these isomiRs were studied in detail, and targets were predicted based on TargetScan custom and miRDB [97, 98], and overlap has been made based on 2 prediction programs. Only isomiRs with more than 50 RC were considered.

Since miR-H1-5p is the third most dominant HSV-1 miRNA detected during productive infection and showed a very high number of variants in our datasets,

especially at the 5' end, which is important for binding to target, we further focused on the analysis of isomiRs for this miRNA. Figure 26A shows the individual modifications for isomiRs that have a high read count (≥ 50) for miR-H1-5p aligned with the annotated miRBase sequence and part of the genomic sequence to differentiate between TA and NTA Figure 26B

IsomiR_1 with 5' deletion and with 3' two nt TA was the most dominant isomiR, and compared to the annotated miRNA, which was ranked 5th among all the sequence variants of this miRNA, the expression profile of the predominant isomiR was about 8 times higher than the canonical sequence. Figure 26C shows the comparison of the targeting potential of the annotated miR-H1-5p sequence compared to the two most abundant isomiRs (1 and 2) using TargetScan and miRDB tools. Both TargetScan and miRDB analyses show that the putative targets of the three variants are very different. Only a smaller number of targets was shared between different isomiRs.

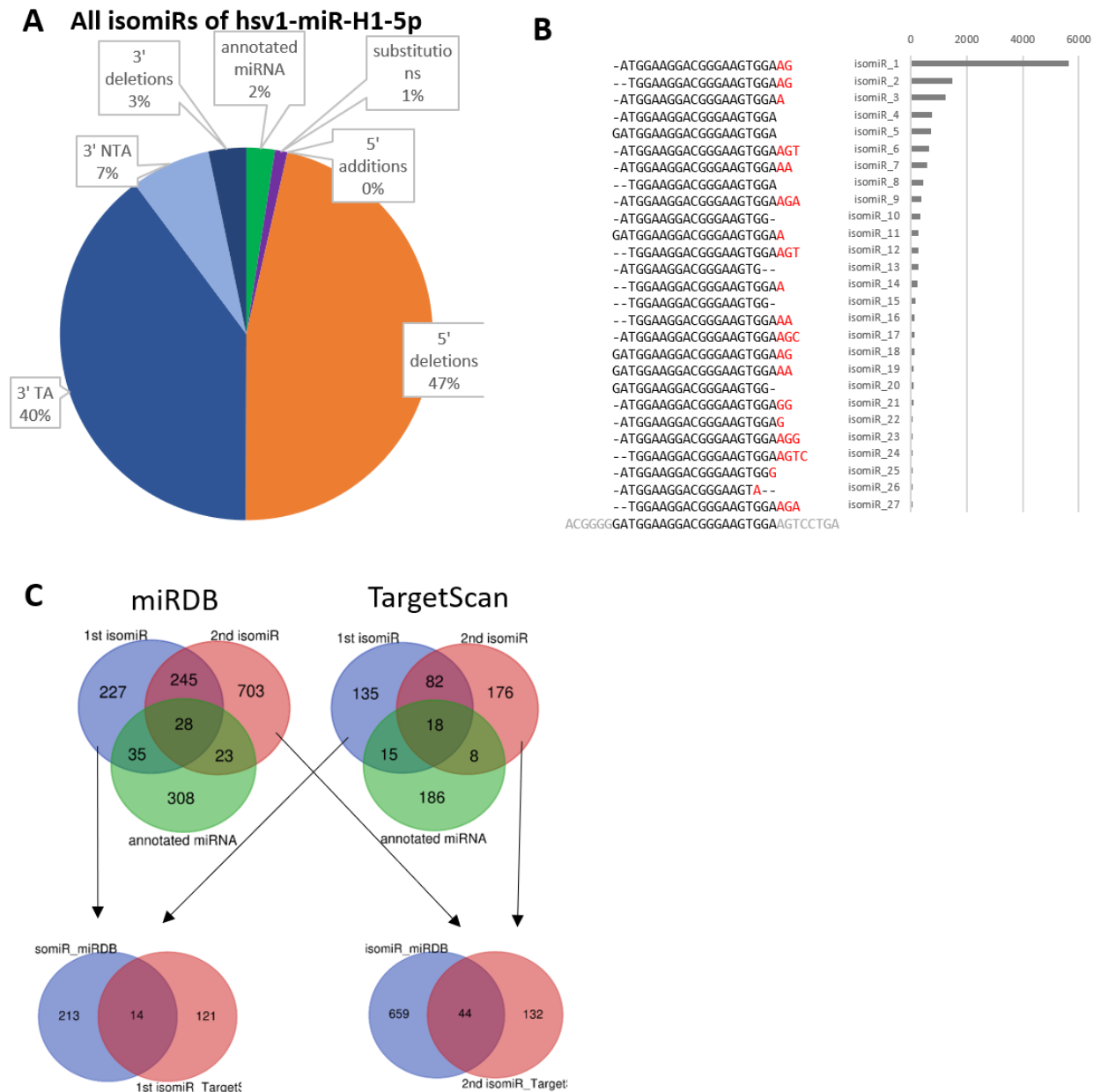


Figure 26: miR-H1-5p isomiR classification and change in the targeting potential of annotated miR-H1-5p and its two most abundant isomiRs. A) miR-H1-5p has a large number of 5' isomiRs which can affect its targeting efficiency. B) Most abundant isomiRs of miR-H1 and their expression. C) Predicted targets of annotated miR-H1 sequence and its two most abundant isomiRs.

4.4.4. HSV-1 miRNA processing and loading into the RISC

Finally, to determine and define all true HSV-1 miRNAs that are actually loaded into the RISC and therefore are likely biologically relevant, we performed Ago immunoprecipitation (Ago IP). We prepared infected HFF samples in triplicates and extracted them at 12 hpi. From each sample, a fraction (1/10) was taken for the total

population of miRNAs before the immunoprecipitation protocol, and the rest of the sample was split and used for Ago and GFP immunoprecipitation (control). Final products were used for the preparation of libraries for small RNA sequencing.

After the bioinformatic analysis, we detected a lot of small reads, probably degradation products, as they map to and match miRNA sequences in a small percentage (Table 8). Further analysis of HSV-1 mapped reads revealed a set of reads that mapped to miRNA hairpins, and remarkably, miR-H8-3p (with p-value less than or equal to 0.001), followed by miR-H2-5p, miR-H3-3p, miR-H6-3p, and miR-H11 (p-value less than or equal to 0.01), and lastly, miR-H1-3p, miR-H2-3p, miR-H3-5p, miR-H4-5p, miR-H4-3p (p-value less than or equal to 0.05) were significantly represented sequences in Ago IP samples (Figure 27).

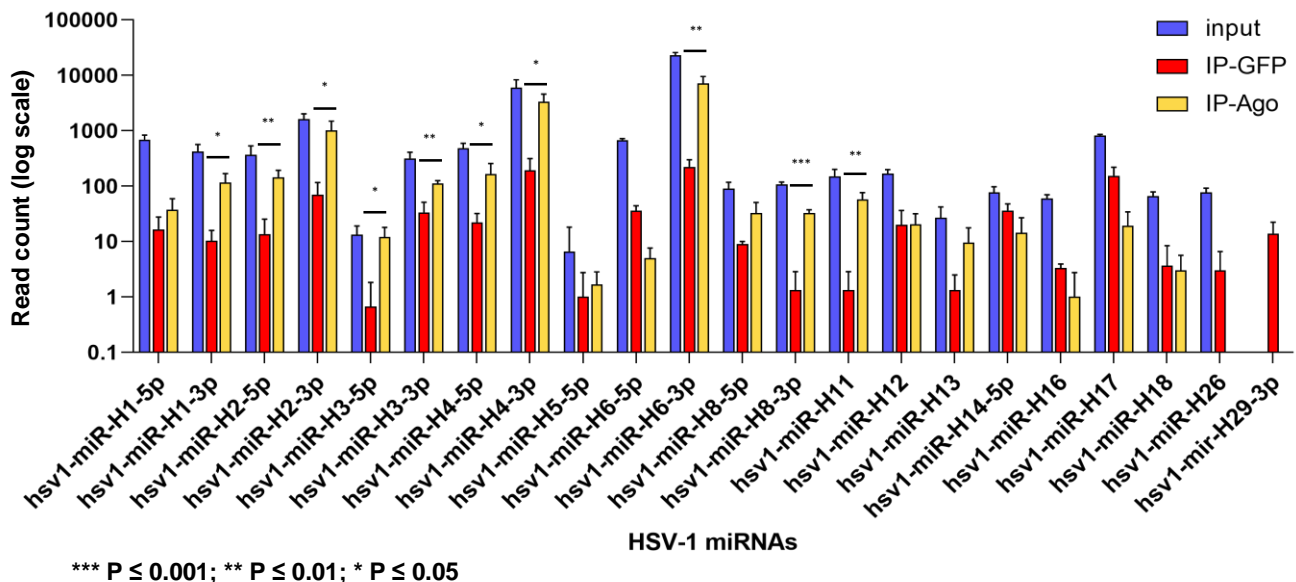


Figure 27: HSV-1 miRNAs found in Ago immunoprecipitation samples and sequencing experiment. The amount of miRNAs is represented in average read counts (RC) found in triplicates. Blue bars represent miRNAs detected in a total fraction multiplied by 10. Red bars represent GFP immunoprecipitation, and yellow bars represent Ago immunoprecipitation samples. The asterisks above bars represent the significance of the difference between miRNAs found in Ago-IP compared to GFP-IP samples: *** p ≤ 0.001; ** p ≤ 0.01; * p ≤ 0.05

5. DISCUSSION

Deregulation of the host miRNAs has been observed in a number of studies of various virus infections, including studies involving HSV-1 [75-87], as viruses profoundly change the landscape of the host miRNA expression during the course of infection. However, the discrepancies between the different studies (i.e., deregulated miRNAs) were quite significant, indicating a strong dependence on the miRNAome of the cells used in the experiments. For that reason, the first aim of this study was to comprehensively investigate changes in host miRNAs expression during productive infection, where we wanted to detect any changes in the expression of other microRNAs that have not been fully explored in previous studies. We analyzed seven host miRNAs in four primary cells (HFF, WI-38, MEF and BMDM) and two cell lines (HEK-293 and SH-SY5Y) at different time points after infection. In addition, we sequenced the whole transcriptome of HFF cells infected with HSV-1. Analysis of host miRNAs revealed a number of deregulated miRNAs in HSV-1 infection.

Our results showed that three miRNAs previously shown as upregulated, miR-182, miR-96 and miR-183, were found significantly and frequently upregulated in fibroblast cells (WI38 and HFFs). A recent study by Kim et al. in which the authors analyzed the miRNA expression in tears of patients with herpes epithelial keratitis and found that among many, miR-182 and miR-183 were upregulated, supports the idea that the activation of miR-183/96/182 represents the innate antiviral response to HSV-1 infection [87]. Similarly, the same cluster has been found upregulated after HSV-1 infection in primary neurons [77] and also in other herpesvirus infections [95] and completely distant RNA viruses [140-142], which indicates a conserved innate antiviral response mechanism.

Surprisingly, we have not detected statistically significant changes for most analyzed miRNAs in any tested cell type, previously reported upregulated in multiple cell lines. The discrepancies in the deregulation of host miRNAs described in studies and our results in cancer cell lines can be explained by the fact that cancer cell lines can have dramatically altered miRNAomes [143], which probably masks the potential upregulation. Another possibility is that the pathways leading to the transcriptional activation of the cluster are lost in cancer cells.

Multiple studies analyzed miR-183/-96/-182 indicating an important role in controlling innate and adaptive immunity (reviewed in [144]). It has been shown that

miRNAs of the cluster target protein phosphatase 2 catalytic subunit alpha (PPP2CA) and tripartite motif containing 27 (TRIM27), a negative regulator of IRF3, STAT1, and TBK1 [142], promote IFN production and signaling. The enhanced IFN signaling can reduce virus replication, as shown for the vesicular stomatitis virus. Moreover, Stittrich et al. showed that the signal transducer and activator of transcription 5 (STAT5)-mediated activation of miR-182 by interleukin 2 receptor (IL-2R) initiates a positive feedback response by targeting FoxO1 and promotes the clonal expansion of activated helper T lymphocytes [145]. Taken together, one might expect that the upregulation of the miR-183/96/182 cluster will affect HSV-1 infection; however, our results show that this is not the case, which is not surprising.

In fact, HSV-1 has developed numerous mechanisms to circumvent the host antiviral defense of the cell, including various functions of incoming virion/tegument proteins and proteins expressed after infection. For example, only the TBK-1/IRF3/IFN axis is targeted by at least five viral proteins, ICP0, ICP27, ICP34.5, US3, and vhs (reviewed in [11, 146]). This indicates that activation of the miR-183/96/182 cluster might be part of an early cellular response to virus infection, preceding the adaptation of large DNA viruses to it. However, Oussaief et al. found that the expression of the miR-183/96/182 cluster is repressed in cells latently infected with EBV, which is facilitated by EBV-encoded latent membrane protein 1 (LMP-1) [96]. These results show that, for the virus, the roles of the miR-183/96/182 cluster in the latency program might be in contrast with productive infection and that their control might be required to enable efficient latent infection. It is difficult to predict a role for these miRNAs in the establishment and/or maintenance of HSV-1 latent infection, particularly in the absence or limited ICP0 expression [78], nonetheless, to elucidate the role of miR-183/96/182 in the establishment and maintenance of latency more research needs to be conducted.

Interestingly, we detected miR-182-5p and miR-183-5p significantly expressed in Ago IP samples (Figure S16), indicating their function in targeting, except miR-96. However, this may be due to the low number of reads for this miRNA.

On the other hand, the question is if miRNAs can have any meaningful role during productive HSV-1 infection. First, productive HSV-1 infection is rather rapid, in contrast to protracted CMV replication, and inevitably leads to the destruction of the infected cell. Second, it has been shown that HSV-1 interferes with miRNA function and biogenesis at the stage of nuclear export [31, 147], which limits the potential of miRNA

regulation in general. Thus, it would be rather surprising that miRNAs, which accumulate late in infection, can exert a relevant control of the genes. Indeed, in our study, we show that the protein levels of members of the FoxO protein family, the confirmed targets of miRNAs of the upregulated cluster, increased early in infection, followed by a decrease late in infection. The late phenomenon might be contributed to the regulation of miRNAs; however, the same observation was true in cells in which we did not detect an increase in miRNAs after infection. Thus, we can conclude that miR-183, -96, and -182, at best, have a minor contributing role in this process. Nonetheless, although we were not able to establish a hypothesized regulatory feedback loop, further analysis of predicted targets mutual among miR-182/96/183 directed us towards the Forkhead box O (FoxO) family of transcription factors.

Given that FoxO transcriptional factors play an important role in cell survival and innate antiviral response [101-103], we hypothesized that they are the target of HSV-1 regulation. We were very intrigued with the expression of the FoxO protein family members – we observed that HSV-1 infection increases FoxO1 and FoxO3 protein and transcript levels but not FoxO4 very early in infection and that early induction depends on MOI. That effect may be caused either by the virus or a cell. Several studies have shown that FoxO1 and FoxO3 inhibit the transcription of IRF3 and IRF7 proteins, resulting in suppression of IFN- β production which is caused by virus or poly(I:C). Also, many studies have shown that certain HSV-1 IE proteins, such as ICP0, ICP27 and regulatory tegument proteins, reduce IFN- β production by different mechanisms in the early stages of infection [148]. Therefore, it is possible that certain HSV-1 factors promote FoxO upregulation for the purpose of cell survival and suppression of the innate immune response at the onset of HSV-1 infection.

Although we focused on studying the phenomenon of FoxO increase in the beginning, we observed a decrease in the later stages of the infection, and one of the potential mechanisms of FoxO inactivation is ICP0-mediated protein degradation. Numerous cellular proteins have been identified as targets of ICP0 ligase that characterizes cellular proteins for ubiquitination for the purpose of regulating the transition from productive to latent infection or merely regulating productive infection. It is possible that, at this stage of infection, the virus limits the infection by increasing the expression level of the above-mentioned host miR-182/96/183, which target FoxO proteins, in order to reduce the visibility of productive infection. However, additional

analyses are necessary to examine these indications, in order to examine potential alternative mechanisms of regulation of FoxO expression.

After investigating the expression profile of FoxO1 and FoxO3 proteins, we wanted to determine their localization in the cell during productive HSV-1 infection. We observed that FoxO1 and FoxO3 proteins accumulated along the nucleus at a certain stage of infection. Further analysis showed that FoxO1 aggregates accumulate in the cis-Golgi network. Late virus protein gC was found in the same compartment alongside FoxO1. The reason for the accumulation of FoxO1 protein in cis-Golgi during the later phase of infection is unknown, but the endoplasmic reticulum and Golgi apparatus are the main sites of accumulation of some other cellular proteins during viral infection, especially proteins necessary for viral particle formation and new viral progeny in which processes Us3 virus kinase plays a major role [149]. Since FoxO1 is a substrate of this kinase, it is possible that these clusters are accumulated phosphorylated FoxO1 proteins, assuming that the antibody used binds the phosphorylated form, as observed by Western Blot analysis (Figure 11).

Finally, to elucidate the importance of FoxO proteins for HSV-1 replication, we required FoxO KO cell lines to observe how their absence affects the progression of HSV-1 infection. In publications, it has been shown that worms lacking homologous gene *daf-16* or *D. melanogaster* lacking dFoxO homolog in flies are viable [150]. However, mice lacking FoxO1 are not viable; it has been demonstrated that they die at embryonic day 10.5 due to angiogenesis defects [151]. FoxO3 and FoxO4 mice are viable [152-154]. In other studies, researchers were successful in generating CRISPR-Cas9 KO cell lines, and for that reason, we employed CRISPR-Cas9 technology to generate FoxO KO cell lines. We showed that in cells devoid of FoxO1 or FoxO3 expression, HSV-1 replication is as efficient as in WT cells, indicating that individual FoxO proteins are not required for efficient replication.

Given that we observed almost the same pattern of behavior of FoxO1 and FoxO3, we hypothesize that they act similarly, potentially because of the possibility of their redundant function, i.e., the ability to take over each other's function in the event of loss of activity of another family member. These compensatory functions of other members might explain the lack of a phenotype, or these proteins might exert their role in latency. It is important to mention that we were not able to generate cells in which FoxO4 or all FoxO proteins were inactivated. In contrast to our observation, roles for individual FoxO proteins have been shown for EBV and KSHV. For example,

it has been shown that in EBV-positive advanced nasopharyngeal carcinoma cells, which exhibit type II latency, EBV LMP1 modulates the PI3K/AKT/FoxO3 pathway, resulting in the accumulation of FoxO3 phosphorylation. This inactivation of FoxO3 led to the induction of miR-21, which, in turn, downregulated programmed cell death 4 (PDCD4) and Fas ligand and reduced apoptosis [106]. In addition, Liu et al. showed that in EBV-associated gastric cancer cells that showed type I/II latency, the FoxO1, FoxO3, and FoxO4 protein levels were significantly lower when compared to the control cells. Interestingly, *FoxO1* mRNA was downregulated, but not *FoxO3* or *FoxO4* mRNAs, suggesting diverse regulatory mechanisms by various EBV latent genes [107]. Similarly, FoxO1 has been shown to sufficiently suppress KSHV lytic replication and maintain latency by controlling the levels of reactive oxygen species (ROS) since the disruption of FoxO1 could trigger KSHV reactivation and induce lytic infection by increasing the cellular ROS level [108]. On the other hand, a recent study investigating HCMV has shown that FoxO1 and FoxO3 positively regulate virus lytic gene expression by activating alternative major immediate-early gene promoters and promoting IE re-expression and virus reactivation [109]. Taken together, our study shows that individual FoxO proteins are not required for efficient virus replication; however, more research, and likely, an adequate in vitro latency model, is needed to understand their roles in HSV-1 latency.

In the second part of the project, we aimed to comprehensively analyze HSV-1 miRNAs and to set the criteria which, in the future, could serve as guidelines for the selection of other viral miRNAs. From the first identification of HSV-1 miRNAs to today, 29 mature HSV-1 miRNAs were defined. However, results were inconsistent and showed great variability in sequence, indicating that, to this day, some basic knowledge, such as their true sequence, is not yet clarified. Reported HSV-1 miRNAs never underwent comprehensive re-analysis, including the same bioinformatics conditions and parameters. Moreover, the difference in virus strains, their expression in both phases of the HSV-1 infection and reproducibility in different hosts were never taken into account. For that reason, we hypothesized that some of them could represent only the degradation products, and our first aim was to evaluate all previously and newly discovered HSV-1 miRNAs.

Our bioinformatics analysis on separate data sets of HSV-1 infected samples went toward a comprehensive and critical analysis of HSV-1 miRNAs. We collected

all publicly available data sets and ones previously prepared in our laboratory. We found that, while all reported miRNA sequences can be detected in productive infection, only a few sequences are abundant in latently infected samples, similar to the profiles shown before [42, 44, 50].

To analyze HSV-1 miRNAs expressed in human tissues in detail (i.e., genuine latent infection in humans), we generated small-RNA libraries from the extracted RNAs (TruSeq small RNA sample preparation kit, Illumina) and sequenced these samples. However, it can be argued that this data set was not deep enough or sufficiently sensitive to detect all possible miRNAs to address our questions regarding HSV-1 miRNAs. Nevertheless, taking that into account, we reasoned that less abundant data sets at least defined a profile of miRNAs, especially including human trigeminal ganglia samples where even in such low abundancies, editing events could be detected. Undoubtedly, deeper sequencing might reveal additional miRNAs in the samples, but the proportion and the importance of the most prevalent miRNAs will not change [114].

We detected only five miRNAs, miR-H2, -H3, -H4, -H6 and miR-H7 (i.e., specific HSV-1 miRNA profile characteristic for latent samples), which resemble the HSV-1 miRNA expression pattern in human ganglia obtained by Umbach et al., however, we did not detect miR-H5 and miR-H8, which were detected previously through a low number of reads [50]. We observed that pre-miRNA and miRNA sequences are remarkably well-conserved among all HSV-1 strains and that sequence preservation in these regions indicates great biological importance in mRNA silencing.

However, in our analysis of productive infection, we show that the sequences of known miRNAs do not precisely match the currently available information in the miRNA databases (miRBase) [121]. The knowledge of the exact sequences of miRNAs is crucial for the target predictions and functional test and detection assays (RT-qPCR). Therefore, we aimed to correct these sequences.

We and others have observed that HSV-1, similar to other viruses (e.g., EBV [137]), shows reduced “arm bias”, a phenomenon that only one arm of the miRNA duplex is retained and functional, whereas the other arm is rapidly degraded, as shown in Figure 27 where both arms of a number of miRNAs are represented bound to Ago. It is unclear why the 3p and 5p arms of the miRNA duplex are similarly represented, but it might be explained by a small coding capacity and a need to exploit the capacity of the genome most efficiently.

Another way for HSV-1 to expand the target repertoire of its miRNAs and exploit the capacity of the genome could be a remarkably high frequency of posttranscriptional modifications. We have combined a number of relevant human HSV-1 latency samples and selected miRNAs that occur reproducibly and a number of latency models. We observed a significant difference within the seed region of miR-H2-3p but not significantly in other HSV-1 miRNAs predominantly in human TG samples. Many factors can be the reason for these differences, for example duration of the latency, i.e. animal latency models were followed up to 30 days [8, 42, 155], and *in vitro* latency models, which may be difficult to establish and are not yet well characterized. The observed phenomenon that includes A-to-I editing of miR-H2-3p can play a role, for example, in miRNA biogenesis processes to regulate Drosha and Dicer cleavage or RISC complex loading potential. Interestingly, while editing of EBV miR-BART6 dramatically reduced the loading of miR-BART6-5p in the RISC [37], we observed the opposite. The percentage of edited HSV-1 miR-H2-3p on position 5 in Ago IP samples was equal to its percentage in productive infection (Figure 23), i.e., loading potential of edited miR-H2 sequences did not change (Table S8). It has been shown multiple times how the change within the seed sequence, even in a single nucleotide, can impact a target sequence and the stability of miRNA (reviewed in [21]). We searched for the targets of edited sequences to determine if the change within the seed sequence of miR-H2-3p would change its selectivity for the ICP0 transcript and/or target other HSV-1 transcripts. Umbach et al. showed that miR-H2 impacts the expression of the ICP0 transcript, which is located antisense to miR-H2, but not ICP4, another important IE gene [50]. However, in our data, we can detect an impact on the expression of ICP4, indicating an increase in targeting potential to target genes important for the reactivation from latency. The fact that edited miR-H2-3p can target both ICP0 and ICP4 strongly indicates the importance of these genes for the maintenance/reactivation process (Figure 25).

We can discuss that the observed differences between our study and the previous studies might be due to differences in applied sequencing technologies. Our results indicate that more basic investigations are needed, particularly a comparative analysis of clinical samples, or a more detailed characterization of latency models and the differences in transcription of transfected samples compared to the truly infected samples, to understand the fundamentals of HSV-1 miRNA expression thoroughly.

6. CONCLUSIONS

- Host miRNAs expressed from a single transcriptional cluster, miR-183, -96, and -182, were reproducibly upregulated and showed the highest level of deregulation in the productive phase of HSV-1 infection in fibroblasts.
- 33 potential targets were identified as shared by all three miRNAs mentioned above, and among these, FoxO1 was identified as a potential target for all three miRNAs, and two other members of the Forkhead box protein family, FoxO3 and FoxO4, were found as potential targets for miR-182 and miR-96, and solely miR-96, respectively.
- We hypothesized that the increase in miRNAs miR-96, -182, and -183 would consequently lead to decreased levels of the FoxO family members. However, we observed FoxO1 and FoxO3 downregulation in cells in which we did not observe upregulated levels of miR-183/96/182 during infection, indicating additional mechanisms other than miRNAs for the depletion of FoxO family members late in infection, and evidence points to viral protein ICP0.
- Additionally, FoxO1 and FoxO3 were upregulated and then downregulated during productive HSV-1 infection, and strongly upregulated during MCMV infection.
- FoxO1 and FoxO3 proteins are induced as a result of an immune response to viral infection. However, they do not play a significant role in HSV-1 replication.
- By categorizing HSV-1 miRNAs, we show that the profile of miRNAs described as “high confidence miRNAs” is similar to Drosha-dependent miRNAs and includes miRNAs from miR-H1-miR-H8; “tentative miRNAs” include miR-H11 - miR-H14, miR-H16 and miR-H27; and “low confidence miRNAs” identify miR-H15, miR-H17 - miR-H26 and miR-H28 - miR-H29, which suggests that some of the previously published miRNAs may not be original regulatory molecules but rather sequencing artifacts.
- We described the high frequency of HSV-1 isomiRs and the most dominant sequence of many HSV-1 miRNAs detected in different phases of the HSV-1 infection, as it was different from the sequences deposited in miRBase, which might significantly affect downstream functional analyses.
- HSV-1 miR-H2-3p seed sequence gets significantly edited in latently infected human TGs. Our functional analysis showed that edited molecules contribute to the downregulation of the HSV-1 ICP0 and ICP4 proteins, which could represent a mechanism of the virus to increase HSV-1 miR-H2 repertoire to target and promote latency.

- Many HSV-1 miRNAs are found, including hsv1-miR-H2-3p-e5 in Ago immunoprecipitation samples suggesting their biological function.

7. REFERENCES

1. James, C., et al., Herpes simplex virus: global infection prevalence and incidence estimates, 2016. *Bull World Health Organ*, **2020**. 98(5): p. 315-329 DOI: 10.2471/BLT.19.237149.
2. Roizman, B.K., DM.; Whitley RJ, *Fields virology*. 6 ed. ed. **2013**, Philadelphia, PA: Lippincott Williams & Wilkins.
3. Elbadawy, H.M., et al., Targeting herpetic keratitis by gene therapy. *J Ophthalmol*, **2012**. 2012: p. 594869 DOI: 10.1155/2012/594869.
4. Madavaraju, K., et al., Herpes Simplex Virus Cell Entry Mechanisms: An Update. *Front Cell Infect Microbiol*, **2020**. 10: p. 617578 DOI: 10.3389/fcimb.2020.617578.
5. Jackson, S.A. and N.A. DeLuca, Relationship of herpes simplex virus genome configuration to productive and persistent infections. *Proc Natl Acad Sci U S A*, **2003**. 100(13): p. 7871-6 DOI: 10.1073/pnas.1230643100.
6. Duarte, L.F., et al., Crosstalk Between Epithelial Cells, Neurons and Immune Mediators in HSV-1 Skin Infection. *Front Immunol*, **2021**. 12: p. 662234 DOI: 10.3389/fimmu.2021.662234.
7. Knipe, D.M. and A. Cliffe, Chromatin control of herpes simplex virus lytic and latent infection. *Nat Rev Microbiol*, **2008**. 6(3): p. 211-21 DOI: 10.1038/nrmicro1794.
8. Kramer, M.F., et al., Herpes simplex virus 1 microRNAs expressed abundantly during latent infection are not essential for latency in mouse trigeminal ganglia. *Virology*, **2011**. 417(2): p. 239-47 DOI: 10.1016/j.virol.2011.06.027.
9. Banerjee, A., S. Kulkarni, and A. Mukherjee, Herpes Simplex Virus: The Hostile Guest That Takes Over Your Home. *Front Microbiol*, **2020**. 11: p. 733 DOI: 10.3389/fmicb.2020.00733.
10. Danastas, K., M. Miranda-Saksena, and A.L. Cunningham, Herpes Simplex Virus Type 1 Interactions with the Interferon System. *Int J Mol Sci*, **2020**. 21(14) DOI: 10.3390/ijms21145150.
11. Su, C., G. Zhan, and C. Zheng, Evasion of host antiviral innate immunity by HSV-1, an update. *Virol J*, **2016**. 13: p. 38 DOI: 10.1186/s12985-016-0495-5.

12. Lanfranca, M.P., H.H. Mostafa, and D.J. Davido, HSV-1 ICP0: An E3 Ubiquitin Ligase That Counteracts Host Intrinsic and Innate Immunity. *Cells*, **2014**. 3(2): p. 438-54 DOI: 10.3390/cells3020438.
13. Everett, R.D., et al., Replication of ICP0-null mutant herpes simplex virus type 1 is restricted by both PML and Sp100. *J Virol*, **2008**. 82(6): p. 2661-72 DOI: 10.1128/JVI.02308-07.
14. Carr, D.J., et al., The lack of RNA-dependent protein kinase enhances susceptibility of mice to genital herpes simplex virus type 2 infection. *Immunology*, **2006**. 118(4): p. 520-6 DOI: 10.1111/j.1365-2567.2006.02403.x.
15. Lussignol, M., et al., The herpes simplex virus 1 Us11 protein inhibits autophagy through its interaction with the protein kinase PKR. *J Virol*, **2013**. 87(2): p. 859-71 DOI: 10.1128/JVI.01158-12.
16. Wylie, K.M., J.E. Schrimpf, and L.A. Morrison, Increased eIF2alpha phosphorylation attenuates replication of herpes simplex virus 2 vhs mutants in mouse embryonic fibroblasts and correlates with reduced accumulation of the PKR antagonist ICP34.5. *J Virol*, **2009**. 83(18): p. 9151-62 DOI: 10.1128/JVI.00886-09.
17. Dauber, B., J. Pelletier, and J.R. Smiley, The herpes simplex virus 1 vhs protein enhances translation of viral true late mRNAs and virus production in a cell type-dependent manner. *J Virol*, **2011**. 85(11): p. 5363-73 DOI: 10.1128/JVI.00115-11.
18. Yu, X. and S. He, The interplay between human herpes simplex virus infection and the apoptosis and necroptosis cell death pathways. *Viol J*, **2016**. 13: p. 77 DOI: 10.1186/s12985-016-0528-0.
19. Gottwein, E. and B.R. Cullen, Viral and cellular microRNAs as determinants of viral pathogenesis and immunity. *Cell Host Microbe*, **2008**. 3(6): p. 375-87 DOI: 10.1016/j.chom.2008.05.002.
20. Cullen, B.R., Viral and cellular messenger RNA targets of viral microRNAs. *Nature*, **2009**. 457(7228): p. 421-5 DOI: 10.1038/nature07757.
21. Bartel, D.P., Metazoan MicroRNAs. *Cell*, **2018**. 173(1): p. 20-51 DOI: 10.1016/j.cell.2018.03.006.
22. Yoshida, T., Y. Asano, and K. Ui-Tei, Modulation of MicroRNA Processing by Dicer via Its Associated dsRNA Binding Proteins. *Noncoding RNA*, **2021**. 7(3) DOI: 10.3390/ncrna7030057.

23. Kim, K., et al., A quantitative map of human primary microRNA processing sites. *Mol Cell*, **2021**. 81(16): p. 3422-3439 e11 DOI: 10.1016/j.molcel.2021.07.002.
24. Stavast, C.J. and S.J. Erkeland, The Non-Canonical Aspects of MicroRNAs: Many Roads to Gene Regulation. *Cells*, **2019**. 8(11) DOI: 10.3390/cells8111465.
25. Yoda, M., et al., ATP-dependent human RISC assembly pathways. *Nat Struct Mol Biol*, **2010**. 17(1): p. 17-23 DOI: 10.1038/nsmb.1733.
26. Khvorova, A., A. Reynolds, and S.D. Jayasena, Functional siRNAs and miRNAs exhibit strand bias. *Cell*, **2003**. 115(2): p. 209-16 DOI: 10.1016/s0092-8674(03)00801-8.
27. Schwarz, D.S., et al., Asymmetry in the assembly of the RNAi enzyme complex. *Cell*, **2003**. 115(2): p. 199-208 DOI: 10.1016/s0092-8674(03)00759-1.
28. Frank, F., N. Sonenberg, and B. Nagar, Structural basis for 5'-nucleotide base-specific recognition of guide RNA by human AGO2. *Nature*, **2010**. 465(7299): p. 818-22 DOI: 10.1038/nature09039.
29. Schirle, N.T., et al., Water-mediated recognition of t1-adenosine anchors Argonaute2 to microRNA targets. *Elife*, **2015**. 4 DOI: 10.7554/eLife.07646.
30. Zhang, F. and D. Wang, The Pattern of microRNA Binding Site Distribution. *Genes (Basel)*, **2017**. 8(11) DOI: 10.3390/genes8110296.
31. Pan, D., et al., Herpes Simplex Virus 1 Lytic Infection Blocks MicroRNA (miRNA) Biogenesis at the Stage of Nuclear Export of Pre-miRNAs. *mBio*, **2019**. 10(1) DOI: 10.1128/mBio.02856-18.
32. Tan, G.C., et al., 5' isomiR variation is of functional and evolutionary importance. *Nucleic Acids Res*, **2014**. 42(14): p. 9424-35 DOI: 10.1093/nar/gku656.
33. Aparicio-Puerta, E., et al., isomiRdb: microRNA expression at isoform resolution. *Nucleic Acids Res*, **2022** DOI: 10.1093/nar/gkac884.
34. Tomasello, L., et al., The MicroRNA Family Gets Wider: The IsomiRs Classification and Role. *Front Cell Dev Biol*, **2021**. 9: p. 668648 DOI: 10.3389/fcell.2021.668648.
35. Lerner, T., F.N. Papavasiliou, and R. Pecori, RNA Editors, Cofactors, and mRNA Targets: An Overview of the C-to-U RNA Editing Machinery and Its Implication in Human Disease. *Genes (Basel)*, **2018**. 10(1) DOI: 10.3390/genes10010013.

36. Paul, D., et al., Human Brain Shows Recurrent Non-Canonical MicroRNA Editing Events Enriched for Seed Sequence with Possible Functional Consequence. *Noncoding RNA*, **2020**. 6(2) DOI: 10.3390/ncrna6020021.
37. Iizasa, H., et al., Editing of Epstein-Barr virus-encoded BART6 microRNAs controls their dicer targeting and consequently affects viral latency. *J Biol Chem*, **2010**. 285(43): p. 33358-70 DOI: 10.1074/jbc.M110.138362.
38. Nachmani, D., et al., MicroRNA editing facilitates immune elimination of HCMV infected cells. *PLoS Pathog*, **2014**. 10(2): p. e1003963 DOI: 10.1371/journal.ppat.1003963.
39. Gandy, S.Z., et al., RNA editing of the human herpesvirus 8 kaposin transcript eliminates its transforming activity and is induced during lytic replication. *J Virol*, **2007**. 81(24): p. 13544-51 DOI: 10.1128/JVI.01521-07.
40. Pfeffer, S., et al., Identification of microRNAs of the herpesvirus family. *Nat Methods*, **2005**. 2(4): p. 269-76 DOI: 10.1038/nmeth746.
41. Cui, C., et al., Prediction and identification of herpes simplex virus 1-encoded microRNAs. *J Virol*, **2006**. 80(11): p. 5499-508 DOI: 10.1128/jvi.00200-06.
42. Jurak, I., et al., Numerous conserved and divergent microRNAs expressed by herpes simplex viruses 1 and 2. *J Virol*, **2010**. 84(9): p. 4659-72 DOI: 10.1128/jvi.02725-09.
43. Jurak, I., A. Griffiths, and D.M. Coen, Mammalian alphaherpesvirus miRNAs. *Biochim Biophys Acta*, **2011**. 1809(11-12): p. 641-53 DOI: 10.1016/j.bbagr.2011.06.010.
44. Umbach, J.L., et al., Analysis of human alphaherpesvirus microRNA expression in latently infected human trigeminal ganglia. *J Virol*, **2009**. 83(20): p. 10677-83 DOI: 10.1128/jvi.01185-09.
45. Enk, J., et al., HSV1 MicroRNA Modulation of GPI Anchoring and Downstream Immune Evasion. *Cell Rep*, **2016**. 17(4): p. 949-956 DOI: 10.1016/j.celrep.2016.09.077.
46. Munson, D.J. and A.D. Burch, A novel miRNA produced during lytic HSV-1 infection is important for efficient replication in tissue culture. *Arch Virol*, **2012**. 157(9): p. 1677-88 DOI: 10.1007/s00705-012-1345-4.
47. Wu, W., et al., A microRNA encoded by HSV-1 inhibits a cellular transcriptional repressor of viral immediate early and early genes. *Sci China Life Sci*, **2013**. 56(4): p. 373-83 DOI: 10.1007/s11427-013-4458-4.

48. Han, Z., et al., miR-H28 and miR-H29 expressed late in productive infection are exported and restrict HSV-1 replication and spread in recipient cells. *Proc Natl Acad Sci U S A*, **2016**. 113(7): p. E894-901 DOI: 10.1073/pnas.1525674113.
49. Jurak, I., et al., Expression of herpes simplex virus 1 microRNAs in cell culture models of quiescent and latent infection. *J Virol*, **2014**. 88(4): p. 2337-9 DOI: 10.1128/jvi.03486-13.
50. Umbach, J.L., et al., MicroRNAs expressed by herpes simplex virus 1 during latent infection regulate viral mRNAs. *Nature*, **2008**. 454(7205): p. 780-3 DOI: 10.1038/nature07103.
51. Tang, S., et al., An acutely and latently expressed herpes simplex virus 2 viral microRNA inhibits expression of ICP34.5, a viral neurovirulence factor. *Proc Natl Acad Sci U S A*, **2008**. 105(31): p. 10931-6 DOI: 10.1073/pnas.0801845105.
52. Tang, S., A. Patel, and P.R. Krause, Novel less-abundant viral microRNAs encoded by herpes simplex virus 2 latency-associated transcript and their roles in regulating ICP34.5 and ICP0 mRNAs. *J Virol*, **2009**. 83(3): p. 1433-42 DOI: 10.1128/jvi.01723-08.
53. Umbach, J.L., et al., Identification of viral microRNAs expressed in human sacral ganglia latently infected with herpes simplex virus 2. *J Virol*, **2010**. 84(2): p. 1189-92 DOI: 10.1128/jvi.01712-09.
54. Tang, S., et al., Herpes simplex virus 2 microRNA miR-H6 is a novel latency-associated transcript-associated microRNA, but reduction of its expression does not influence the establishment of viral latency or the recurrence phenotype. *J Virol*, **2011**. 85(9): p. 4501-9 DOI: 10.1128/jvi.01997-10.
55. Du, T., et al., Patterns of accumulation of miRNAs encoded by herpes simplex virus during productive infection, latency, and on reactivation. *Proc Natl Acad Sci U S A*, **2015**. 112(1): p. E49-55 DOI: 10.1073/pnas.1422657112.
56. Flores, O., et al., Mutational inactivation of herpes simplex virus 1 microRNAs identifies viral mRNA targets and reveals phenotypic effects in culture. *J Virol*, **2013**. 87(12): p. 6589-603 DOI: 10.1128/jvi.00504-13.
57. Pan, D., et al., Mutations Inactivating Herpes Simplex Virus 1 MicroRNA miR-H2 Do Not Detectably Increase ICP0 Gene Expression in Infected Cultured Cells or Mouse Trigeminal Ganglia. *J Virol*, **2017**. 91(2) DOI: 10.1128/jvi.02001-16.

58. Jiang, X., et al., A herpes simplex virus type 1 mutant disrupted for microRNA H2 with increased neurovirulence and rate of reactivation. *J Neurovirol*, **2015**. 21(2): p. 199-209 DOI: 10.1007/s13365-015-0319-1.
59. Kawamura, Y., et al., Herpes Simplex Virus 2 Latency-Associated Transcript (LAT) Region Mutations Do Not Identify a Role for LAT-Associated MicroRNAs in Viral Reactivation in Guinea Pig Genital Models. *J Virol*, **2018**. 92(14) DOI: 10.1128/jvi.00642-18.
60. Zhao, H., et al., MicroRNA-H4-5p encoded by HSV-1 latency-associated transcript promotes cell proliferation, invasion and cell cycle progression via p16-mediated PI3K-Akt signaling pathway in SHSY5Y cells. *Int J Clin Exp Med*, **2015**. 8(5): p. 7526-34.
61. Duan, F., et al., HSV-1 miR-H6 inhibits HSV-1 replication and IL-6 expression in human corneal epithelial cells in vitro. *Clin Dev Immunol*, **2012**. 2012: p. 192791 DOI: 10.1155/2012/192791.
62. Barrozo, E.R., et al., Deletion of Herpes Simplex Virus 1 microRNAs miR-H1 and miR-H6 Impairs Reactivation. *J Virol*, **2020** DOI: 10.1128/jvi.00639-20.
63. Pribanic Matesic, M., Puzzling functions of HSV-1 miRNAs in productive and latent infection. *Periodicum Biologorum*, **2020**. 121-122(3-4): p. 107-113 DOI: 10.18054/pb.v121-122i3-4.10561.
64. Jurak, I., et al., Herpes simplex virus is equipped with RNA- and protein-based mechanisms to repress expression of ATRX, an effector of intrinsic immunity. *J Virol*, **2012**. 86(18): p. 10093-102 DOI: 10.1128/jvi.00930-12.
65. Zheng, K., et al., HSV-1-encoded microRNA miR-H1 targets Ubr1 to promote accumulation of neurodegeneration-associated protein. *Virus Genes*, **2018**. 54(3): p. 343-350 DOI: 10.1007/s11262-018-1551-6.
66. Naqvi, A.R., et al., Viral miRNAs Alter Host Cell miRNA Profiles and Modulate Innate Immune Responses. *Front Immunol*, **2018**. 9: p. 433 DOI: 10.3389/fimmu.2018.00433.
67. Zhao, Y., et al., HSV-2-encoded miRNA-H4 Regulates Cell Cycle Progression and Act-D-induced Apoptosis in HeLa Cells by Targeting CDKL2 and CDKN2A. *Virol Sin*, **2019**. 34(3): p. 278-286 DOI: 10.1007/s12250-019-00101-8.
68. Barrozo, E.R., et al., Herpes Simplex Virus 1 MicroRNA miR-H8 Is Dispensable for Latency and Reactivation In Vivo. *J Virol*, **2021**. 95(4) DOI: 10.1128/JVI.02179-20.

69. Duan, Y., et al., Herpes Simplex Virus Type 1-Encoded miR-H2-3p Manipulates Cytosolic DNA-Stimulated Antiviral Innate Immune Response by Targeting DDX41. *Viruses*, **2019**. 11(8) DOI: 10.3390/v11080756.
70. Cullen, B.R., Viruses and microRNAs. *Nat Genet*, **2006**. 38 Suppl: p. S25-30 DOI: 10.1038/ng1793.
71. Pedersen, I.M., et al., Interferon modulation of cellular microRNAs as an antiviral mechanism. *Nature*, **2007**. 449(7164): p. 919-22 DOI: 10.1038/nature06205.
72. Lecellier, C.H., et al., A cellular microRNA mediates antiviral defense in human cells. *Science*, **2005**. 308(5721): p. 557-60 DOI: 10.1126/science.1108784.
73. Skalsky, R.L. and B.R. Cullen, Viruses, microRNAs, and host interactions. *Annu Rev Microbiol*, **2010**. 64: p. 123-41 DOI: 10.1146/annurev.micro.112408.134243.
74. Zhang, Y., et al., Marek's Disease Virus-Encoded MicroRNA 155 Ortholog Critical for the Induction of Lymphomas Is Not Essential for the Proliferation of Transformed Cell Lines. *J Virol*, **2019**. 93(17) DOI: 10.1128/JVI.00713-19.
75. Ru, J., et al., MiR-23a facilitates the replication of HSV-1 through the suppression of interferon regulatory factor 1. *PLoS One*, **2014**. 9(12): p. e114021 DOI: 10.1371/journal.pone.0114021.
76. Lagos, D., et al., miR-132 regulates antiviral innate immunity through suppression of the p300 transcriptional co-activator. *Nat Cell Biol*, **2010**. 12(5): p. 513-9 DOI: 10.1038/ncb2054.
77. Majer, A., et al., Induction of Multiple miR-200/182 Members in the Brains of Mice Are Associated with Acute Herpes Simplex Virus 1 Encephalitis. *PLoS One*, **2017**. 12(1): p. e0169081 DOI: 10.1371/journal.pone.0169081.
78. Lutz, G., et al., Viral Ubiquitin Ligase Stimulates Selective Host MicroRNA Expression by Targeting ZEB Transcriptional Repressors. *Viruses*, **2017**. 9(8) DOI: 10.3390/v9080210.
79. Zheng, S.Q., et al., MiR-101 regulates HSV-1 replication by targeting ATP5B. *Antiviral Res*, **2011**. 89(3): p. 219-26 DOI: 10.1016/j.antiviral.2011.01.008.
80. Hill, J.M., et al., HSV-1 infection of human brain cells induces miRNA-146a and Alzheimer-type inflammatory signaling. *Neuroreport*, **2009**. 20(16): p. 1500-5 DOI: 10.1097/WNR.0b013e3283329c05.

81. Mulik, S., et al., Role of miR-132 in angiogenesis after ocular infection with herpes simplex virus. *Am J Pathol*, **2012**. 181(2): p. 525-34 DOI: 10.1016/j.ajpath.2012.04.014.
82. Bhela, S., et al., Role of miR-155 in the pathogenesis of herpetic stromal keratitis. *Am J Pathol*, **2015**. 185(4): p. 1073-84 DOI: 10.1016/j.ajpath.2014.12.021.
83. Wang, X., et al., ICP4-induced miR-101 attenuates HSV-1 replication. *Sci Rep*, **2016**. 6: p. 23205 DOI: 10.1038/srep23205.
84. Zhang, Y., et al., MicroRNA-649 promotes HSV-1 replication by directly targeting MALT1. *J Med Virol*, **2017**. 89(6): p. 1069-1079 DOI: 10.1002/jmv.24728.
85. Xie, Y., S. He, and J. Wang, MicroRNA-373 facilitates HSV-1 replication through suppression of type I IFN response by targeting IRF1. *Biomed Pharmacother*, **2018**. 97: p. 1409-1416 DOI: 10.1016/j.biopha.2017.11.071.
86. Sharma, N., et al., Herpes simplex virus 1 evades cellular antiviral response by inducing microRNA-24, which attenuates STING synthesis. *PLoS Pathog*, **2021**. 17(9): p. e1009950 DOI: 10.1371/journal.ppat.1009950.
87. Kim, Y.J., et al., Analysis of MicroRNA Expression in Tears of Patients with Herpes Epithelial Keratitis: A Preliminary Study. *Invest Ophthalmol Vis Sci*, **2022**. 63(4): p. 21 DOI: 10.1167/iovs.63.4.21.
88. Cokaric Brdovcak, M., A. Zubkovic, and I. Jurak, Herpes Simplex Virus 1 Deregulation of Host MicroRNAs. *Noncoding RNA*, **2018**. 4(4) DOI: 10.3390/ncrna4040036.
89. Choi, B., et al., The relevance of miRNA-21 in HSV-induced inflammation in a mouse model. *Int J Mol Sci*, **2015**. 16(4): p. 7413-27 DOI: 10.3390/ijms16047413.
90. Lee, S., et al., Polymerase chain reaction reveals herpes simplex virus DNA in saliva of patients with Behcet's disease. *Arch Dermatol Res*, **1996**. 288(4): p. 179-83 DOI: 10.1007/BF02505221.
91. Stirnweiss, A., et al., IFN regulatory factor-1 bypasses IFN-mediated antiviral effects through viperin gene induction. *J Immunol*, **2010**. 184(9): p. 5179-85 DOI: 10.4049/jimmunol.0902264.
92. Kobayashi, K., et al., MiR-199a Inhibits Secondary Envelopment of Herpes Simplex Virus-1 Through the Downregulation of Cdc42-specific GTPase

- Activating Protein Localized in Golgi Apparatus. *Sci Rep*, **2017**. 7(1): p. 6650 DOI: 10.1038/s41598-017-06754-3.
93. Pan, D., et al., A neuron-specific host microRNA targets herpes simplex virus-1 ICP0 expression and promotes latency. *Cell Host Microbe*, **2014**. 15(4): p. 446-56 DOI: 10.1016/j.chom.2014.03.004.
 94. Sun, B., et al., Regulation of host and virus genes by neuronal miR-138 favours herpes simplex virus 1 latency. *Nat Microbiol*, **2021**. 6(5): p. 682-696 DOI: 10.1038/s41564-020-00860-1.
 95. Stark, T.J., et al., High-resolution profiling and analysis of viral and host small RNAs during human cytomegalovirus infection. *J Virol*, **2012**. 86(1): p. 226-35 DOI: 10.1128/JVI.05903-11.
 96. Oussaief, L., et al., Modulation of MicroRNA Cluster miR-183-96-182 Expression by Epstein-Barr Virus Latent Membrane Protein 1. *J Virol*, **2015**. 89(23): p. 12178-88 DOI: 10.1128/JVI.01757-15.
 97. Agarwal, V., et al., Predicting effective microRNA target sites in mammalian mRNAs. *Elife*, **2015**. 4 DOI: 10.7554/eLife.05005.
 98. Chen, Y. and X. Wang, miRDB: an online database for prediction of functional microRNA targets. *Nucleic Acids Res*, **2020**. 48(D1): p. D127-D131 DOI: 10.1093/nar/gkz757.
 99. Weigel, D., et al., The homeotic gene fork head encodes a nuclear protein and is expressed in the terminal regions of the Drosophila embryo. *Cell*, **1989**. 57(4): p. 645-58 DOI: 10.1016/0092-8674(89)90133-5.
 100. Accili, D. and K.C. Arden, FoxOs at the crossroads of cellular metabolism, differentiation, and transformation. *Cell*, **2004**. 117(4): p. 421-6 DOI: 10.1016/s0092-8674(04)00452-0.
 101. Burgering, B.M. and G.J. Kops, Cell cycle and death control: long live Forkheads. *Trends Biochem Sci*, **2002**. 27(7): p. 352-60 DOI: 10.1016/s0968-0004(02)02113-8.
 102. Ito, Y., H. Daitoku, and A. Fukamizu, Foxo1 increases pro-inflammatory gene expression by inducing C/EBPbeta in TNF-alpha-treated adipocytes. *Biochem Biophys Res Commun*, **2009**. 378(2): p. 290-5 DOI: 10.1016/j.bbrc.2008.11.043.

103. Su, D., et al., FoxO1 links insulin resistance to proinflammatory cytokine IL-1beta production in macrophages. *Diabetes*, **2009**. 58(11): p. 2624-33 DOI: 10.2337/db09-0232.
104. Lei, C.Q., et al., FoxO1 negatively regulates cellular antiviral response by promoting degradation of IRF3. *J Biol Chem*, **2013**. 288(18): p. 12596-604 DOI: 10.1074/jbc.M112.444794.
105. Litvak, V., et al., A FOXO3-IRF7 gene regulatory circuit limits inflammatory sequelae of antiviral responses. *Nature*, **2012**. 490(7420): p. 421-5 DOI: 10.1038/nature11428.
106. Yang, G.D., et al., Epstein-Barr Virus_Encoded LMP1 upregulates microRNA-21 to promote the resistance of nasopharyngeal carcinoma cells to cisplatin-induced Apoptosis by suppressing PDCD4 and Fas-L. *PLoS One*, **2013**. 8(10): p. e78355 DOI: 10.1371/journal.pone.0078355.
107. Liu, W., et al., Dysregulation of FOXO transcription factors in Epstein-Barr virus-associated gastric carcinoma. *Virus Res*, **2020**. 276: p. 197808 DOI: 10.1016/j.virusres.2019.197808.
108. Gao, R., et al., FoxO1 Suppresses Kaposi's Sarcoma-Associated Herpesvirus Lytic Replication and Controls Viral Latency. *J Virol*, **2019**. 93(3) DOI: 10.1128/JVI.01681-18.
109. Hale, A.E., et al., FOXO transcription factors activate alternative major immediate early promoters to induce human cytomegalovirus reactivation. *Proc Natl Acad Sci U S A*, **2020**. 117(31): p. 18764-18770 DOI: 10.1073/pnas.2002651117.
110. Strazic Geljic, I., et al., Cytomegalovirus protein m154 perturbs the adaptor protein-1 compartment mediating broad-spectrum immune evasion. *Elife*, **2020**. 9 DOI: 10.7554/eLife.50803.
111. Sandri-Goldin, R.M., R.E. Sekulovich, and K. Leary, The alpha protein ICP0 does not appear to play a major role in the regulation of herpes simplex virus gene expression during infection in tissue culture. *Nucleic Acids Res*, **1987**. 15(3): p. 905-19 DOI: 10.1093/nar/15.3.905.
112. Sekulovich, R.E., K. Leary, and R.M. Sandri-Goldin, The herpes simplex virus type 1 alpha protein ICP27 can act as a trans-repressor or a trans-activator in combination with ICP4 and ICP0. *J Virol*, **1988**. 62(12): p. 4510-22 DOI: 10.1128/JVI.62.12.4510-4522.1988.

113. Depledge, D.P., et al., A spliced latency-associated VZV transcript maps antisense to the viral transactivator gene 61. *Nat Commun*, **2018**. 9(1): p. 1167 DOI: 10.1038/s41467-018-03569-2.
114. Cokaric Brdovcak, M., et al., Herpes simplex virus 1 miRNA sequence variations in latently infected human trigeminal ganglia. *Virus Res*, **2018**. 256: p. 90-95 DOI: 10.1016/j.virusres.2018.08.002.
115. Stutika, C., et al., Comprehensive Small RNA-Seq of Adeno-Associated Virus (AAV)-Infected Human Cells Detects Patterns of Novel, Non-Coding AAV RNAs in the Absence of Cellular miRNA Regulation. *PLoS One*, **2016**. 11(9): p. e0161454 DOI: 10.1371/journal.pone.0161454.
116. Shi, J., et al., Deep RNA Sequencing Reveals a Repertoire of Human Fibroblast Circular RNAs Associated with Cellular Responses to Herpes Simplex Virus 1 Infection. *Cell Physiol Biochem*, **2018**. 47(5): p. 2031-2045 DOI: 10.1159/000491471.
117. Sanson, K.R., et al., Optimized libraries for CRISPR-Cas9 genetic screens with multiple modalities. *Nat Commun*, **2018**. 9(1): p. 5416 DOI: 10.1038/s41467-018-07901-8.
118. Doench, J.G., et al., Optimized sgRNA design to maximize activity and minimize off-target effects of CRISPR-Cas9. *Nat Biotechnol*, **2016**. 34(2): p. 184-191 DOI: 10.1038/nbt.3437.
119. Barturen, G.R., A.; Hamberg, M.; Alganza, A.; Lebron, R.; Kotsyfakis, M.; Shi, B.; Koppers-Lalic, D.; Hackenberg, M., sRNAbench: profiling of small RNAs and its sequence variants in single or multi-species high-throughput experiments. *Methods Next-Generation Seq.*, **2014**: p. 21-31.
120. Rueda, A., et al., sRNAtoolbox: an integrated collection of small RNA research tools. *Nucleic Acids Res*, **2015**. 43(W1): p. W467-73 DOI: 10.1093/nar/gkv555.
121. Kozomara, A., M. Birgaoanu, and S. Griffiths-Jones, miRBase: from microRNA sequences to function. *Nucleic Acids Res*, **2019**. 47(D1): p. D155-D162 DOI: 10.1093/nar/gky1141.
122. Alles, J., et al., An estimate of the total number of true human miRNAs. *Nucleic Acids Res*, **2019**. 47(7): p. 3353-3364 DOI: 10.1093/nar/gkz097.
123. Chiang, H.R., et al., Mammalian microRNAs: experimental evaluation of novel and previously annotated genes. *Genes Dev*, **2010**. 24(10): p. 992-1009 DOI: 10.1101/gad.1884710.

124. Kuleshov, M.V., et al., Enrichr: a comprehensive gene set enrichment analysis web server 2016 update. *Nucleic Acids Res*, **2016**. 44(W1): p. W90-7 DOI: 10.1093/nar/gkw377.
125. Chuluunbaatar, U., et al., Constitutive mTORC1 activation by a herpesvirus Akt surrogate stimulates mRNA translation and viral replication. *Genes Dev*, **2010**. 24(23): p. 2627-39 DOI: 10.1101/gad.1978310.
126. Meyers, B.C., et al., Criteria for annotation of plant MicroRNAs. *Plant Cell*, **2008**. 20(12): p. 3186-90 DOI: 10.1105/tpc.108.064311.
127. Kozomara, A. and S. Griffiths-Jones, miRBase: annotating high confidence microRNAs using deep sequencing data. *Nucleic Acids Res*, **2014**. 42(Database issue): p. D68-73 DOI: 10.1093/nar/gkt1181.
128. Fromm, B., et al., MirGeneDB 2.1: toward a complete sampling of all major animal phyla. *Nucleic Acids Res*, **2022**. 50(D1): p. D204-D210 DOI: 10.1093/nar/gkab1101.
129. Fromm, B., et al., A Uniform System for the Annotation of Vertebrate microRNA Genes and the Evolution of the Human microRNAome. *Annu Rev Genet*, **2015**. 49: p. 213-42 DOI: 10.1146/annurev-genet-120213-092023.
130. Ambros, V., et al., A uniform system for microRNA annotation. *RNA*, **2003**. 9(3): p. 277-9 DOI: 10.1261/rna.2183803.
131. Axtell, M.J. and B.C. Meyers, Revisiting Criteria for Plant MicroRNA Annotation in the Era of Big Data. *Plant Cell*, **2018**. 30(2): p. 272-284 DOI: 10.1105/tpc.17.00851.
132. Starega-Roslan, J., et al., Structural basis of microRNA length variety. *Nucleic Acids Res*, **2011**. 39(1): p. 257-68 DOI: 10.1093/nar/gkq727.
133. Dabney, J. and M. Meyer, Length and GC-biases during sequencing library amplification: a comparison of various polymerase-buffer systems with ancient and modern DNA sequencing libraries. *Biotechniques*, **2012**. 52(2): p. 87-94 DOI: 10.2144/000113809.
134. Starega-Roslan, J., P. Galka-Marciniak, and W.J. Krzyzosiak, Nucleotide sequence of miRNA precursor contributes to cleavage site selection by Dicer. *Nucleic Acids Res*, **2015**. 43(22): p. 10939-51 DOI: 10.1093/nar/gkv968.
135. Bogerd, H.P., et al., A mammalian herpesvirus uses noncanonical expression and processing mechanisms to generate viral MicroRNAs. *Mol Cell*, **2010**. 37(1): p. 135-42 DOI: 10.1016/j.molcel.2009.12.016.

136. Szpara, M.L., L. Parsons, and L.W. Enquist, Sequence variability in clinical and laboratory isolates of herpes simplex virus 1 reveals new mutations. *J Virol*, **2010**. 84(10): p. 5303-13 DOI: 10.1128/jvi.00312-10.
137. Hooykaas, M.J., et al., Comprehensive profiling of functional Epstein-Barr virus miRNA expression in human cell lines. *BMC Genomics*, **2016**. 17: p. 644 DOI: 10.1186/s12864-016-2978-6.
138. Kawahara, Y., et al., Frequency and fate of microRNA editing in human brain. *Nucleic Acids Res*, **2008**. 36(16): p. 5270-80 DOI: 10.1093/nar/gkn479.
139. Rehmsmeier, M., et al., Fast and effective prediction of microRNA/target duplexes. *RNA*, **2004**. 10(10): p. 1507-17 DOI: 10.1261/rna.5248604.
140. Shaheen, N.M.H., et al., Role of circulating miR-182 and miR-150 as biomarkers for cirrhosis and hepatocellular carcinoma post HCV infection in Egyptian patients. *Virus Res*, **2018**. 255: p. 77-84 DOI: 10.1016/j.virusres.2018.07.004.
141. El Sobky, S.A., et al., Contradicting roles of miR-182 in both NK cells and their host target hepatocytes in HCV. *Immunol Lett*, **2016**. 169: p. 52-60 DOI: 10.1016/j.imlet.2015.10.013.
142. Singaravelu, R., et al., A conserved miRNA-183 cluster regulates the innate antiviral response. *J Biol Chem*, **2019**. 294(51): p. 19785-19794 DOI: 10.1074/jbc.RA119.010858.
143. Melo, S.A. and M. Esteller, Dysregulation of microRNAs in cancer: playing with fire. *FEBS Lett*, **2011**. 585(13): p. 2087-99 DOI: 10.1016/j.febslet.2010.08.009.
144. Mehta, A. and D. Baltimore, MicroRNAs as regulatory elements in immune system logic. *Nat Rev Immunol*, **2016**. 16(5): p. 279-94 DOI: 10.1038/nri.2016.40.
145. Stittrich, A.B., et al., The microRNA miR-182 is induced by IL-2 and promotes clonal expansion of activated helper T lymphocytes. *Nat Immunol*, **2010**. 11(11): p. 1057-62 DOI: 10.1038/ni.1945.
146. Kurt-Jones, E.A., M.H. Orzalli, and D.M. Knipe, Innate Immune Mechanisms and Herpes Simplex Virus Infection and Disease. *Adv Anat Embryol Cell Biol*, **2017**. 223: p. 49-75 DOI: 10.1007/978-3-319-53168-7_3.
147. Wu, Z., et al., Herpes simplex virus type 1 suppresses RNA-induced gene silencing in mammalian cells. *J Virol*, **2009**. 83(13): p. 6652-63 DOI: 10.1128/JVI.00260-09.

148. Melchjorsen, J., S. Matikainen, and S.R. Paludan, Activation and evasion of innate antiviral immunity by herpes simplex virus. *Viruses*, **2009**. 1(3): p. 737-59 DOI: 10.3390/v1030737.
149. Poon, A.P., L. Benetti, and B. Roizman, U(S)3 and U(S)3.5 protein kinases of herpes simplex virus 1 differ with respect to their functions in blocking apoptosis and in virion maturation and egress. *J Virol*, **2006**. 80(8): p. 3752-64 DOI: 10.1128/JVI.80.8.3752-3764.2006.
150. Junger, M.A., et al., The Drosophila forkhead transcription factor FOXO mediates the reduction in cell number associated with reduced insulin signaling. *J Biol*, **2003**. 2(3): p. 20 DOI: 10.1186/1475-4924-2-20.
151. Dharaneeswaran, H., et al., FOXO1-mediated activation of Akt plays a critical role in vascular homeostasis. *Circ Res*, **2014**. 115(2): p. 238-251 DOI: 10.1161/CIRCRESAHA.115.303227.
152. Hinman, R.M., et al., Foxo3^{-/-} mice demonstrate reduced numbers of pre-B and recirculating B cells but normal splenic B cell sub-population distribution. *Int Immunol*, **2009**. 21(7): p. 831-42 DOI: 10.1093/intimm/dxp049.
153. Li, H., et al., FoxO4 regulates tumor necrosis factor alpha-directed smooth muscle cell migration by activating matrix metalloproteinase 9 gene transcription. *Mol Cell Biol*, **2007**. 27(7): p. 2676-86 DOI: 10.1128/MCB.01748-06.
154. Castrillon, D.H., et al., Suppression of ovarian follicle activation in mice by the transcription factor Foxo3a. *Science*, **2003**. 301(5630): p. 215-8 DOI: 10.1126/science.1086336.
155. Du, T., G. Zhou, and B. Roizman, HSV-1 gene expression from reactivated ganglia is disordered and concurrent with suppression of latency-associated transcript and miRNAs. *Proc Natl Acad Sci U S A*, **2011**. 108(46): p. 18820-4 DOI: 10.1073/pnas.1117203108.
156. Oliveros, J.C., VENNY. An interactive tool for comparing lists with Venn Diagrams. **2007**.
157. Babicki, S., et al., Heatmapper: web-enabled heat mapping for all. *Nucleic Acids Res*, **2016**. 44(W1): p. W147-53 DOI: 10.1093/nar/gkw419.
158. Lorenz, R., I.L. Hofacker, and P.F. Stadler, RNA folding with hard and soft constraints. *Algorithms Mol Biol*, **2016**. 11: p. 8 DOI: 10.1186/s13015-016-0070-z.

159. Hung, J.H. and Z. Weng, Sequence Alignment and Homology Search with BLAST and ClustalW. *Cold Spring Harb Protoc*, **2016**. 2016(11) DOI: 10.1101/pdb.prot093088.

SUPPLEMENTAL DATA

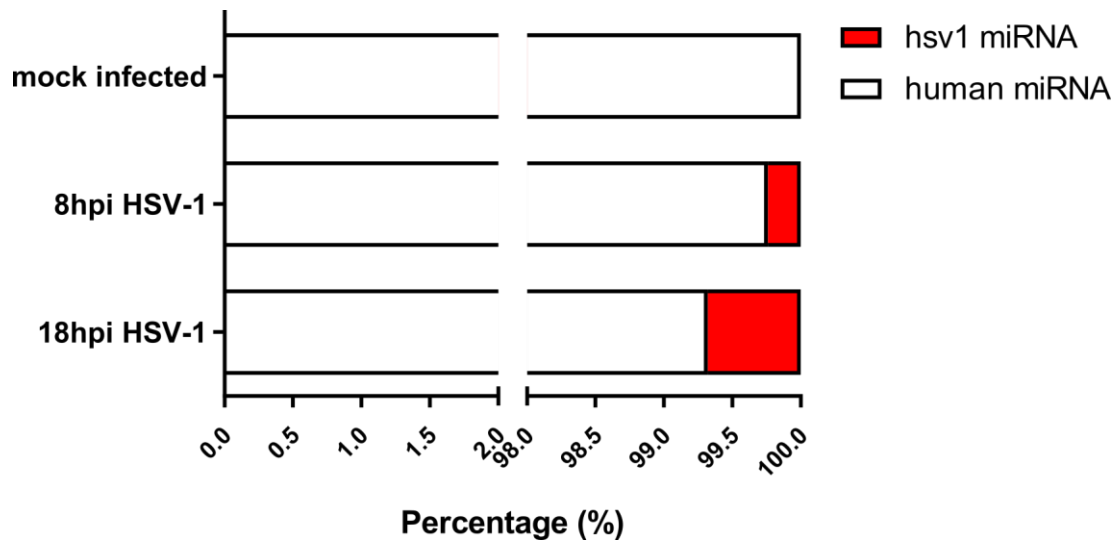


Figure S1: HSV-1 miRNAs represent only a small fraction of miRNAs in infected cells. The percentage of HSV-1 miRNAs in the total number of reads aligned to human and HSV-1 miRNA. The results represent the average of four replicates.

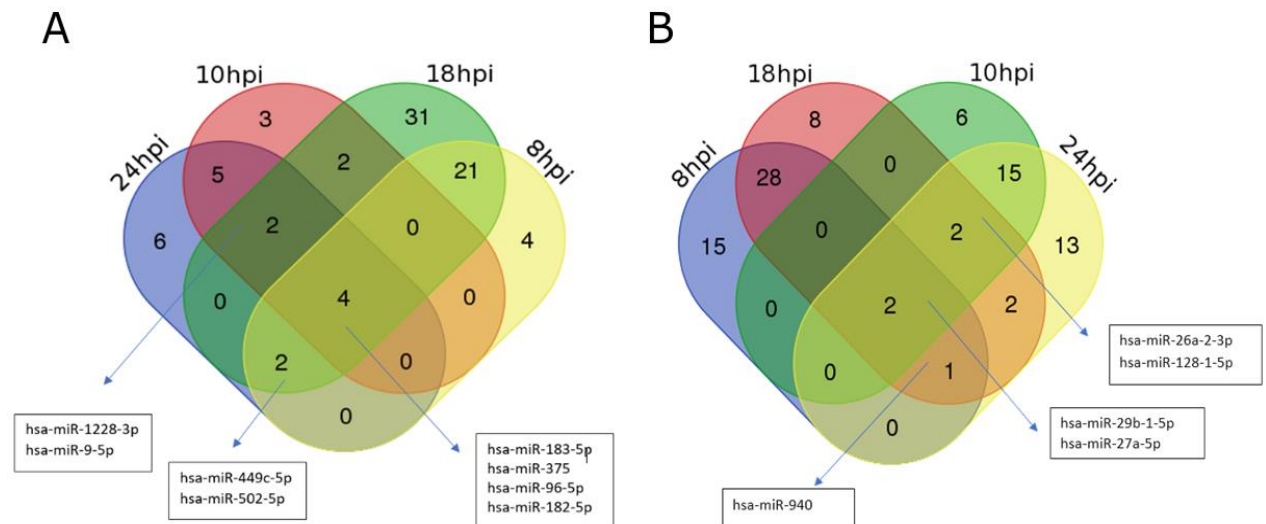


Figure S2. A number of miRNAs found reproducibly deregulated between two data sets. Deregulated miRNAs were extracted from data sets obtained by sequencing samples of HFF cells productively infected with HSV-1 at different time points. The number of miRNAs shared between data sets is shown, and miRNAs found shared between at least three data sets are listed as (A) upregulated or (B) downregulated [156].

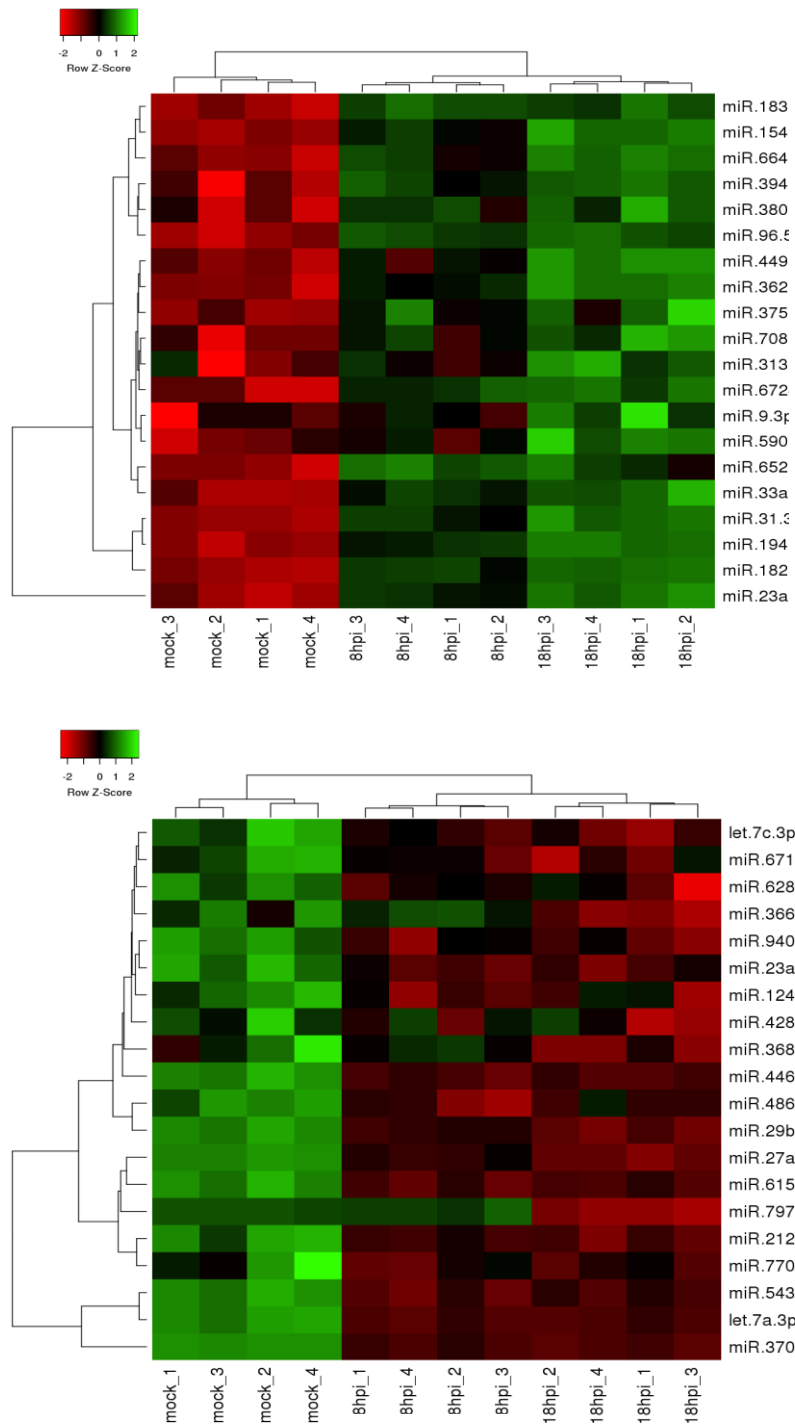


Figure S3: Heatmap of the most informative miRNAs shows perfect clustering pattern. HFF cells were infected with MOI 5 and samples were extracted at 8 and 18 hpi. The upper heatmap shows 20 most upregulated miRNAs, while the lower panel shows 20 most downregulated miRNAs. Samples are clustered based on their expression profile. [157].

Table S1: Example of TargetScan search for miR-182-5p

Target gene	Gene name	Link to sites in UTRs	Conserved sites				Total context++ score
			total	8mer	7mer-m8	7mer-A1	
PPP1R1C	protein phosphatase 1, regulatory (inhibitor) subunit 1C	Sites in UTR	1	1	0	0	-1
RGS17	regulator of G-protein signaling 17	Sites in UTR	4	2	1	1	-1.1
LHX1	LIM homeobox 1	Sites in UTR	2	2	0	0	-0.9
CTTN	cortactin	Sites in UTR	2	2	0	0	-0.8
NCALD	neurocalcin delta	Sites in UTR	1	1	0	0	-0.8
HAS2	hyaluronan synthase 2	Sites in UTR	3	0	0	3	-0.8
ZFP36L1	ZFP36 ring finger protein-like 1	Sites in UTR	2	1	0	1	-1
FLOT1	flotillin 1	Sites in UTR	1	1	0	0	-0.8
PEG10	paternally expressed 10	Sites in UTR	1	1	0	0	-0.8
SLC35G1	solute carrier family 35, member G1	Sites in UTR	1	0	0	1	-0.8

Table S2 .: Example of miRDB search for miR-182-5p

Target Detail	Target Rank	Target Score	miRNA Name	Gene Symbol	Gene Description
Details	1	100	hsa-miR-182-5p	PRKACB	protein kinase cAMP-activated catalytic subunit beta
Details	2	100	hsa-miR-182-5p	RGS17	regulator of G protein signaling 17
Details	3	100	hsa-miR-182-5p	BNC2	basonuclein 2
Details	4	100	hsa-miR-182-5p	SNX30	sorting nexin family member 30
Details	5	100	hsa-miR-182-5p	LPP	LIM domain containing preferred translocation partner in lipoma
Details	6	100	hsa-miR-182-5p	MITF	melanocyte inducing transcription factor
Details	7	100	hsa-miR-182-5p	FRS2	fibroblast growth factor receptor substrate 2
Details	8	100	hsa-miR-182-5p	CAMSAP2	calmodulin regulated spectrin associated protein family member 2
Details	9	100	hsa-miR-182-5p	HAS2	hyaluronan synthase 2
Details	10	99	hsa-miR-182-5p	PRRG3	proline rich and Gla domain 3

Table S3: Overlap between TargetScan and MiRDB search

33 common elements in "miRDB " and "Targetscan":

FRS2
COL25A1
SOX6
FRMD5
FOXO1
ARHGAP6
CEP170B
REV1
BNC2
SPRY3
NTN4
PLCB4
RAPGEF4
CNOT6L
BRMS1L
FNDC3B
TCF7L2
QKI
DAAM1
DMXL1
MFAP3
RHPN2
REPS2
KCNJ14
CELF2
DGCR2
DCX
NR4A3
RHOBTB1
BACH2
PTPN4
SLC6A6
CELF1

Position 265-271 of FOXO1 3' UTR	5' . . . UUCAUUACAAGAGUGCCAAAC . . .
hsa-miR-182-5p	3' UCACACUCAAGAUGGUAACGGUUU
<pre> 230 240 250 260 270 Human AGAUAAAGGACUGU-GCCAUUGGAAAUUU---CAUUACAAGAGUGCCAAACUCACUA- Chimp AGAUAAAGGACUGU-GCCAUUGGAAAUUU---CAUUACAAGAGUGCCAAACUCACUA- Rhesus AGAUAAAGGACCGU-GCCAUUGGAAAUUU---CAUUACAAGAGUGCCAAACUCACUA- Squirrel AGAUAAAGGACUGU-GCCAUUGGAAAUUU---CAUUACAAGAGUGCCAAACUCACUA- Mouse AGAUAAAGGACUGU-GCCAUUGGAAAUUU---CAUUACAAGAGUGCCAAACUCACUA- Rat AGAUAAAGGACUGU-GCCAUUGGAAAUUU---CAUGACAGCAAGUGCCAAACUCACUA- Rabbit AGAUAAAGGACUGU-GCCAUUGGAAAUUU---CAUUACAAGAGUGCCAAACUCACUA- Pig AGAUAAAGGACUGU-GCCAUUGGAAAUUU---CAUUACAAGAGUGCCAAACUCACUA- Cow AGAUAAAGGACUGU-GCCAUUGGAAAUUU---CAUUACAAGAGUGCCAAACUCACUA- Cat AGAUAAAGGACUGU-GCCAUUGGAAAUUU---CAUUACAAGAGUGCCAAACUCACUA- Dog AGAUAAAGGACUGU-GCCAUUGGAAAUUU---CAUUACAAGAGUGCCAAACUCACUA- Brown bat AGAUAAAGGACUGU-GCCAUUGGAAAUUU---CAUUACAAGAGUGCCAAACUCACUA- Elephant AGAUAAAGGACUGU-GCCAUUGGAAAUUU---CGUUACAAGAGUGCCAAACUCACUA- Opossum AGAUAAAGGACUGU-GCCAUUGGAGAUUUCAUUCAUUAAGAGUGCCAAACUCACUA- Macaw AGAUAAAGGACUGU-GCCAUUGGAAAUUU---CAUUACUCUGAGUGCCAAAUUCACUA- Chicken AGAUAAAGGACUGU-GCCAUUGGAAAUUU---CAUUACUCUGAGUGCCAAAUUCACUA- Lizard A----AGGAAGU-GCCGUUGGAAGUGU---CUUUUUUUGAGUGCCAAACUCACUA- X. tropicalis -----UUGGACCUCU-----UAUCACUAUAAAGUGCCAAACUCACUA- </pre>	

miR-182-5p binding site

Position 264-271 of FOXO1 3' UTR	5' . . . UUCAUUACAAGAA---GUGCCAAA . . .
hsa-miR-96-5p	3' UCGUUUUUACACGAUCACGGUUU
<pre> 230 240 250 260 270 280 Human JAGAUAAAGGACUGU-GCCAUUGGAAAUUU---CAUUACAAGAGUGCCAAACUCACUA-CA-- Chimp JAGAUAAAGGACUGU-GCCAUUGGAAAUUU---CAUUACAAGAGUGCCAAACUCACUA-CA-- Rhesus JAGAUAAAGGACCGU-GCCAUUGGAAAUUU---CAUUACAAGAGUGCCAAACUCACUA-CA-- Squirrel JAGAUAAAGGACUGU-GCCAUUGGAAAUUU---CAUUACAAGAGUGCCAAACUCACUA-CA-- Mouse JAGAUAAAGGACUGU-GCCAUUGGAAAUUU---CAUUACAAGAGUGCCAAACUCACUA-CA-- Rat JAGAUAAAGGACUGU-GCCAUUGGAAAUUU---CAUGACAGCAAGUGCCAAACUCACUA-CA-- Rabbit JAGAUAAAGGACUGU-GCCAUUGGAAAUUU---CAUUACAAGAGUGCCAAACUCACUA-CA-- Pig JAGAUAAAGGACUGU-GCCAUUGGAAAUUU---CAUUACAAGAGUGCCAAACUCACUA-CA-- Cow JAGAUAAAGGACUGU-GCCAUUGGAAAUUU---CAUUACAAGAGUGCCAAACUCACUA-CA-- Cat JAGAUAAAGGACUGU-GCCAUUGGAAAUUU---CAUUACAAGAGUGCCAAACUCACUA-CA-- Dog JAGAUAAAGGACUGU-GCCAUUGGAAAUUU---CAUUACAAGAGUGCCAAACUCACUA-CA-- Brown bat JAGAUAAAGGACUGU-GCCAUUGGAAAUUU---CAUUACAAGAGUGCCAAACUCACUA-CA-- Elephant JAGAUAAAGGACUGU-GCCAUUGGAAAUUU---CGUUACAAGAGUGCCAAACUCACUA-CA-- Opossum JAGAUAAAGGACUGU-GCCAUUGGAGAUUUCAUUCAUUAAGAGUGCCAAACUCACUA-CA-- Macaw JAGAUAAAGGACUGU-GCCAUUGGAAAUUU---CAUUACUCUGAGUGCCAAAUUCACUA-CA-- Chicken JAGAUAAAGGACUGU-GCCAUUGGAAAUUU---CAUUACUCUGAGUGCCAAAUUCACUA-CA-- Lizard JA----AGGAAGU-GCCGUUGGAAGUGU---CUUUUUUUGAGUGCCAAACUCACUA-CAAL X. tropicalis -----UUGGACCUCU-----UAUCACUAUAAAGUGCCAAACUCACUA-GA-- </pre>	

miR-96-5p binding site

Position 236-242 of FOXO1 3' UTR	5' . . . CUGUAGAUAAAGGACUGUGCCAUU . . .
hsa-miR-183-5p.1	3' UCACUUAAGAUGGUCACGGUUAU
<pre> 90 200 210 220 230 240 250 Human SUUUGGCCCAAGUGUGCAGGUUAUGUGGUGUAGAUAAAGGACUGU-GCCAUUGGAAAUUU-- Chimp SUUUGGCCCAAGUGUGCAGGUUAUGUGGUGUAGAUAAAGGACUGU-GCCAUUGGAAAUUU-- Rhesus SUUUGGCCCAAGUGUGCAGGUUAUGUGGUGUAGAUAAAGGACCGU-GCCAUUGGAAAUUU-- Squirrel SUUUGGCCCAAGUGUGCAGGUUAUGUGGUGUAGAUAAAGGACUGU-GCCAUUGGAAAUUU-- Mouse SUUUGGCCCAGCGUCCGAGGUUUUGUGGUGUAGAUAAAGGACUGU-GCCAUUGGAAAUUU-- Rat SUUUGGCCCAGCACCACAGGUUAUGUGGUGUAGAUAAAGGACUGU-GCCAUUGGAAAUUU-- Rabbit SUUUGGCCCAAGUGUGCAGGUUAUGUGGUGUAGAUAAAGGACUGU-GCCAUUGGAAAUUU-- Pig SUUUGGCCCAAGUGUGCAGGUUAUGUGGUGUAGAUAAAGGACUGU-GCCAUUGGAAAUUU-- Cow SUUUGGCCCAGUGUUGCAGGUUAUGUGGUGUAGAUAAAGGACUGU-GCCAUUGGAAAUUU-- Cat SUUUGGCCCAAGUGUGCAGGUUAUGUGGUGUAGAUAAAGGACUGU-GCCAUUGGAAAUUU-- Dog SUUUGGCCCAAGUGUGCAGGUUAUGUGGUGUAGAUAAAGGACUGU-GCCAUUGGAAAUUU-- Brown bat SUUUGGCCCAAGUGUGCAGGUUAUGUGGUGUAGAUAAAGGACUGU-GCCAUUGGAAAUUU-- Elephant SUUUGGCCCAAGUGUGCAGGUUAUGUGGUGUAGAUAAAGGACUGU-GCCAUUGGAAAUUU-- Opossum SUUUGGCCCAAGUGUGCAGGUUAUGUGGUGUAGAUAAAGGACUGU-GCCAUUGGAGAUUUA Macaw SUUUGGCCCAAGUGUGCAGGUUAUGUGGUGUAGAUAAAGGACUGU-GCCAUUGGAAAUUU-- Chicken SUUUGGCCCAAGUGUGCAGGUUAUGUGGUGUAGAUAAAGGACUGU-GCCAUUGGAAAUUU-- Lizard SUUUGGCCCAAGUGUGCAGGUUAUGUGGUGUAGAUAAAGGACUGU-GCCAUUGGAAAUUU-- X. tropicalis CUUUGACCAGAACACGAGGUUUGUGGUGGUC-----UUGGACCUCU----- </pre>	

miR-183-5p.1 binding site

Figure S4: Example of miR-182/-96/-183 binding sites at 3' UTR of FoxO 1 gene. TargetScan was used to predict miRNAs: miR-182, miR-96, miR-183 pairing to FoxO targets and their conservation across different species. The white area represents a highly conserved region for all target sites.

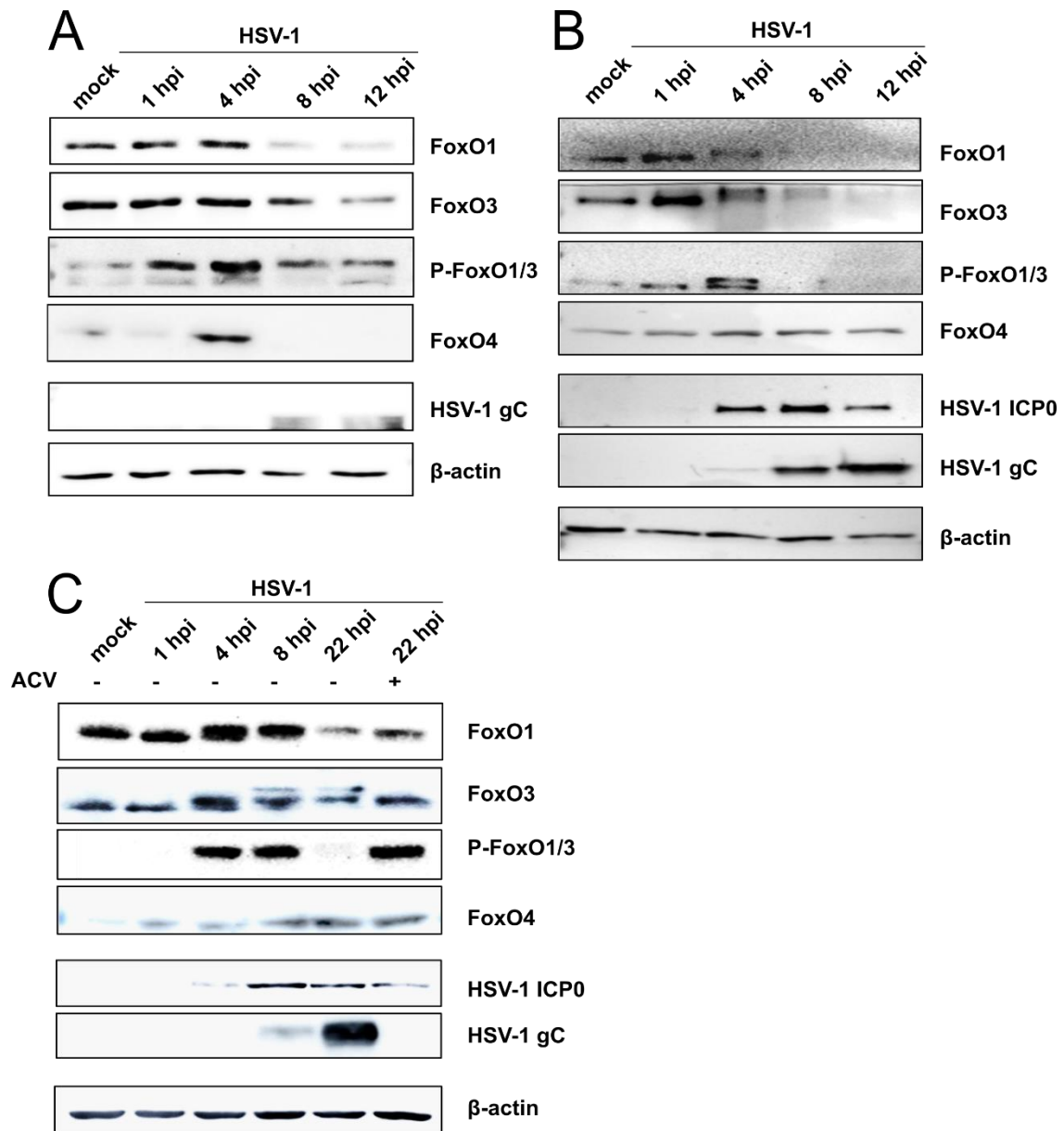


Figure S5: FoxO1 and FoxO3 proteins are upregulated in HEK293, SH-SY5Y and HFF cells. (A) HEK293 cells, (B) SH-SY5Y cells, and (C) HFF cells were mock-infected or infected with HSV-1, where indicated, cells were pretreated with acyclovir (ACV). Cells were collected at indicated time points and analyzed by western blot. ICP0, immediate-early viral gene, and gC, late viral gene.

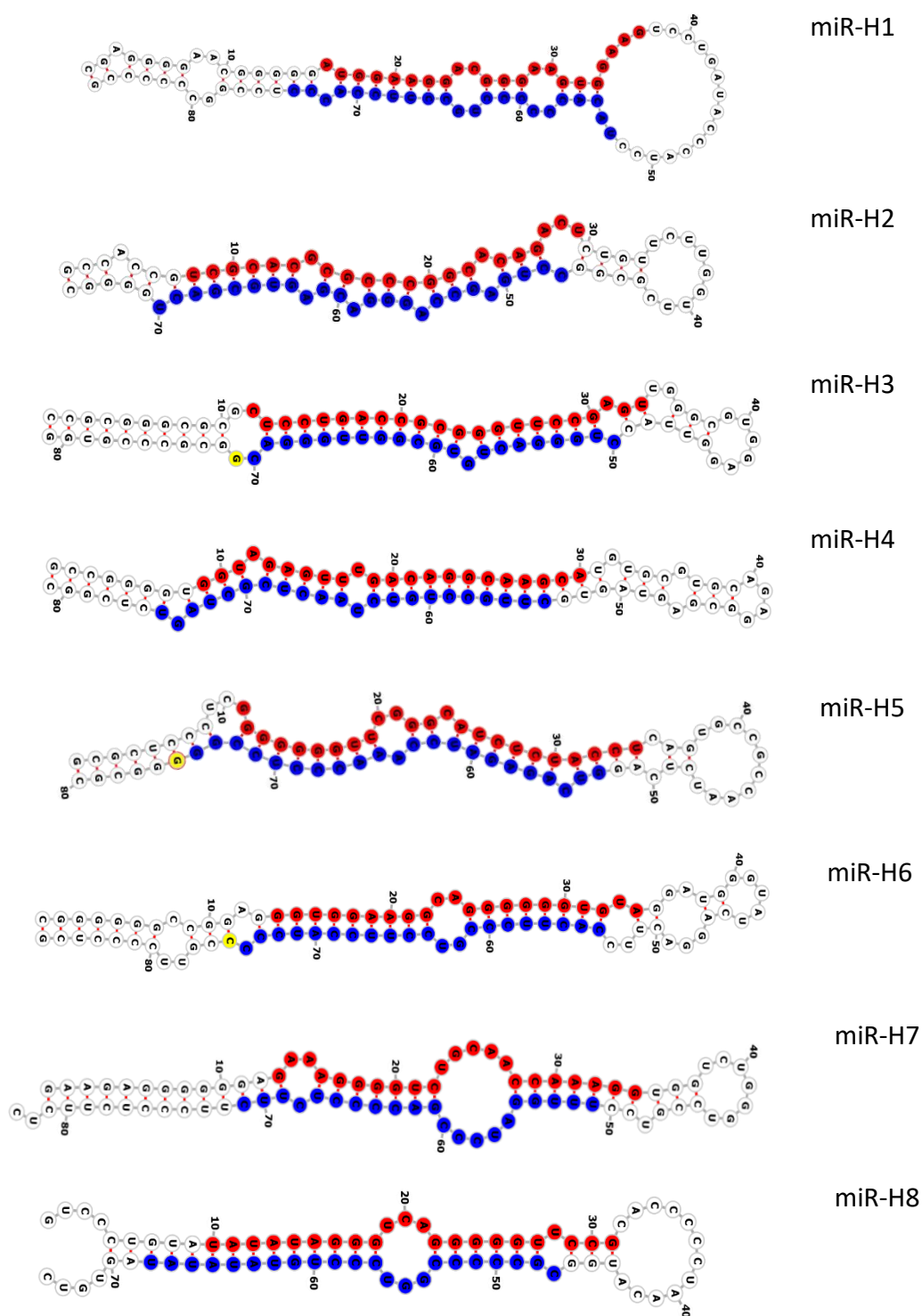
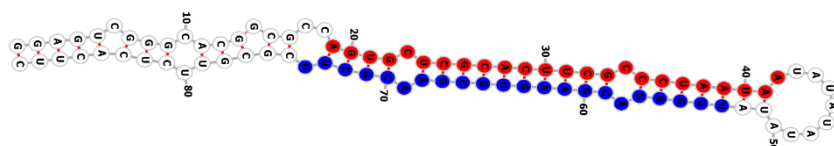


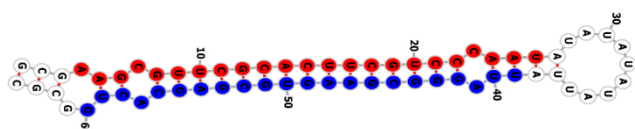
Figure S6: Both arms of HSV-1 miR-H1-H8 are classified as true miRNAs. Hairpin sequences are folded with RNAfold, and the minimum free energy structure is chosen. The most dominant 5p sequence is marked with red, and the most dominant 3p sequence is marked with blue. 3' additions are marked with yellow [158].



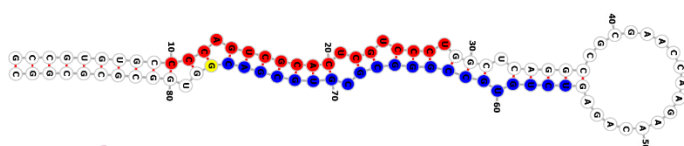
miR-H11



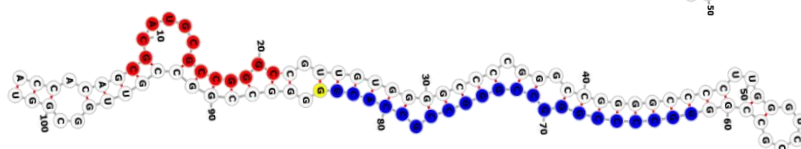
miR-H12



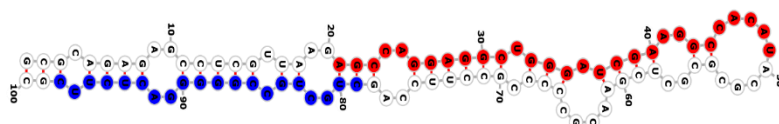
miR-H13



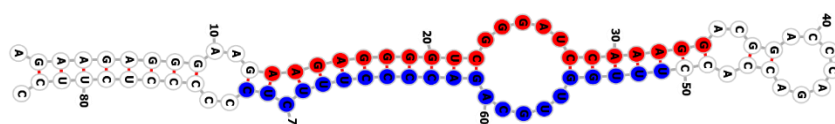
miR-H14



miR-H15



miR-H16



miR-H27

Figure S7: At least one arm of HSV-1 miR-H11-H16 and miR-H27 are classified as tentative miRNAs. Hairpin sequences are folded with RNAfold, and the minimum free energy structure is chosen. The most dominant 5p sequence is marked with red, and the most dominant 3p sequence is marked with blue. 3' additions are marked with yellow. Purple color signifies the most dominant 5p and 3p sequence overlapping.

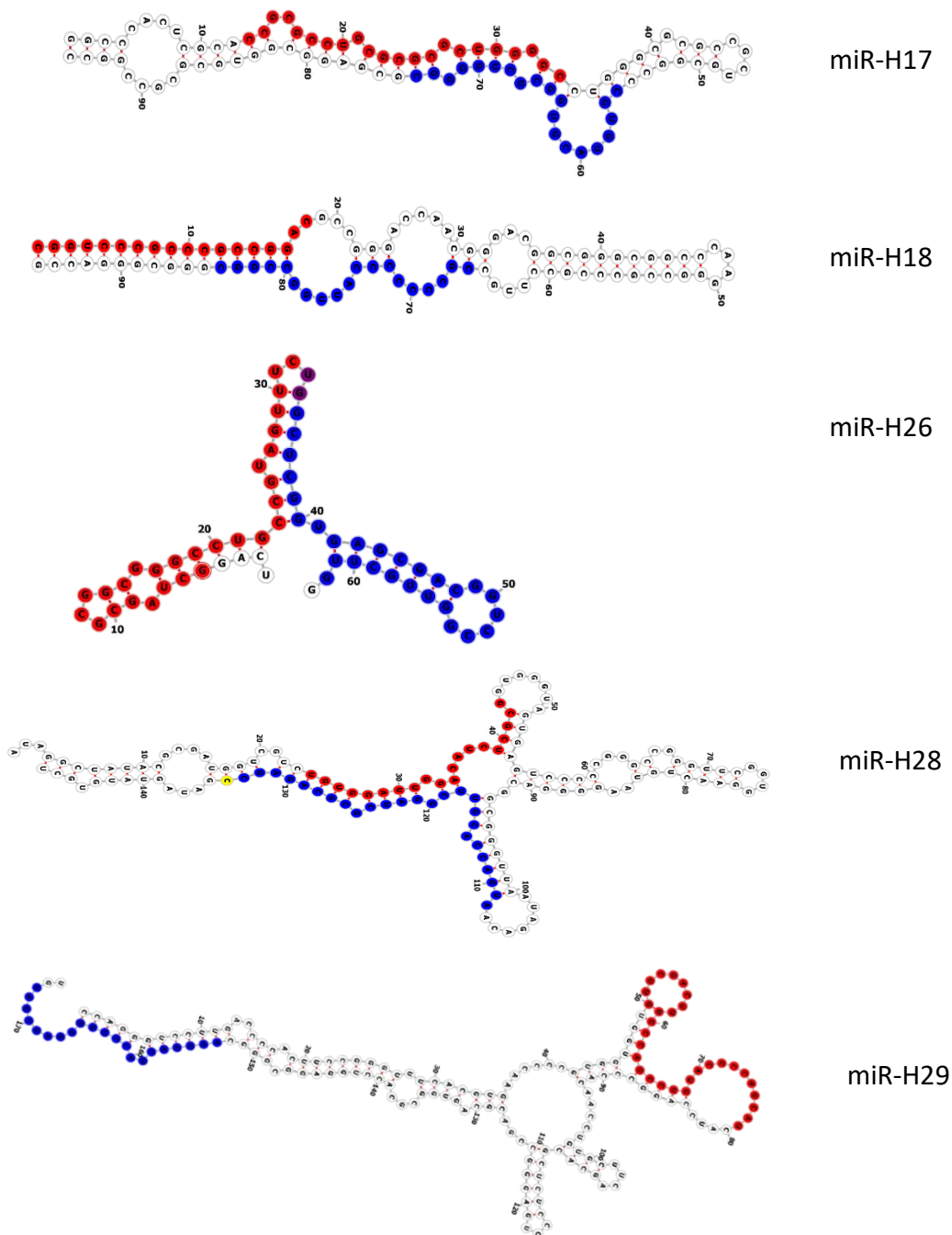
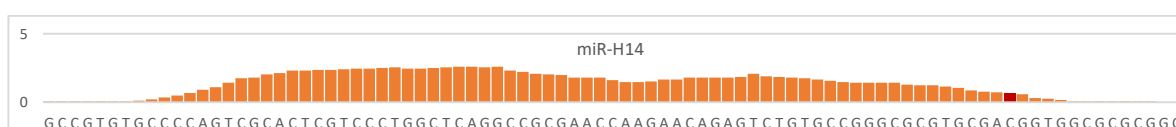
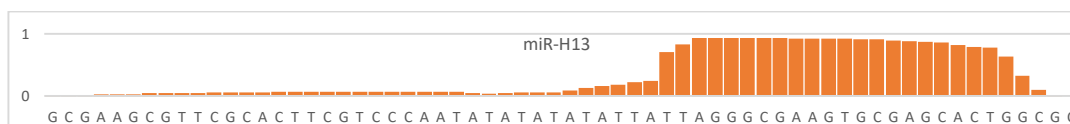
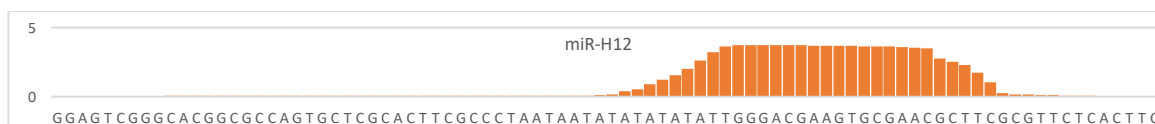
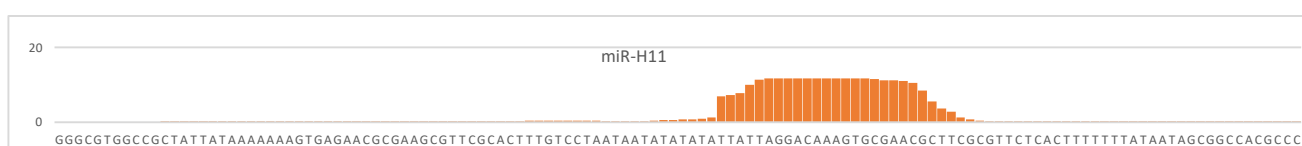
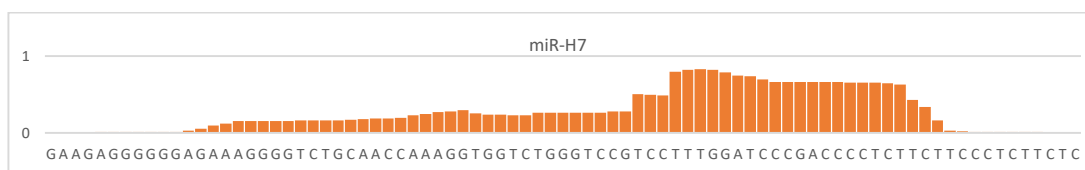
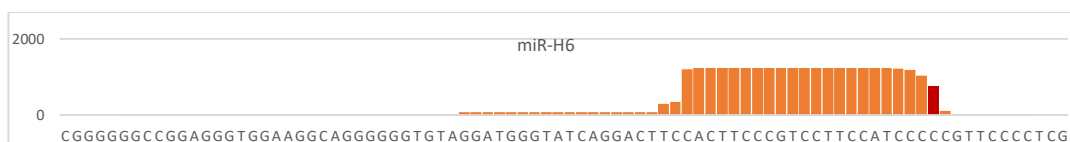
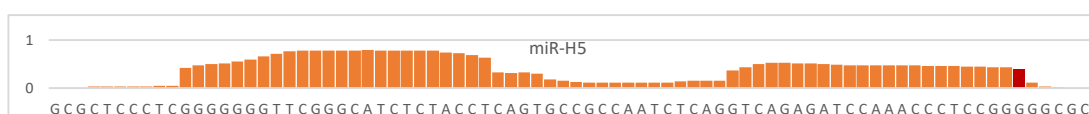
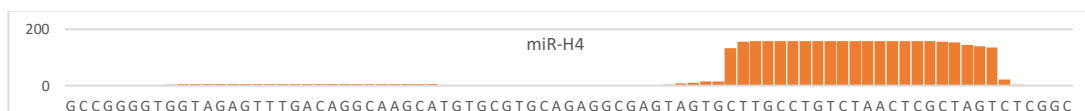
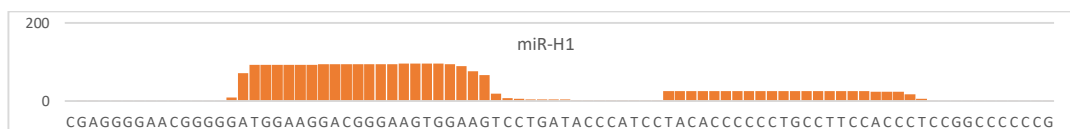


Figure S8: All arms of the HSV-1 miR-H17-H18 and miR-H26, miR-H28-H29 are classified as miRNAs that need confirmation. Hairpin sequences are folded with RNAfold, and the minimum free energy structure is chosen. The most dominant 5p sequence is marked with red, and the most dominant 3p sequence is marked with blue. 3' additions are marked with yellow. Purple color signifies the most dominant 5p and 3p sequence overlapping.



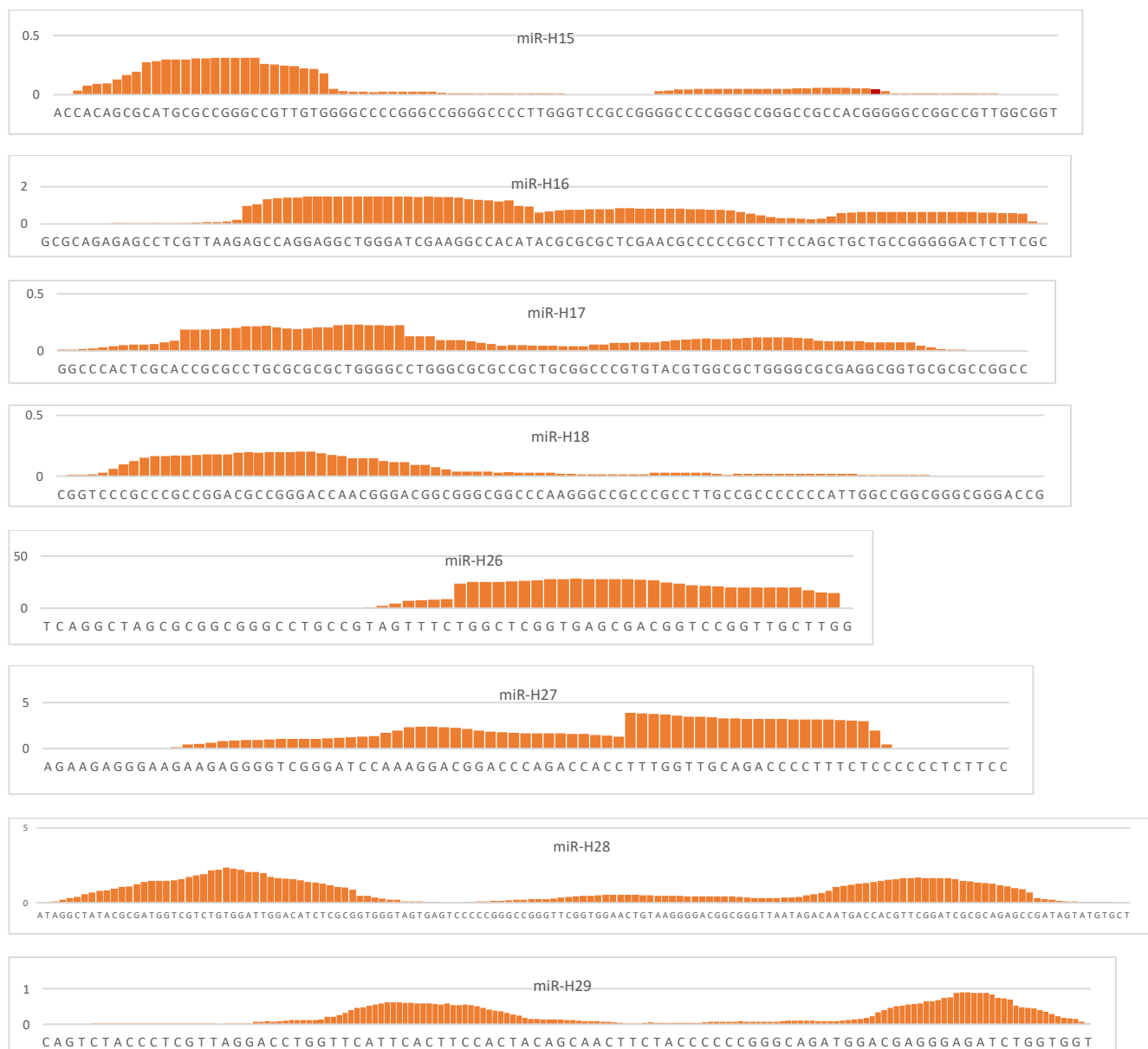


Figure S9: 5' homogeneity profiles. Profiles of expression of each HSV-1 miRNA. The hairpin sequence of individual HSV-1 miRNAs is shown below the graph, and each bar represents the expression value of each base. NTAs are marked with brown.

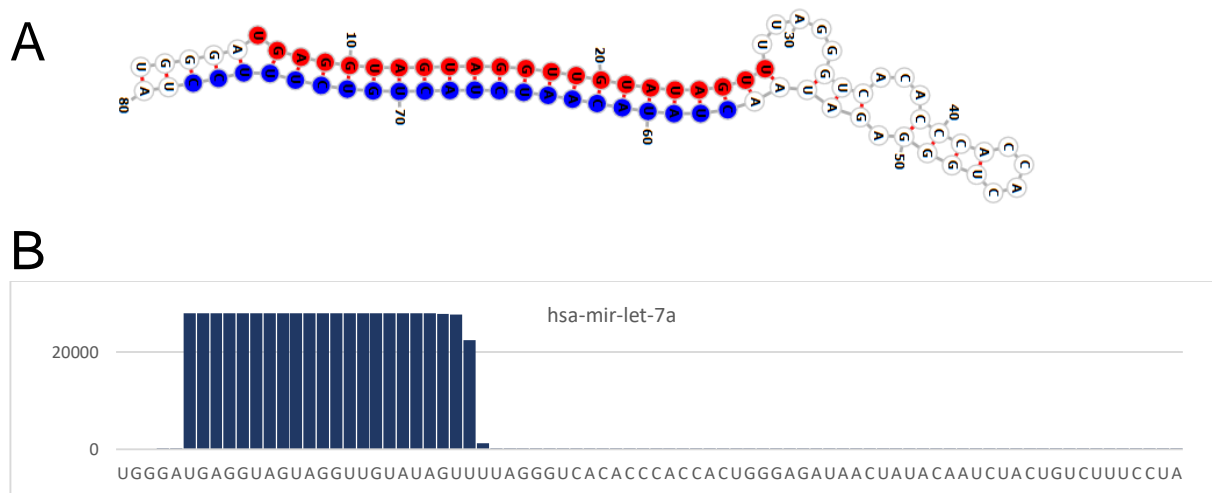


Figure S10: 5' homogeneity profile and folding of *bona fide* host miRNA mir-let-7a. (A) Hairpin sequences are folded with RNAfold, and the minimum free energy structure is chosen. The most dominant 5p sequence is marked with red, and the most dominant 3p sequence is marked with blue. (B) The hairpin sequence of mir-let-7a is shown below the graph, and each bar represents the expression value of each base.

Table S4: Second HSV-1 miRNA arms introduced to the analysis.

>hsv1-miR-H1-5p MIMAT0003744 Herpes Simplex miR-H1-5p
AUGGAAGGACGGGAAGUGGAAG
>hsv1-miR-H1-3p MIMAT0015220 Herpes Simplex miR-H1-3p
UACACCCCCUGCCUCCACCCU
>hsv1-miR-H2-5p MIMAT0008398 Herpes Simplex miR-H2-5p
UCGCACGCGCCCGGCACAGACU
>hsv1-miR-H2-3p MIMAT0008399 Herpes Simplex miR-H2-3p
CCUGAGCCAGGGACGAGUGCGACU
>hsv1-miR-H3-5p MIMAT0015279 Herpes Simplex miR-H3-5p
CUCCUGACCGCGGGUUCGAGU
>hsv1-miR-H3-3p MIMAT0008400
CUGGGACUGUGCGGUUGGGACC
>hsv1-miR-H4-5p MIMAT0008401 Herpes Simplex miR-H4-5p
GGUAGAGUUUGACAGGCAAGCA
>hsv1-miR-H4-3p MIMAT0008402 Herpes Simplex miR-H4-3p
CUUGCCUGUCUAAUCGCUAGU
>hsv1-miR-H5-5p MIMAT0015280
GGGGGGGUUCGGGCAUCUCUACCU
>hsv1-miR-H5-3p MIMAU0008403
GUCAGAGAUCCAAACCUCCGGA
>hsv1-miR-H6-5p MIMAT0015281 Herpes Simplex miR-H6-5p
GGUGGAAGGCAGGGGGGUGUA
>hsv1-miR-H6-3p MIMAU0008404
CACUUCCCGUCCUCCAUCCCU
>hsv1-miR-H7-5p MIMAT0012595 Herpes Simplex miR-H7-5p
AAAGGGGUCUGCAACCAAAGG
>hsv1-miR-H7-3p MIMAT0012596 Herpes Simplex miR-H7-3p
UUUGGAUCCCGACCCUUCUUCU
>hsv1-miR-H8-5p MIMAT0012597 Herpes Simplex miR-H8-5p
UAUAUAGGGUCAGGGGGUCCG
>hsv1-miR-H8-3p MIMAT0012598 Herpes Simplex miR-H8-3p
CGCCCCGUGCCUGUAUAUAU
>hsv1-miR-H11-5p MIMAT0037307 Herpes Simplex miR-H11-5p
UUCGCACUUUGUCCUAAUAUAU
>hsv1-miR-H11-3p MIMAT0014688 Herpes Simplex miR-H11-3p
UUAUUAGGACAAAGUGCGAACG
>hsv1-miR-H12-5p MIMAT0037308 Herpes Simplex miR-H12-5p
AGUGCUCGCACUUCGCCUAA
>hsv1-miR-H12-3p MIMAT0014689 Herpes Simplex miR-H12-3p
UUGGGACGAAGUGCGAACGCUU
>hsv1-miR-H13-5p MIMAT0037309 Herpes Simplex miR-H13-5p
AAGCGUUCGCACUUCGUCCCAAU
>hsv1-miR-H13-3p MIMAT0014690 Herpes Simplex miR-H13-3p
UUAGGGCGAAGUGCGAGCACUG
>hsv1-miR-H14-5p MIMAT0014691 Herpes Simplex miR-H14-5p
AGUCGCACUCGUCCUGGCUCAGG
>hsv1-miR-H14-3p MIMAT0014692 Herpes Simplex miR-H14-3p
UCUGUGCCGGGCGCGUGCGACU
>hsv1-miR-H15-5p MIMAT0037310 Herpes Simplex miR-H15-5p
TGTGGGGCCCCGGGCCGGGGCC
>hsv1-miR-H15-3p MIMAT0014693 Herpes Simplex miR-H15-3p
GGCCCCGGGCCGGGCCGCCACGT
>hsv1-miR-H16-5p MIMAT0014694 Herpes Simplex miR-H16-5p
AGCCAGGAGGCTGGGATCGAAGGCCAC
>hsv1-miR-H16-3p MIMAT0037311 Herpes Simplex miR-H16-3p
CGCUCGAACGCCCCGCCUCC
>hsv1-miR-H17-5p MIMAT0037312 Herpes Simplex miR-H17-5p
CCGCGCCUGCGCGCGUGGGGC

>hsv1-miR-H17-3p MIMAT0014695 Herpes Simplex miR-H17-3p
 UGGCGCUGGGGCGCGAGGCGG
 >hsv1-miR-H18-5p MIMAT0014696 Herpes Simplex miR-H18-5p
 CCCGCCCGCCGGACGCCGGGACC
 >hsv1-miR-H18-3p MIMAT0037313 Herpes Simplex miR-H18-3p
 TTGGCCGGCGGGCGGGAC
 >hsv1-miR-H26-5p MIMAT0037314 Herpes Simplex miR-H26-5p
 TTTCTGGCTCGGTGAGCGAC
 >hsv1-miR-H26-3p MIMAT0025022 Herpes Simplex miR-H26-3p
 GCGCGGCGGGCCTGCCGTAG
 >hsv1-miR-H27-5p MIMAT0037315 Herpes Simplex miR-H27-5p
 AAGAGGGAAGAAGAGGGGUCGG
 >hsv1-miR-H27a-3p Herpes Simplex miR-H27-3p
 UUUGGUUGCAGACCCUUUCUC
 >hsv1-miR-H28-5p MIMAT0037305 Herpes Simplex miR-H28-5p
 CGATGGTCGTCTGTGGAT
 >hsv1-miR-H28-3p MIMAT0037316 Herpes Simplex miR-H28-3p
 ATCGCGCAGAGCCGATAG
 >hsv1-miR-H29-5p MIMAT0037317 Herpes Simplex miR-H29-5p
 GGGTCCTTGACCCCACTTCCGG
 >hsv1-miR-H29-3p MIMAT0037306 Herpes Simplex miR-H29-3p
 CTGGAGGCGGGCAAGGACTACC

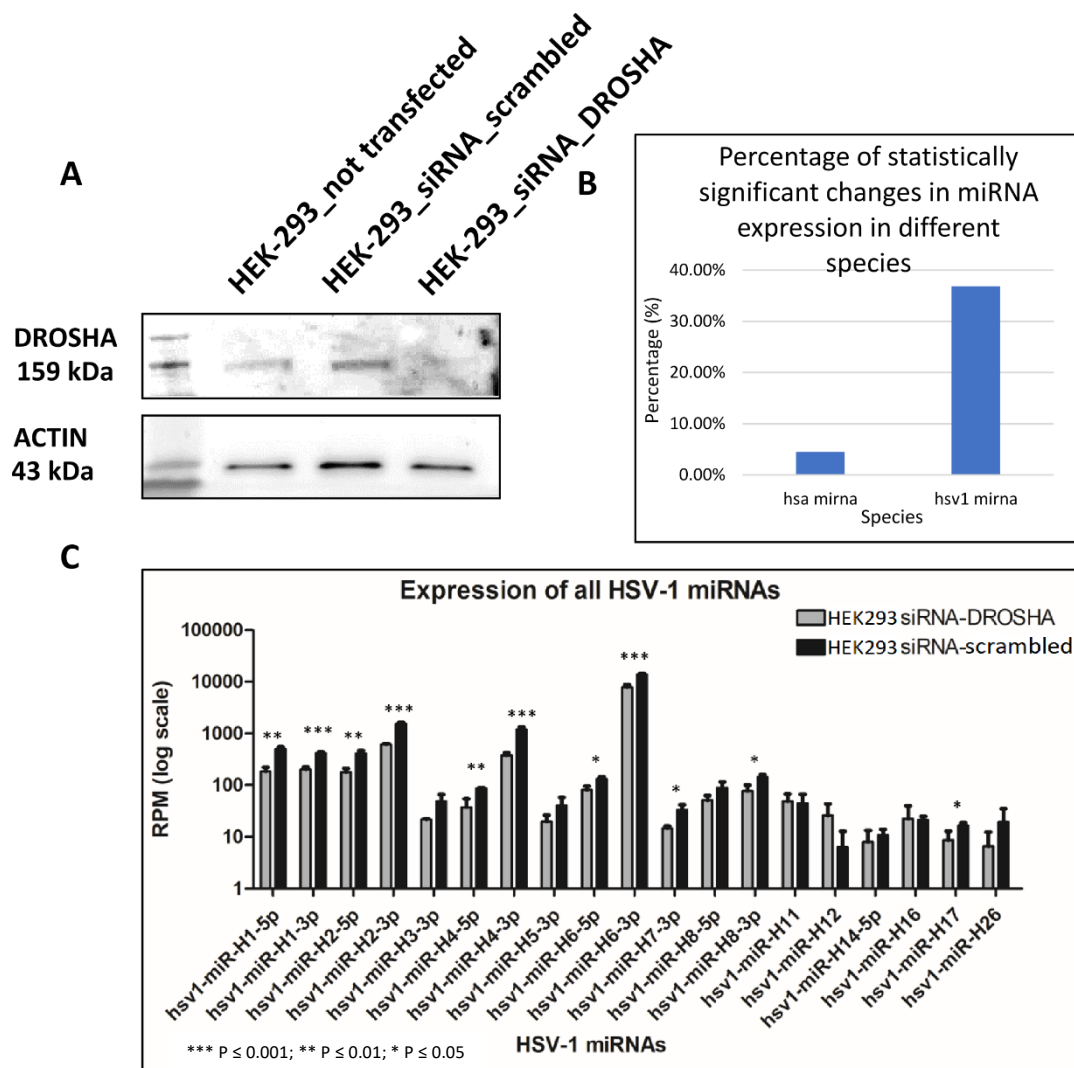


Figure S11: Generating siRNA Drosha^{-/-} cell line and the profile of Drosha-dependent miRNAs. HEK293 cells were transfected with siRNA that targets DROSHA and siRNA scrambled sequence as a negative control. A) DROSHA downregulation was successful using siRNA DROSHA. Cells were infected, and after 12hpi, samples were collected. B) HSV-1 miRNAs are largely affected in our experiment. C) A few HSV-1 miRNAs are significantly affected by DROSHA. Samples were performed in triplicates, and statistical significance is marked with asterisks.

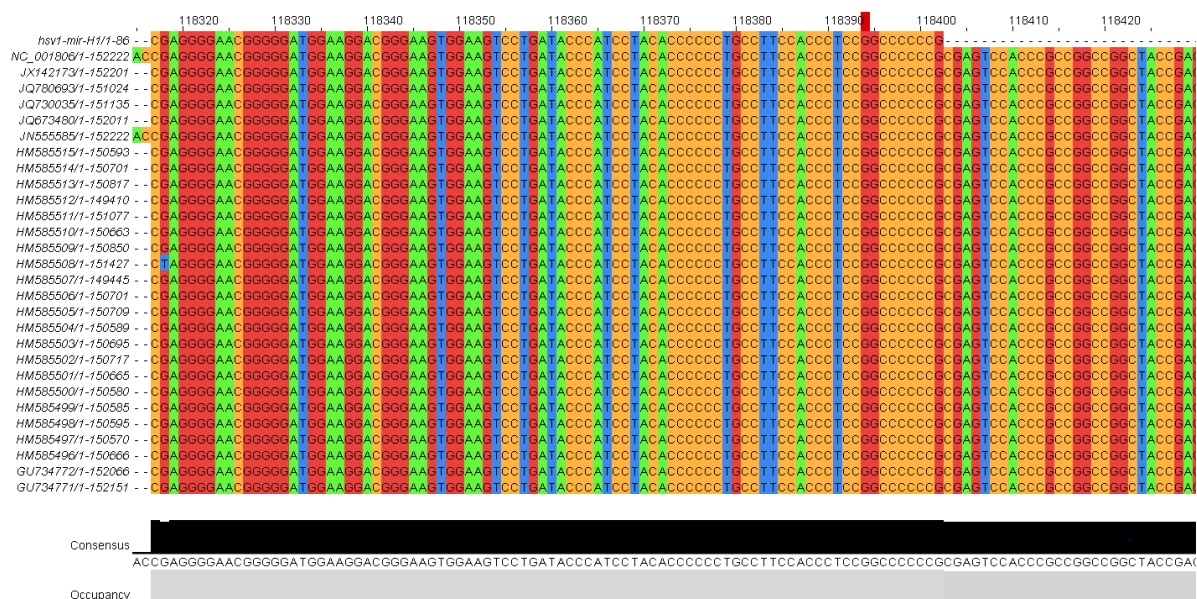


Figure S12: Example of the analysis of the conservation of the HSV-1 pre-miRNA region of mir-H1 among different HSV-1 strains and clinical isolates. The region of pre-mir-H1 is highly conserved. All pre-miRNA sequences were individually mapped to the 26 publicly available strains of HSV-1 using ClustalW [159]. A representative example of the conserved region is shown on the example of mir-H1 region. The other miRNA precursor regions all show high conservation as well (not shown).


```

hsv1-mir-H8      1  GTCCCTGTATATATAGGGTCAGGGGGTTCCGCACCCCTAACATGGCGCC      50
|||||
NC_001806      123803 GTCCCTGTATATATAGGGTCAGGGGGTTCCGCACCCCTAACATGGCGCC      123852
hsv1-mir-H8      51  CCCGGTCCCTGTATATATAGTTGTC      75
|||||
NC_001806      123853 CCCGGTCCCTGTATATATAGTTGTC      123876

hsv1-mir-H17     1  GGCCCACTCGCATCGCGCCTGCGCGCTGGGGCCTGGGCGCGCCGCTGC      50
|||||
NC_001806      150560 GGCCCACTCGCATCGCGCCTGCGCGCTGGGGCCTGGGCGCGCCGCTGC      150609
hsv1-mir-H17     51  GGCCCGTGACGTGGCGCTGGGGCGCGAGGCGGTGCGCGCCGGCC      95
|||||
NC_001806      150610 GGCCCGTGACGTGGCGCTGGGGCGCGAGGCGGTGCGCGCCGGCC      150654

hsv1-mir-H28     1  ATAGGCTATACGCGATGGTCTGTGGATTGGACATCTCGCGGTGGGTA      50
|||||
NC_001806      12386  ATAGGCTATACGCGATGGTCTGTGGATTGGACATCTCGCGGTGGGTA      12435
hsv1-mir-H28     51  GTGAGTCCCCCGGGCCGGGTTCTGGTGGAACTGTAAGGGGACGGCGGGTTA      100
|||||
NC_001806      12436  GTGAGTCCCCCGGGCCGGGTTCTGGTGGAACTGTAAGGGGACGGCGGGTTA      12485
hsv1-mir-H28     101 ATATACAATGACCACGTTCCGATCGCGCAGAGCCGATAGTATGTGCT      147
|||
NC_001806      12486  ATATACAATGACCACGTTCCGATCGCGCAGAGCCGATAGTATGTGCT      12532

hsv1-mir-H29     1  CCAGGGTCCTTGACCCCACTTCCGGGTTTCACTGAACCCCGTGGTGGTG      50
|||||
NC_001806      64902  CCAGGGTCCTTGACCCCACTTCCGGGTTTCACTGAACCCCGTGGTGGTG      64951
hsv1-mir-H29     51  TTCGACTTTGCCAGCCTGTACCCAGCATCATCCAGGCCACAACTGTG      100
|||||
NC_001806      64952  TTCGACTTTGCCAGCCTGTACCCAGCATCATCCAGGCCACAACTGTG      65001
hsv1-mir-H29     101 CTTAGCAGCTCTCCCTGAGGGCCGACGAGTGGCGCACCTGGAGGCGG      150
|||||
NC_001806      65002  CTTAGCAGCTCTCCCTGAGGGCCGACGAGTGGCGCACCTGGAGGCGG      65051
hsv1-mir-H29     151 GCAAGGACTACCTGGAGATCGAGGT      175
|||||
NC_001806      65052  GCAAGGACTACCTGGAGATCGAGGT      65076

```

Figure S13: Error in the annotation of several HSV-1 miRNAs. Published sequences of hsv1-mir-H8, -H17, -H28, and -H29 are different from their origin sequence, which is highly conserved among different HSV-1 strains and clinical isolates (Figure S11). HSV-1 strain 17 is used as the main reference (NC_001806).

Table S5: Representative sequences of two most dominant reads for each HSV-1 miRNA.

miRNA	Sequence	RC	miRNA	Sequence	RC	miRNA	Sequence	RC
miR-H1-5p		16845	miR-H12-5p			miR-H28-5p		66
miRBase	<u>GATGGAAGACGGGAAGTGGA</u>		miRBase	not annotated		miRBase	<u>CGATGGTCGTCTGTGGAT</u>	
1st dominant	<u>ATGGAAGACGGGAAGTGGAAG</u>	5656	1st dominant	CACGGCCGAGTGCTC	2	1st dominant	<u>ATGGTCGTCTGTGGATTGGAC</u>	5
2nd dominant	<u>TGGAAGACGGGAAGTGGAAG</u>	1495	2nd dominant	CACGGCCGGTGCTCGCACC	2	2nd dominant	<u>CGCATGGTCGTCTGTGGATT</u>	4
other		9694	other			other		57
miR-H1-3p		4872	miR-H12-3p		432	miR-H28-3p		
miRBase	<u>TACACCCCCCTGCCTTCCACCCT</u>		miRBase	<u>TTGGGACGAAGTGCGAACGCTT</u>		miRBase	not annotated	
1st dominant	<u>TACACCCCCCTGCCTTCCACC</u>	1118	1st dominant	<u>TTGGGACGAAGTGCGAACGCTT</u>	52	1st dominant	<u>ATGACCACGTTTGGATCGCGCAGAGCT</u>	5
2nd dominant	<u>TACACCCCCCTGCCTTCCACCCT</u>	628	2nd dominant	<u>ATTGGGACGAAGTGCGAAC</u>	30	2nd dominant	<u>ACAATGACCACGTTTGGATCGC</u>	4
other		3126	other		350	other		
miR-H2-5p		9058	miR-H13-5p			miR-H29-5p		
miRBase	<u>TCGCACGCGCCGGCACAGACT</u>		miRBase	not annotated		miRBase	not annotated	
1st dominant	<u>TCGCACGCGCCGGCACAGACT</u>	5630	1st dominant	AAGCGTTTCGCACCTTCGCCAAT	14	1st dominant	<u>CGACTTTGCGAGCTGTACCC</u>	4
2nd dominant	<u>TCGCACGCGCCGGCACAGAC</u>	606	2nd dominant	AGCGTTTCGCACCTTCGCCAAT	1	2nd dominant	<u>TTGCCAGCTGTACCCAGCATC</u>	2
other		2822	other			other		
miR-H2-3p		127592	miR-H13-3p		168	miR-H29-3p		100
miRBase	<u>CCTGAGCCAGGACGAGTGCGACT</u>		miRBase	<u>TTAGGGCGAAGTGCGAGCACTGG</u>		miRBase	<u>CTGGAGGCGGCAAGGACTACC</u>	
1st dominant	<u>CCTGAGCCAGGACGAGTGCGACT</u>	30755	1st dominant	<u>TTAGGGCGAAGTGCGAGCACTGG</u>	24	1st dominant	<u>CCTGGAGGCGGCAAGGACTACC</u>	7
2nd dominant	<u>GAGCCAGGACGAGTGCGACTGT</u>	23885	2nd dominant	<u>TTAGGGCGAAGTGCGAGCAC</u>	20	2nd dominant	<u>CTGGAGGCGGCAAGGACTACC</u>	4
other		72952	other		124	other		89
miR-H3-5p		1153	miR-H14-5p		335			
miRBase	<u>CTCCTGACCGCGGTTCCGAGT</u>		miRBase	<u>AGTCGCACTCGTCCCTGGCTCAGG</u>				
1st dominant	<u>CTCCTGACCGCGGTTCCGAGT</u>	459	1st dominant	<u>CAGTCGCACTCGTCCCTGGCTCAGGCTT</u>	15			
2nd dominant	<u>TCCTGACCGCGGTTCCGAGT</u>	366	2nd dominant	<u>T</u>	14			
other		328	other	<u>AGTCGCACTCGTCCCTGGCTCAGG</u>	306			
miR-H3-3p		5823	miR-H14-3p		124			
miRBase	<u>CTGGGACTGTGCGGTTGGGAC</u>		miRBase	<u>TCTGTGCGGGCGGTGCGAC</u>				
1st dominant	<u>CTGGGACTGTGCGGTTGGGACC</u>	1151	1st dominant	<u>TCTGTGCGGGCGGTGCGACT</u>	16			
2nd dominant	<u>CTGGGACTGTGCGGTTGGGAC</u>	1040	2nd dominant	<u>AACAGAGTCTGTGCGGGCG</u>	7			
other		3632	other		101			
miR-H4-5p		2708	miR-H15-5p					
miRBase	<u>GGTAGAGTTTGACAGGCAAGCA</u>		miRBase	not annotated				
1st dominant	<u>GGTAGAGTTTGACAGGCAAG</u>	655	1st dominant	<u>CATGCGCCGGGCGTTGTG</u>	8			
2nd dominant	<u>GGTAGAGTTTGACAGGCAAGCA</u>	428	2nd dominant	<u>CGCAGCGCATGCGCCGGG</u>	7			
other		1625	other					
miR-H4-3p		31888	miR-H15-3p		8			
miRBase	<u>CTTGCTGTCTAACTCGCTAGT</u>		miRBase	<u>GGCCCCGGGCGGGCCGCCACG</u>				
1st dominant	<u>CTTGCTGTCTAACTCGCTAGT</u>	15081	1st dominant	<u>GGCCCCGGGCGGGCCGCCACGT</u>	2			
2nd dominant	<u>TTGCTGTCTAACTCGCTAGT</u>	2326	2nd dominant	<u>GCCCCGGGCGGGCCGCCACGCT</u>	1			
other		14481	other		5			
miR-H5-5p		104	miR-H16-5p		250			
miRBase	<u>GGGGGGGTTCGGGCATCTCTAC</u>		miRBase	<u>CCAGGAGGCTGGGATCGAAGGC</u>				
1st dominant	<u>GGGGGGGTTCGGGCATCTCTACT</u>	54	1st dominant	<u>AGCCAGGAGGCTGGGATCGAAGGCCACA</u>	60			
2nd dominant	<u>GGGGGGGTTCGGGCATCTCTACC</u>	4	2nd dominant	<u>T</u>	46			
other		46	other	<u>AGCCAGGAGGCTGGGATCGAAGGCCAC</u>	144			
miR-H5-3p		87	miR-H16-3p					
miRBase	<u>GTCAGAGATCCAAACCTCCGG</u>		miRBase	not annotated				
1st dominant	<u>GTCAGAGATCCAAACCTCCGGA</u>	25	1st dominant	<u>CTGCTGCCGGGGACTCTTC</u>	146			
2nd dominant	<u>GTCAGAGATCCAAACCTCCGGT</u>	4	2nd dominant	<u>TGCTGCCGGGGACTCTTC</u>	83			
other		58	other					
miR-H6-5p		2202	miR-H17-5p					
miRBase	<u>GGTGAAGGACGGGGGTGTA</u>		miRBase	not annotated				
1st dominant	<u>GGTGAAGGACGGGGGTGTA</u>	395	1st dominant	<u>CCGCGCTGCGCGCTGGGGC</u>	15			
2nd dominant	<u>GGTGAAGGACGGGGGTGT</u>	196	2nd dominant	<u>CTCGCACCGCGCTGCGCGCTGGGGC</u>	2			
other		1611	other					
miR-H6-3p		228611	miR-H17-3p		14			
miRBase	<u>CACTTCCGCTCCTTCCATCCC</u>		miRBase	<u>TGGCGTGGGGCGCGAGGCGG</u>				
1st dominant	<u>CACTTCCGCTCCTTCCATCCCT</u>	40376	1st dominant	<u>GCCTGGGGCGCGAGGCGGT</u>	2			
2nd dominant	<u>CACTTCCGCTCCTTCCATCCA</u>	31543	2nd dominant	<u>GGCGTGGGGCGCGAGGCGGT</u>	1			
other		156692	other		11			
miR-H7-5p		930	miR-H18-5p		22			
miRBase	<u>AAAGGGGTCTGCAACCAAGG</u>		miRBase	<u>CCCGCCCGCGAGCCGGGACC</u>				
1st dominant	<u>AAAGGGGTCTGCAACCAAGG</u>	237	1st dominant	<u>CGCCCGCGGACGCGGGA</u>	2			
2nd dominant	<u>AAAGGGGTCTGCAACCAAGGT</u>	71	2nd dominant	<u>GCCCGCGGACGCGGACCAACG</u>	2			
other		622	other		18			
miR-H7-3p		8537	miR-H18-3p					
miRBase	<u>TTTGGATCCCGACCCCTCTTC</u>		miRBase	not annotated				
1st dominant	<u>TTTGGATCCCGACCCCTCTTCT</u>	3906	1st dominant	<u>CGCCTTGCCGCCCCCATT</u>	2			
2nd dominant	<u>TTTGGATCCCGACCCCTCTTC</u>	2466	2nd dominant	<u>CGCCCCCATTGGCCGGC</u>	2			
other		2165	other					
miR-H8-5p		641	miR-H26-5p					
miRBase	<u>TATATAGGGTCAGGGGTTTC</u>		miRBase	not annotated				
1st dominant	<u>TATATAGGGTCAGGGGTTTC</u>	173	1st dominant	<u>CAGGCTAGCGGGCGGGC</u>	2			
2nd dominant	<u>TATATAGGGTCAGGGGTTCC</u>	98	2nd dominant	<u>GGCGGGCTGCGTGAATTTCTG</u>	1			
other		370	other					
miR-H8-3p		1722	miR-H26-3p		266			
miRBase	<u>GCCCCGGTCCCTGTATATA</u>		miRBase	<u>TGGCTCGGTGAGCGACGTC</u>				
1st dominant	<u>GCCCCGGTCCCTGTATATAT</u>	955	1st dominant	<u>TGGCTCGGTGAGCGACGG</u>	37			
2nd dominant	<u>GCCCCGGTCCCTGTATAT</u>	180	2nd dominant	<u>TGGCTCGGTGAGCGACGTTCC</u>	15			
other		587	other		214			
miR-H11-5p			miR-H27-5p					
miRBase	not annotated		miRBase	not annotated				
1st dominant	<u>TTGCTCAATAATATATATATT</u>	7	1st dominant	<u>AAGAGGGGTGCGGATCCAAAGG</u>	16			
2nd dominant	<u>AGCGTTTCGCACTTTGTCTTAAT</u>	5	2nd dominant	<u>AAGACGACGCCAGACACC</u>	10			
other			other					
miR-H11-3p		1903	miR-H27-3p		1			
miRBase	<u>TTAGGACAAAGTGCGAACGC</u>		miRBase	<u>CAGACCCCTTTCTCCCCCTCTT</u>				
1st dominant	<u>TTATTAGGACAAAGTGCGAACGC</u>	194						
2nd dominant	<u>TTAGGACAAAGTGCGAACGCTT</u>	121						
other		1588						
				<u>GACCCCTTTCTCCCCCTCTTC</u>	1			
			1st dominant	<u>TTTGGTTGACAGACCCCTTCTC</u>	218			
			2nd dominant	<u>TTTGGTTGACAGACCCCTTCT</u>	127			
			other					

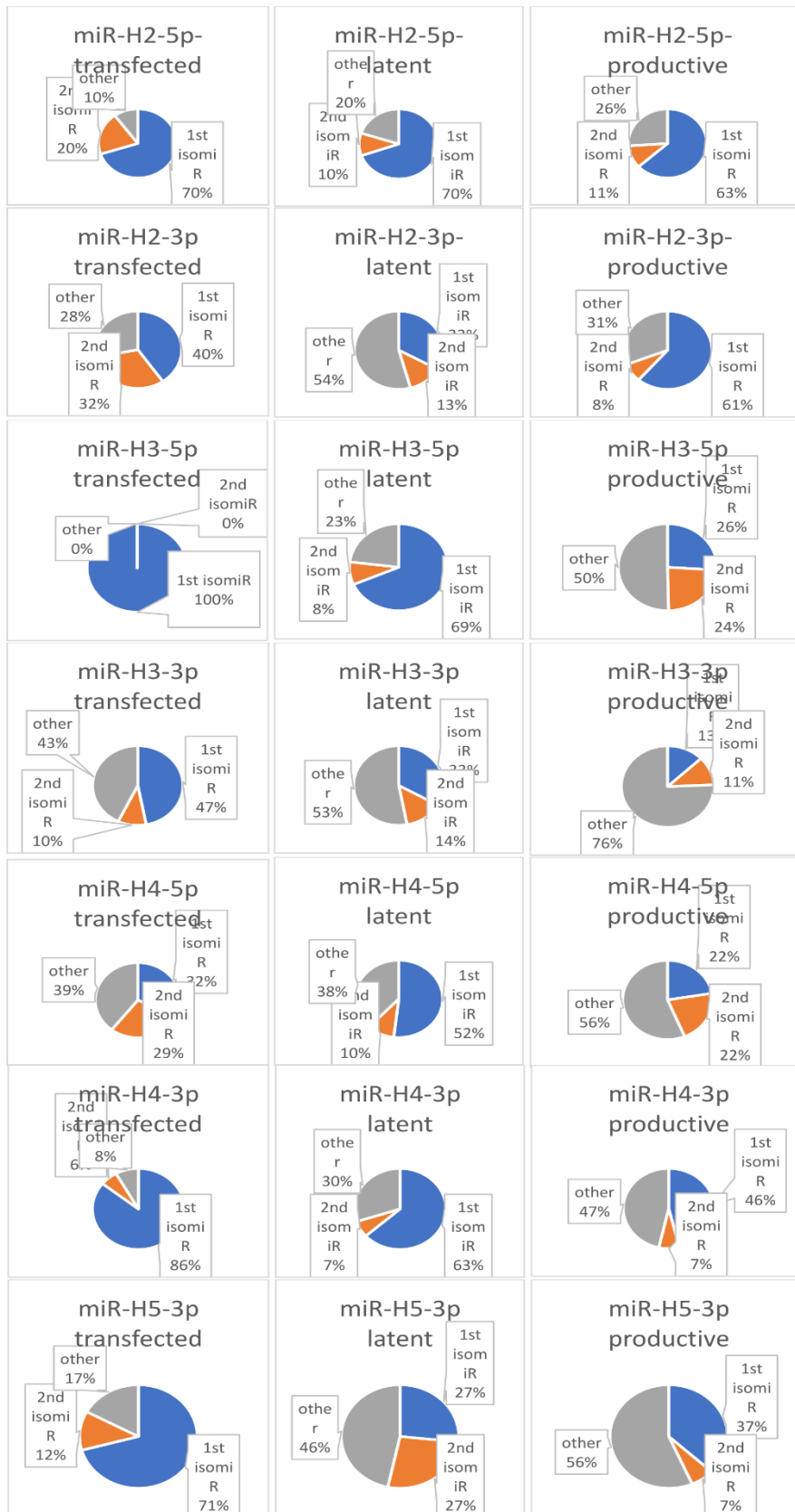


Figure S14: The frequency of isomiRs of HSV-1 miRNAs in productive or latent HSV-1 infection or transfected samples with HSV-1 fragments. The first two most dominant isomiRs are shown, and all others are labeled as other.

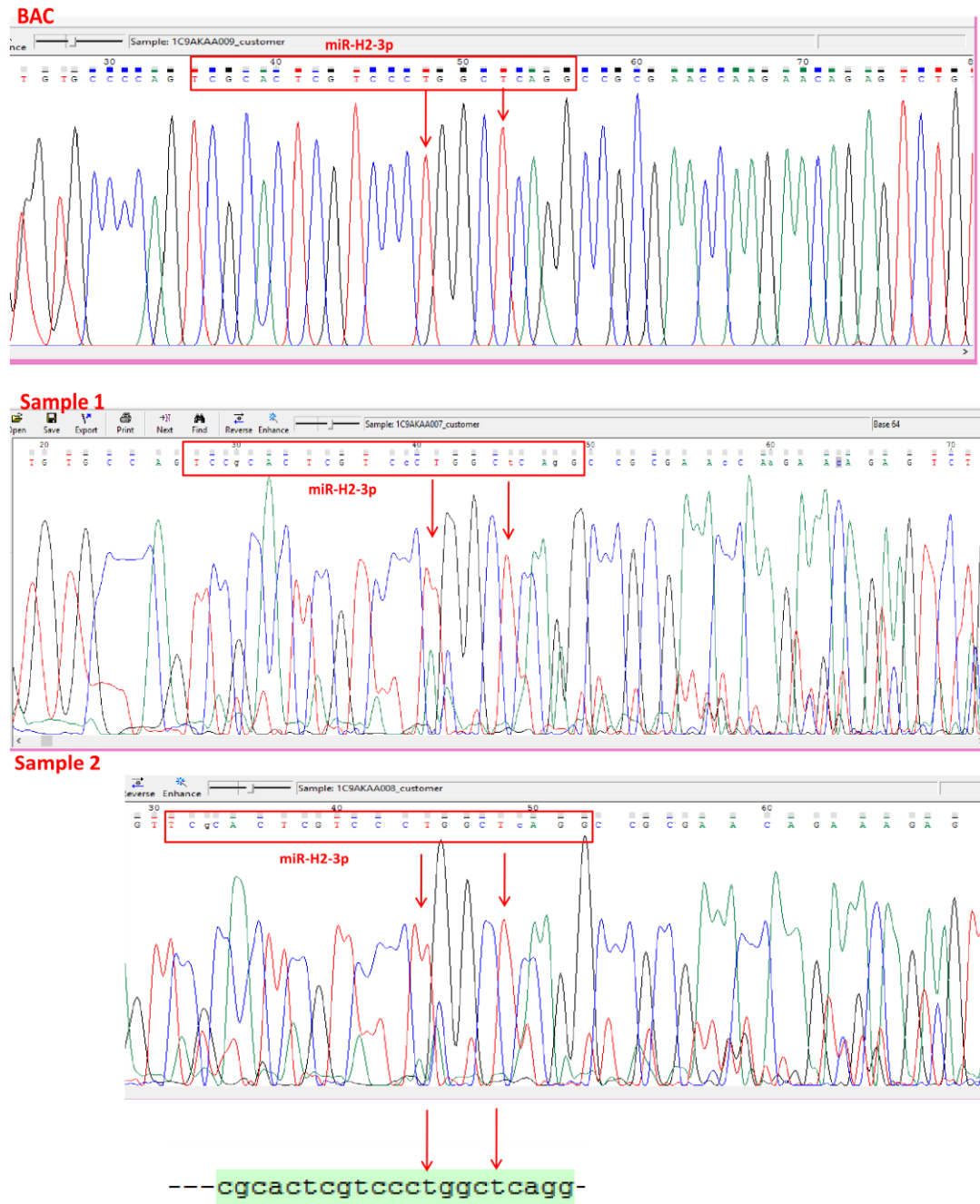


Figure S15: miR-H2 locus amplification and sequencing. Genomic miR-H2 locus sequences from HSV-1-BAC, and hTG sample 4 and hTG sample 5 were amplified and sequenced. The miR-H2-3p sequence is outlined in red. Sequencing results show a consensus sequence equal to the wt sequence of miR-H2 in the green box on positions 5 and 9 marked with red arrows where we can strongly detect a pattern of seed editing event.

Table S6: Full list of predicted targets for wt miR-H2-3p and edited sequences

miR-H2-3p-wt

RL2_1/miR-H14 – SEED -ICP0
UL32 no seed - L2 - cleavage and packaging of viral DNA
UL55 no seed
UL39 no seed
UL26 -no seed

miR-H2-3p-e5

RL2_1/miR-H14 - no seed
UL12 no seed - E - processes replication intermediates that would interfere with the packaging of viral DNA into capsids
UL32 no seed - L2 - cleavage and packaging of viral DNA
UL15 intron - SEED - L1 -
UL17 - no seed 2x - L1 - essential for DNA cleavage and packaging
UL17 - SEED - L1 - essential for DNA cleavage and packaging
UL19 - SEED - L1 - VP5 - major capsid protein
UL21 - SEED - L1 - tegument protein weakly associated with capsids
UL22 - no seed - L1 - gH essential for virion infectivity
UL25 - no seed - L2 - capsid protein
UL32 - no seed - L2 - cleavage and packaging of viral DNA
UL36 - no seed 2x - L2 - tegument protein required for egress of virions through cytoplasm
UL39 SEED - E - PK activity
UL39 no seed - E - PK activity

miR-H2-3p-e9

RL2 ICP0
UL3 - L2 - colocalizes with ICP22
UL12 - E - processes replication intermediates that would interfere with the packaging of viral DNA into capsids
UL17 - L1 - essential for DNA cleavage and packaging
UL25 - L2 - capsid protein
UL43 - L1 - integral membrane protein
RS1 - ICP4

miR-H2-3p-e5-9

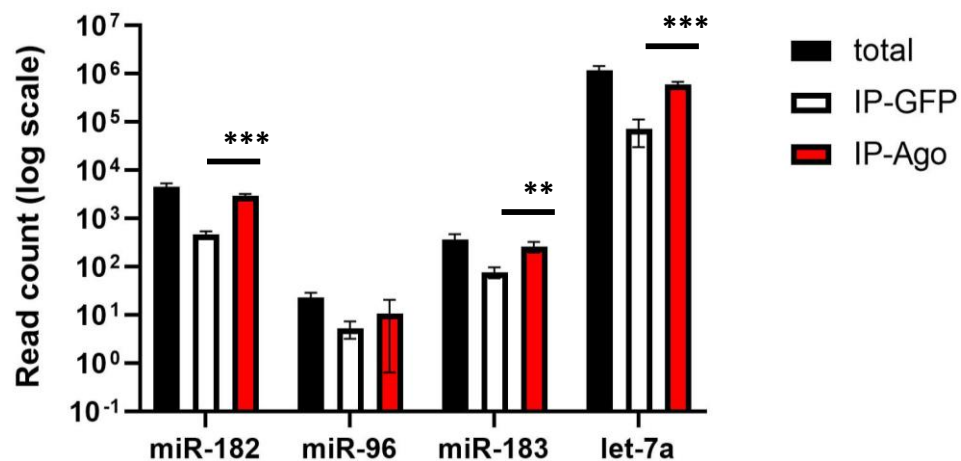
RL2 2x - ICP0
UL9 SEED - E - initiation of DNA synthesis
UL12- E - processes replication intermediates that would interfere with the packaging of viral DNA into capsids
UL17 seed - L1 - essential for DNA cleavage and packaging
UL19 - L1 - VP5 - major capsid protein
UL21 - L1 - tegument protein weakly associated with capsids
UL22 - L1 - gH essential for virion infectivity
UL23 - E - TK
UL27 - L1 - gB - essential for entry
UL29 - E - ICP8 - key role in viral gene expression and synthesis of viral DNA
UL30 - E - catalytic subunit of viral DNA polymerase

UL39 - E - PK activity
UL43 - L1 - integral membrane protein
UL44 - L2 - gC - attachment to cells
UL47 - L1 - RNA binding
126 500 5x
RS1 - ICP4
US4 - gG
US8 - gE

Table S7: miR-H2-3p-wt and edited sequences binding sites on ICP0 and ICP4. Targets were visualized using RNAhybrid 2.2 and the table shows minimum free energy (MFE). Perfect seed sequence match was marked with asterisks

ICP0 binding sites	MFE		ICP4 binding sites	MFE	
miR-H2-3p-WT					
2391	-58.5	*	2582	-34.6	*
27	-33.5		3904	-32.7	
2622	-31.7		185	-32	
3341	-31.6		2090	-31.6	
1906	-30.7		2303	-31.5	
2455	-30.5		2871	-30.8	
3435	-30.4		3543	-30.7	
849	-29.4		1509	-30.6	
2586	-29.4		3121	-30.5	
2903	-29.2		3331	-30.3	
miR-H2-3p-MUT					
2391	-43.5		3904	-36.3	*
27	-33.4		185	-35.5	
2970	-32.5		290	-34.7	*
2622	-32.1		986	-34.3	
2432	-31	*	2728	-33.5	
2330	-30.2		1509	-32.6	
2007	-29.8		404	-32.3	
1231	-29.7		3047	-32.2	
1906	-29.7		1922	-31.5	
1850	-29.4		1066	-31.3	
miR-H2-3p-e5					
2391	-57.6	*	3904	-37.3	*
3341	-37.5	*	2511	-36.7	*
27	-33.9		2728	-36.4	
3435	-33.9		796	-36.3	*
2007	-33.8		713	-35.9	*
2455	-33.1		2303	-35	
2697	-32.8	*	3560	-34.1	*
2903	-32.6		3331	-34	
2622	-32.5		2582	-33.7	*
2306	-31.5	*	3674	-33.7	*
miR-H2-3p-e9					
2391	-57.8	*	2582	-40.6	*
27	-37.8		713	-34.9	
2622	-35.3		334	-34	
2007	-34.4		1385	-34	
3160	-34.2		3904	-33.7	
1906	-32.6		796	-33.2	
2442	-32.3	*	290	-32.9	

2236	-32.2		2320	-32.9	
1213	-31.8		1509	-32.7	
2330	-31.6		185	-32.5	
miR-H2-3p-e5-9					
2391	-56.9	*	713	-41.9	*
27	-38.2		3904	-40.7	*
3341	-36.8	*	796	-40.2	*
2622	-35.9		2582	-39.7	*
2325	-35.6		2722	-39.1	
2903	-34.7		3560	-39.1	*
2169	-34.4		3674	-38.7	*
3160	-34.2		2940	-38.1	
2007	-33.9		1509	-36.9	
1906	-33.4		2511	-36.9	*



*** $P \leq 0.001$; ** $P \leq 0.01$; * $P \leq 0.05$

Figure S16. Host miR-183/-96/-182 in Ago immunoprecipitation and sequencing experiment. The amount of miRNAs is represented in average read counts (RC) found in triplicates. Black bars represent miRNAs detected in total fraction multiplied by 10. White bars represent GFP immunoprecipitation, and red bars represent Ago immunoprecipitation samples. The asterisks above bars represent the significance of the difference between miRNAs found in Ago-IP compared to GFP-IP samples: *** $p \leq 0.001$; ** $p \leq 0.01$; * $p \leq 0.05$

Table S8. Percentage of miR-H2-3p edited at position 5 in Ago immunoprecipitation and sequencing experiment.

mir-H2-3p	A>G e5 RC	Total RC	Percentage of e5 (%)
input	390	4820	8.09
IP-Ago	309	3020	10.23

CURRICULUM VITAE

ANDREJA ZUBKOVIĆ

Laboratory for Molecular Virology, Department of Biotechnology, University of Rijeka |
<https://portal.uniri.hr/Portfelj/2524> | azubkovic@uniri.hr

Education

- 2014 – today **PhD Candidate**, PhD program *Medicinal chemistry*,
Department of Biotechnology, University of Rijeka
- 2009 – 2014 **Masters in Biotechnology in Medicine** (magna cum laude)
Department of Biotechnology, University of Rijeka

Work experience

- 2017 – today **Assistant and young researcher**
- Teaching experience: assistance in conducting seminars and sessions for
Courses: Microbiology, Virology, Biochemistry, Methods in DNA technologies,
Basics of Bioinformatics
- Young researcher in Laboratory for Molecular Virology, Department of
Biotechnology, University of Rijeka, principal investigator associate professor
Igor Jurak, PhD
- 2017 / 2019 Erasmus+ traineeship in Genetics Department & Biotechnology Institute,
Biomedical Research Center (CIBM), University of Granada, Spain, topic of
research: advanced bioinformatics analysis of small RNA molecules, in period
of 5 months
- 2015 – 2016 Young researcher at the Department of Biotechnology, University of Rijeka,
involved in European Social Fund research project "Host microRNA role in
herpes simplex virus replication"

Professional education

- 2019 Workshop *Better Skills for Better Jobs: Education and Training for Successful
Research Careers*, Congress of the Croatian Society of Biochemistry and
Molecular Biology *Crossroads in Life Sciences*, Lovran, Croatia, 25. – 28.
September, 2019.
- 2019 Attending lifelong learning program: Language training for English in higher
education, University of Rijeka, February -April 2019.
- 2019 Bioinformatics training by attending workshop *Bioinformatics: computer
methods in molecular and systems biology*, ICGEB, Trieste, Italy, 24.- 28. June
2019

2016	Bioinformatics training by attending workshop <i>BioBash Essentials</i> , Ljubljana, Slovenia, February 2015
------	--------------------------------------------------------------------------------------------------------------

Languages

Mother tongue	Croatian
Other languages	English, proficiency level C2

Scholarships and awards

2020	Croatian Society of Biochemistry and Molecular Biology Scholarship for attending 45 th FEBS Congress, 4. – 9. July, 2020, Ljubljana, Slovenia (virtual)
2019	FEMS Meeting Attendance Grant for attending <i>44th Annual International Herpesvirus Workshop</i> , Knoxville, TN, USA
2017 / 2019	Erasmus+ scholarship for period of 5 months' traineeship in Genetics department & Biotechnology Institute, University of Granada, Spain
2018	FEMS Meeting Attendance Grant for attending congress <i>Power of Viruses</i>
2016	Award for the best poster presentation at 6th Croatian Congress of Microbiology
2015	Support for University of Rijeka PhD students for realization of their projects with the aim of achieving strategic goals
2010 – 2014	City of Rijeka scholarship for talented students

Memberships

2019 – today	Croatian Society of Biochemistry and Molecular Biology (HDBMB)
2017 – today	Croatian Microbiology Society (HMD)

Selected conferences

2021	Poster presentation at <i>45th Annual International Herpesvirus Workshop: Host microRNAs Indicated to Target FoxO Protein Family are Upregulated During Herpes Simplex Virus 1 Productive Infection</i> , 2. – 6. August, 2021. (virtual)
2019	Poster presentation at <i>44th Annual International Herpesvirus Workshop: Herpes simplex virus 1 miRNA sequence variations during productive and latent infection</i> , Knoxville, TN, USA, 20-24. July, 2019.
2018	Oral presentation at <i>Power of Viruses</i> conference: <i>Comprehensive analysis of herpes simplex virus 1 encoded miRNAs and host miRNAs during productive and latent infection – the need for a revision</i> – Poreč, 16. May 2018.
2017	Oral presentation at <i>7th Congress of Slovenian Microbiology Society on Virology Day: A subset of host miRNAs is upregulated during herpes simplex virus 1 infection</i> – Bled, 22. September 2017.

Publications

- 2022** **Zubković, Andreja**; Žarak, Ines; Ratkaj, Ivana; Rokić, Filip; Jekić, Maja; Pribanić Matešić, Marina; Lebrón, Ricardo; Gómez Martín, Cristina; Lisnić, Berislav; Juranić Lisnić, Vanda; Jonjić, Stipan; Pan, Dongli; Vugrek, Oliver; Hackenberg, Michael; Jurak, Igor. The Virus-Induced Upregulation of the miR-183/96/182 Cluster and the FoxO Family Protein Members Are Not Required for Efficient Replication of HSV-1, *Viruses*, 2022.
- 2020** Pribanić Matešić, Marina; **Zubković, Andreja**; Đukić, Nina; Mihalac, Josip; Jurak, Igor. Puzzling functions of HSV-1 miRNAs in productive and latent infection, *Periodicum biologorum*, 2020.
- 2019** Aparicio-Puerta, Ernesto; Lebrón, Ricardo; Rueda, Antonio; Gómez-Martín, Cristina; Giannoukakos, Stavros; Jaspez, David; Medina, José María; **Zubković, Andreja**; Jurak, Igor; Fromm, Bastian et al. *sRNAbench and sRNAtoolbox 2019: intuitive fast small RNA profiling and differential expression*, *Nucleic acids research*, 2019.
- 2018** Cokarić Brdovčak M, **Zubković A**, Jurak I., *Herpes Simplex Virus 1 Deregulation of Host MicroRNAs*, *Noncoding RNA*, 2018.
- 2018** Cokarić Brdovčak M, **Zubković A**, Ferencić A, Šoša I, Stemberga V, Cuculić D, Rokić F, Vugrek O, Hackenberg M, Jurak I., *Herpes simplex virus 1 miRNA sequence variations in latently infected human trigeminal ganglia*, *Virus research*, 2018.
- Other**
- 2014-2019.** Science popularization on Department of Biotechnology, University of Rijeka with activities: Open doors of the Laboratory for Molecular Virology and Isolation of DNA from Banana Workshop

